

Proteomic Architecture of Human Coronary and Aortic

Atherosclerosis: Supplemental Materials

Expanded Methods

The data, analytic methods, and study materials are available to other researchers for purposes of reproducing the results or replicating procedures. Specifically, The DDA MS and the MRM MS data along with the Skyline document have been uploaded to Peptide Atlas. The Spectral Library used for DIA MS quantitation has also been uploaded to Peptide Atlas. The data can be accessed at <http://www.peptideatlas.org/PASS/PASS01066> or via FTP using the following credentials: Servername: [ftp.peptideatlas.org](ftp://ftp.peptideatlas.org); Username: PASS01066; Password: KV454u.

Arterial Sample Acquisition and Pathology Grading Methods

Male and female cases of any race, aged 18-50 years (men) or 18-60 years (women) with no ante mortem clinical suspicion of coronary disease autopsied < 24 hours of death were eligible for inclusion. This report includes data from the first 100 adult coroner cases included in the study (age range: 15-55 yrs., 75% males, 67% White, 26% Black, 7% other). The Medico-Legal Death Investigators obtain signed family consent for retrieval of anatomic specimens prior to the autopsy. During the autopsy the pathologist dissects the aorta (ligamentum arteriosum to aortic bifurcation) and LAD and removes branching arteries and adventitial or epicardial adipose tissue. Both the aorta and LAD are opened longitudinally, cleansed of blood and photographed (**Supplemental Fig. 1**). In each of the regions to be sampled, the pathologist inspects the intimal surface and categorizes the type and percent involvement of the following atherosclerotic changes: a) fatty streaks (FS); b) fibrous plaques (FP); c) complicated lesions (CL); and d) calcified lesions (CO), and records the data on a data collection form. Consistent with the age and cause of death (trauma), the fibrous plaques were almost exclusively early lesions - only one specimen had any macroscopic evidence of calcification and <3% of samples had any evidence of plaque hemorrhage, ulceration or thrombosis. Next the pathologist collects up to 1

gram of tissue from each of three standardized sections of the thoracic and abdominal aorta and two sections from the coronary artery¹ (**Supplemental Fig. 1**). The specimens are snap frozen in cryotubes with liquid nitrogen and remain in a 34L WWR Cryogenic Dewar until transferred to a -80 freezer equipped with temperature alarms and automated generator back-up systems in the Department of Pathology at LSU. Additionally, targeted “pure” samples of grossly normal (non-lesion) and, if available, grossly atherosclerotic (lesion) are taken and divided into three 100mg portions and 1.) snap frozen, 2.) placed in RNALater solution and frozen, and 3.) placed in formalin and stored at room temperature for possible future immunohistochemistry analyses. A 50 gram sample of liver is also collected and frozen for future studies. All samples received at LSU are checked for label accuracy and entered in a database using an unlinked anonymous code for further processing, analyses and storage.

Protein Extraction, MS Analysis and Protein Identification

Aorta and LAD tissues were pulverized in liquid nitrogen and homogenized in 8M urea, 2M thiourea, 4% CHAPs and 1% DTT using Dounce homogenizer for 100 strokes, centrifuged at 16000 rpm for 20 mins. These conditions will solubilize the majority of proteins except cross-linked extracellular matrix (ECM) proteins which require additional solubilization strategies not used here^{2,3}. However, by using two different MS based methods we were able to obtain extensive coverage of soluble ECM proteins (**Supplemental Table 1**). Protein concentration of the supernatant was assessed by CB-X assay kit (G-Biosciences MO, USA). 100 µg of protein was precipitated using 2-D clean-up kit (GE Healthcare MA, USA) and then reconstitute in 6M urea, 50mM ammonium bicarbonate. The protein was reduced, alkylated and digested with trypsin (1:20). Peptides were desalted using Oasis HLB 96-well Plate (Waters MA, USA). A total of 2.0 µg of peptides per sample were then analyzed using label-free quantification on a reversed-phase liquid chromatography tandem mass spectrometry (RPLC–MS/MS) online with an Orbitrap Elite mass spectrometer (Thermo Scientific, USA) coupled to an Easy-nLC 1000 system (Thermo Scientific, USA). Peptides concentrated on a C18 trap column (Acclaim PepMap 100, 300 µm × 5 mm, C18, 5 µm, 100 Å; maximum pressure 800bar) in 0.1% TFA,

then separated on a C18 analytical column (Acclaim PepMap RSLC, 75 µm × 15 cm, nano Viper, C18, 2 µm, 100 Å) using a linear gradient from 5% to 35% solvent B over 155 mins (solvent A: 0.1% aqueous formic acid and solvent B: 0.1% formic acid in acetonitrile; flow rate 350 nL/min; column oven temperature 45 °C). The analysis was operated in a data-dependent mode with full scan MS spectra acquired at a resolution of 60,000 in the Orbitrap analyzer, followed by tandem mass spectra of the 20 most abundant peaks in the linear ion trap after peptide fragmentation by collision-induced dissociation (CID).

To eliminate batch effect, the same parameters were used for mass spectra acquisition and the peptides from each individual were analyzed randomly in one batch. To minimize cross contamination, a blank run was performed between each sample. To monitor column performance, 200fmol BSA digested peptides were analyzed to make sure elution time of same peptide were within 0.2 minutes and signal intensity and total spectra counts variation were less than 10%. One LAD and one AA sample (from different subjects) were excluded because of poor protein yield leaving n=99 samples from each territory for analysis.

The MS/MS data obtained from the Orbitrap Elite were converted to mzXML and mgf format using Msconvert version 3.0.3858 from ProteoWizard⁴ for peaklist generation. All data were searched using the X!Tandem⁵ algorithm version 2009.10.01.1 and OMSSA⁶ algorithm version 2.1.9. The dataset was searched against the concatenated target/decoy⁷ Human Uniprot⁸ database as of July 24, 2015, with only reviewed and canonical sequences used. The search parameters were as follows: Fixed modification of Carbamidomethyl (C) and variable modifications of Oxidation (M), Phosphorylation (STY); Enzyme: Trypsin with 2 maximum missed cleavages; Parent Tolerance: 0.050.08 Da; Fragment tolerance: 1.00 Da. Post-search analysis was performed using Trans Proteomic Pipeline⁹ version v4.6, rev 1 with protein group and peptide probability thresholds set to 90% and 90%, respectively, and one or more distinct peptide required for identification. PeptideProphet¹⁰ was used for peptide validation from each individual search algorithm and iProphet¹¹ was used to merge results from the separate algorithms and further refine the identification probabilities. Lastly, ProteinProphet¹² was then

used to infer protein identifications from the resulting combined peptide list and perform grouping of ambiguous hits. Protein Group and Peptide False Discovery Rates were calculated automatically using a target-decoy method for the above probability thresholds (0.72% and 0.06% respectively). Protein isoforms were only reported if a peptide comprising an amino acid sequence that was unique to the isoform was identified. Label-free quantification of each protein was performed using weighted spectral counting¹³. The distribution of protein spectral counts for each data file was inspected to verify equivalence in sample loading and instrument performance between files. Based on this analysis, a median normalization (adjustment of the raw spectral counts for each protein of a given file to the median of all spectral counts observed for the same file) was performed.

Post-processing Quality Control and Data Imputation

A total of 1925 unambiguous proteins were detected in one or more of the 99 LAD samples. Of these proteins 944 had $\leq 50\%$ missingness and 375 had no missingness in all 99 samples (**Supplemental Fig. 2**). PCA analysis of the 375 proteins with complete data from every sample failed to identify significant sample outliers or important batch effects (**Supplemental Fig. 2**). Missing values for the 944 proteins with $\leq 50\%$ missingness were imputed using a low rank approximation derived from non-linear iterative partial least squares (NIPALS) PCA¹⁴ (**Supplemental Fig. 2**). All subsequent analyses including regression, WCNA, and CAM were performed on this imputed data set. Exploratory regression analysis of proteins with $> 50\%$ missingness using missingness encoding failed to identify proteins with compelling association with disease and these proteins were subsequently dropped from further consideration. In a similar manner the AA samples revealed 1495 unambiguous proteins including 725 with $\leq 50\%$ missingness and no important batch effects or extreme outliers.

Analysis of Association with Extent of Atherosclerosis or Anatomic Location

Three orthogonal strategies (regression, weighted co-expression analysis, convex analysis of mixtures) were employed to identify proteins individually or jointly associated with extent of disease or anatomic location.

Regression Models: MANOVA models with adjustment for age, sex, and race were used to model the joint distributions of % intimal surface demonstrating fibrous plaque (FP), streaks (FS), and normal (NL) intima as a function of each individual protein. Separately, generalized linear models (GLM) were used to examine the association between individual proteins and %FP or %NL after adjustment for age, sex, and race. In the models of %FP the reference was, by definition, the % intimal surface demonstrating fatty streaks or normal intima. In contrast, in models of %NL the reference was, by definition, the % intimal surface demonstrating fatty streaks or fibrous plaques. Accordingly we developed separate models using each trait (%FP or %NL) as the dependent variable with the expectation that direction of effect would be inversely related depending on the dependent variable used. Proteins with beta coefficients in the same direction for both %FP and %NL were excluded from further consideration. In a similar manner ordinal regression was also used to examine the association between individual proteins and % FP or % NL treated as three level ordinal variables (FP: 0%, 1-59%, \geq 60%; NL: 100%, 99-61%, <60%). Exploratory models using robust GLM with logit link produced qualitatively similar lists of significantly associated proteins (data not shown).

When modeling the association between proteins identified using data-independent acquisition (SWATH) and disease or location we also adjusted for several housekeeping proteins (Proteasome subunit beta type-2, Small nuclear ribonucleoprotein Sm D3, Receptor expression-enhancing protein 5, Ras-related protein Rab-7a) and Myosin-11 (a vascular smooth muscle cell marker protein) to account for possible differences in tissue sample volumes, cellular composition, or protein yields.

Weighted Co-Expression Network Modelling: The WGCNA package in R was used to identify distinct protein modules among the 94 proteins used for analysis ¹⁵. A weighted power adjacency matrix was constructed using signed bi-correlations between proteins and mapping

the results onto the 0-1 interval. The power parameter was selected such that the topological overlap connectivity (k) of the entire network approximated a scale-free topology. The topological overlap was used to create a dissimilarity matrix for hierarchical clustering to identify modules. To assess stability of module assignments, 50 bootstrap samples of the data were created and each one interrogated using identical WCGNA parameters. Once the modules were determined, regression models were developed to examine the association between module eigengenes and the arterial phenotypes (%FP and % NL) after adjustment for age, sex, and race.

Convex Analysis of Mixtures and Protein Expression Differences in Complex Tissues Analysis

Tissue heterogeneity is present in our samples where multiple tissue types are variably mixed and co-exist^{16, 17}, representing a major confounder when studying tissue-specific disease markers¹⁸⁻²⁰. We have recently devised CAM, a fully unsupervised data deconvolution method that exploits the strong parallelism between a latent variable model and the theory of convex sets²¹. With the newly-proven mathematical theorems, we showed that the simplex of mixed expressions is a rotated and compressed version of the simplex of tissue expressions in scatter space²² (**Fig. 3**). The vertices of the scatter simplex, characterized by the molecular markers whose expressions are maximally enriched in a particular tissue, define the optimal data-derived distinctive tissue types present in the heterogeneous samples. CAM has distinct advantages over other competing deconvolution methods (e.g. PCA, ICA, etc) because it can handle protein profiles that are not statistically independent or geometrically orthogonal and which are intrinsically non-negative.

CAM works by geometrically identifying the vertices (and their resident molecular markers) of the scatter simplex of globally measured expressions (**Fig. 3**), i.e., determining the multifaceted simplex that most tightly encloses the mixed expression profiles, and subsequently estimating the proportions and specific expression profiles of constituent subpopulations²² (**Fig. 3**). Tissue samples to be analyzed by CAM contain unknown number and varying proportions of molecularly distinctive (including novel) tissue types. Molecular expression in a specific tissue is

modeled as being linearly proportional to the abundance of that tissue and the number of tissues present is determined by the newly-derived minimum description length (MDL) criterion
22

We first eliminate proteins whose signal intensity (vector norm) is lower than 5% (noise) or higher than 95% (outlier) of the mean value over all proteins. The signals from these proteins are unreliable and could have a negative impact on the subsequent deconvolution. Second, dimension reduction is performed on the raw measurements using principal component analysis with 10 PCs. To further reduce the impact of noise/outlier data points and permit appropriate parameterization of the MDL criterion to determine the number of tissues, we aggregate protein vectors into representative clusters using affinity propagation clustering (APC)^{23-25, 22}. As an initialization-free and near-global-optimum clustering method, APC simultaneously considers all protein vectors as potential exemplars and recursively exchanges real-valued ‘messages’ between protein vectors until a high-quality set of exemplars and corresponding clusters gradually emerge. CAM detected four tissues from LAD simplex (**Fig. 3**) and three tissues from AA simplex (**Supplemental Fig. 10**). On the basis of the expression levels of tissue-specific marker proteins detected by CAM, the relative proportions of constituent tissues are estimated using standardized averaging that are then used to deconvolute the mixed expressions into tissue-specific profiles by non-negative least-square regression techniques²². Upregulated maker proteins associated with specific tissues can be detected by One-Versus-Everyone (OVO) fold change thresholding, e.g., currently set to 2 for FP tissue.

GO Term and Pathway Enrichment Analysis

GO Term and pathway enrichment analyses using GO Term Finder²⁶, and IPA (Ingenuity Pathway Analysis, Ingenuity Systems, Redwood City, CA) tools were used to characterize the evaluable proteins obtained from the arterial samples. For the GO term enrichment analysis, clustering based on semantic similarity was used to indicate which child nodes could be represented by higher level parent nodes²⁷. For the pathway analysis, the significant differentially expressed proteins with |fold change| ≥ 1.7 and the false discovery rate (FDR)

corrected p-value of 0.05 were analyzed with IPA for pathways, upstream regulators, and associated diseases and biological functions. The fold change cut-point of ≥ 1.7 was chosen to yield approximately 100 proteins for further analysis. The following parameters were used for these analyses: 1) Human genes in the Ingenuity Knowledge Base were used as the reference set; 2) Both the direct and indirect relationships were considered; 3) The confidence level was set to be “Experimentally Observed” and “High predicted” with high confidence scores; 4) The following selected tissues/cell types were used: heart, smooth muscle, fibroblasts, cardiomyocytes, endothelial cells, smooth muscle cells, and macrophages. The p-values for the identified canonical pathways, disease associations and functions were calculated using Fisher's exact test. The Benjamini-Hochberg method was used to estimate the false discovery rate, and an FDR-corrected p-value of 0.05 was used to select significantly enriched pathways. The significant upstream regulators were selected using p-value ≤ 0.05 and $|Z\text{-score}| \geq 2$. Similar analyses were also performed using proteins selected purely on the basis of q-value ≤ 0.01 for FP vs NL. (**Supplemental Tables 15 and 19** for data extracts of the IPA analyses.)

Differential Dependent Network Analyses

Modeling biological networks is an important tool in systems biology to study the orchestrated activities of gene products in cells²⁸. Significant rewiring of these networks provides a unique perspective on phenotypic transitions that can occur in biological systems²⁹. Thus, instead of asking “which genes are differentially expressed”, a more interesting question is “which genes are differentially connected?”^{28, 30}. To systematically characterize selectively activated or deactivated regulatory components and mechanisms, the modeling tools must effectively distinguish significant rewiring from random background fluctuations. We have developed an integrated molecular network learning method, within a well-grounded mathematical framework, to construct differential dependency networks with significant rewiring^{23, 31}. This knowledge-fused differential dependency networks (kDDN) method, implemented as a Java Cytoscape app, can be used to optimally integrate prior biological knowledge with measured data to simultaneously construct both common and differential networks^{32, 33}.

kDDN algorithm jointly learns the shared biological network and statistically significant rewiring across different phenotypes. Phenotype-specific data and prior knowledge are quantitatively fused via an extended Lasso model with l_1 regularized convex optimization formulation³². Based on the unique nature of the problem, we derive an efficient closed-form solution for the embedded sub-problem solved by the block-wise coordinate descent (BCD) algorithm. Since existing knowledge is often nonspecific or imperfect, kDDN uses a “minimax” strategy to maximize the benefit of prior knowledge while confining its negative impact under the worst-case scenario. Furthermore, kDDN matches the values of model parameters to the expected false positive rates on network edges at a specified significance level, and assesses edge-specific p-values on each of the differential connections³².

We use kDDN to construct the network and detect significant network rewiring between FP and NL groups, where an extended Lasso-based sparse Gaussian graphic model is used to capture the network structure. The network rewiring under different phenotypes is inferred jointly by performing the BCD algorithms sequentially for all nodes. We then used permutation-based significance test to estimate p-values of the detected differential dependence edges^{31, 32}.

Those detected differential dependence edges with p-values larger than 0.05 were filtered out for control of false positive rate. We used different colors to distinguish differential dependency edges under each phenotype, and use solid/dashed lines to indicate positive/negative dependences between nodes. The linewidths of edges correspond to the dependency strength to give a straightforward illustration and a better comparison within the network.

Multiple Reaction Monitoring Assay Design

The 38 proteins identified by DDA-MS analysis to be most highly associated with fibrous plaques were selected as candidate circulating biomarker proteins. A peptide assay library was assembled for these proteins using the DDA-MS search results and the open-source Skyline MS-data analysis software³⁴ (**Supplemental Figure 13**). To streamline peptide selection for MRM-assay design, the top 6 fragment mass-to-charge values from library peptides identified from these 38 candidate proteins were extracted against an existing Data Independent

Acquisition file derived from normal, control human plasma. The top three to four performing peptides from each protein identified by this initial screen were included for downstream MRM-method building. Five proteins (DRB1, LCP1, RNASE1, MTHFD1, and CALU) were excluded at this step for absence of any detectable peptides in the reference plasma sample. Unscheduled MRM methods were developed for peptides from the remaining 33 proteins and pools of the processed CAD and Control plasma (described below) were injected and acquired against these methods for data refinement. A final scheduled, multiplexed MRM method against 323 fragments from 86 peptides of 33 putative FP marker proteins was optimized using the Skyline software, and included the addition of stable isotope labeled ‘heavy’ reference peptides (SIS peptides) in a subset of 7 proteins (C1R, APOE, APOB, VTNC, CO5, IGHM, ITIH1).

Scheduled MRM-MS Data Acquisition

The multiplexed method, described above, was acquired on a SCIEX QTRAP6500 using multiple reaction monitoring (MRM) scanning in positive mode (Framingham, MA). Ion spray voltage was set to 5500 and source temperature set to 500 °C. Curtain gas was set at 35 to reduce contamination and Source Gases 1 and 2 were set to 60 and 70, respectively. 9 ug of digested samples was placed onto a Waters XBridge Peptide BEH C18 130Å, 3.5 µm, 2.1mm x 100mm column (Waters, Milford, Massachusetts). Mobile phase A was 0.1% formic acid, 2% acetonitrile, and 98% water, while mobile phase B was 0.1% formic acid, 5% water, and 95% acetonitrile. The sample was eluted over a 20-minute gradient moving from 1% to 35% mobile phase B. Retention times for MRM scheduling were gathered by first running subsets of the selected transitions to determine retention time. Afterwards, all transitions were combined into a single scheduled method using the previously determined retention times.

MRM Data Processing

Raw files were analyzed in the Skyline software and peaks were manually investigated for quality, with care taken to ensure that retention times were well aligned across replicates, all monitored fragments co-eluted, and peptide peak areas could be easily discerned from

chemical noise and were free from interference. Manual filtering eliminated an additional eight proteins from further analysis due to low or undetectable signal-to-noise ratios (CATB, TSP1, NNMT, S100A9, ITIH2, POSTN, CORO1A, and HTRA). The final 25 candidate proteins were processed to generate protein-level abundance data from endogenous peptides as follows: (1) raw signals for both the heavy SIS and endogenous targets were analyzed across each of the 10 pooled replicates; (2) Normalization of each analyte in a given specimen to the median signal from the SIS-peptides in that specimen was performed to address signal drift across the acquisition block; (3) the coefficient of variation for endogenous peptide fragments across the 10 pool samples was calculated, and fragments were filtered to include only those with <20% CV (after normalization) were used for downstream analysis, with the exception of fragments from BCAM, BGH3, and CATZ which had no fragments <20% (but all fragments were still less than 40%) so all fragments from these proteins were still included; (4) the correlation matrices for all quantified peptides / fragments of a given protein were manually inspected and fragments / peptides with low correlation to the rest of the observations for a given protein were excluded; (5) the final normalized, filtered fragment-level intensities were averaged to yield protein level abundance for each specimen. For the seven proteins with corresponding SIS-peptides, the ratio of endogenous-to-heavy signal area was calculated per specimen and the same %CV filtering and correlation analysis from pooled replicates was performed on this ratio data, with all fragments meeting the filter criteria for inclusion. For a given protein, all ratio observations were averaged to yield protein level ratio abundances. As a validation index for the endogenous-quantitation workflow, the correlation between the SIS-based and endogenous quantitative pipeline was analyzed for the seven proteins with available SIS-peptides.

Validation of Candidate Plasma Fibrous Plaque Biomarkers

Initially, an adaptive elastic net model ($\alpha=0.9$)³⁵⁻³⁷ optimized by leave-one-out validation was used to select among the 25 candidate biomarkers for prediction of case status. Bias-corrected bootstrap sampling (n=10,000) was used to evaluate overall performance of the optimized

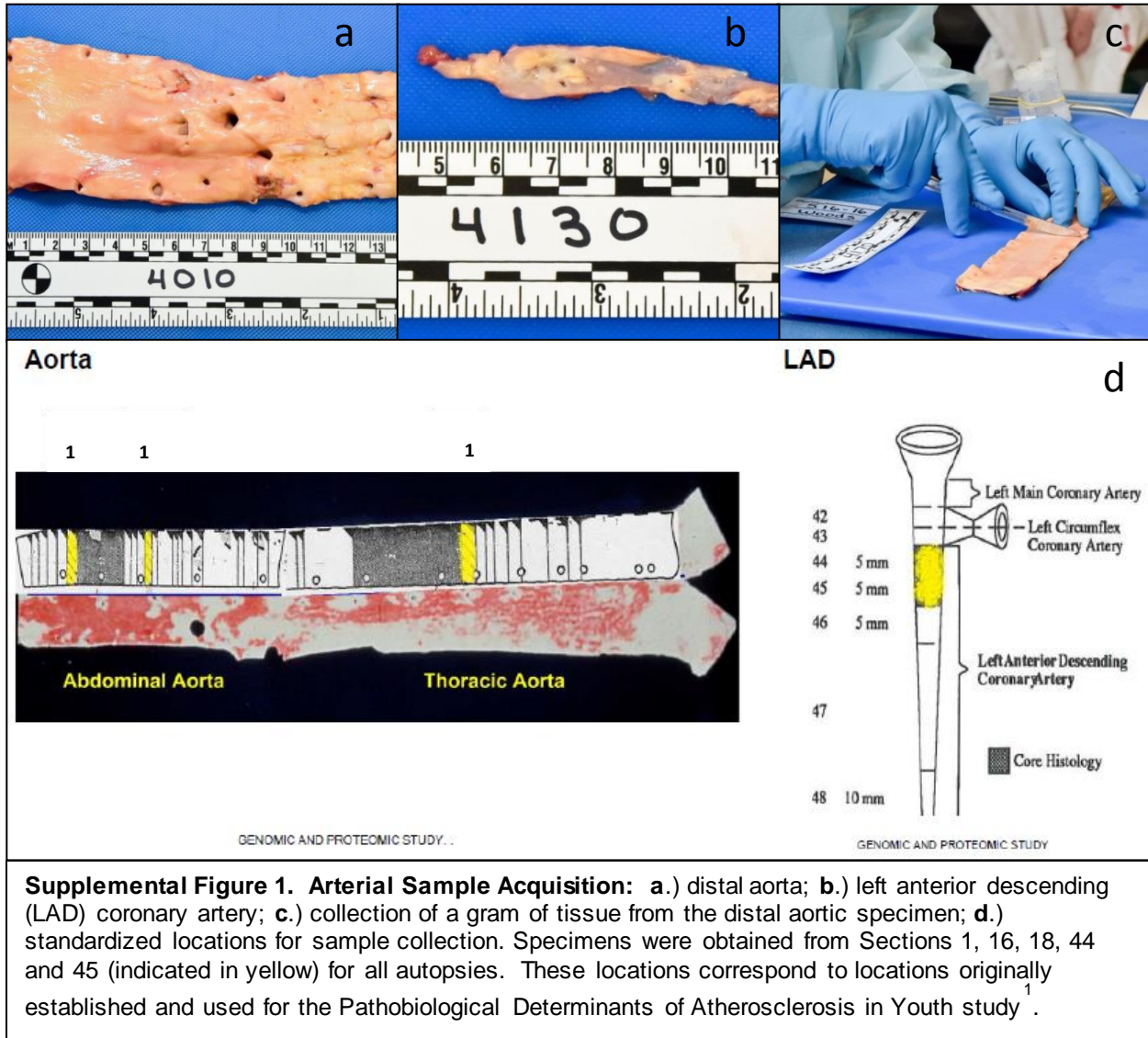
model based on median (95% CI) AUC from the bootstrap samples³⁸. Qualitatively similar models were obtained when the elastic net model was optimized using K-fold (K=5) cross-validation or by minimizing AICc (data not shown).

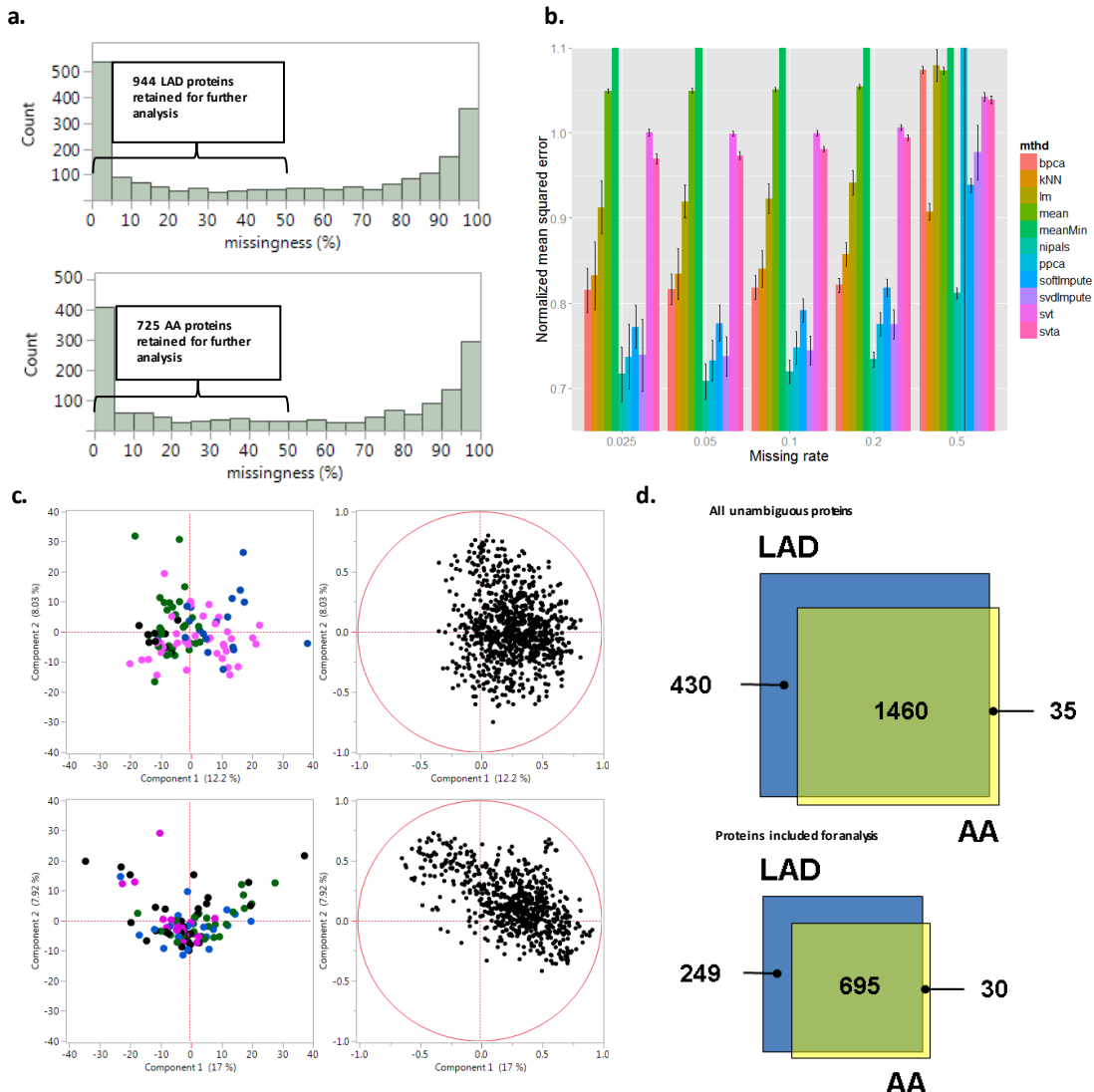
Proteomic Architecture of Human Coronary and Aortic Atherosclerosis

Online Supplemental Figures

Table of Contents

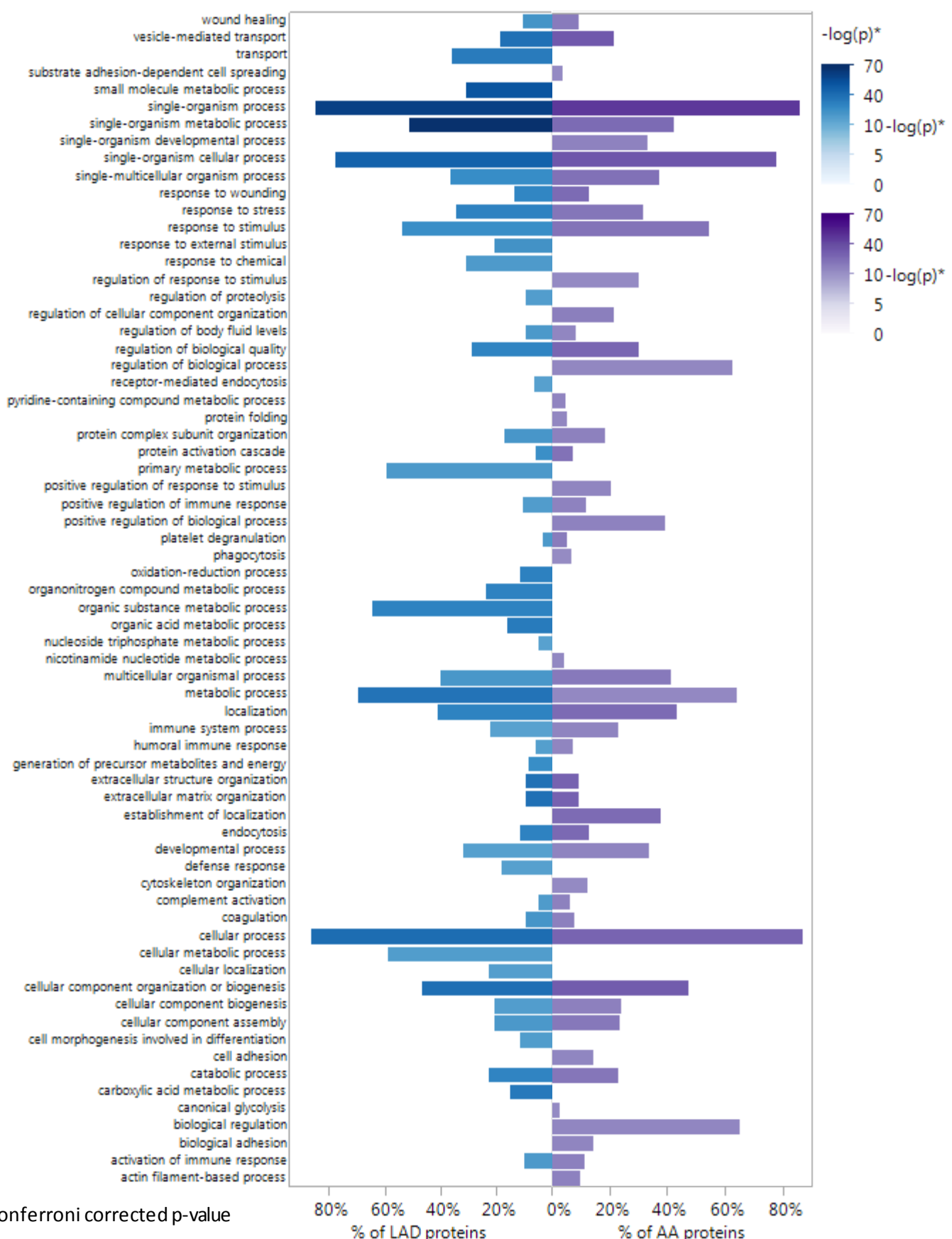
Supplemental Figure 1	Arterial Sample Acquisition
Supplemental Figure 2	Data Missingness, Imputation, Batch Effects and Anatomic Overlap
Supplemental Figure 3	Enriched GO: Biological Process Terms From Human LAD and AA Proteins
Supplemental Figure 4	Enriched GO: Molecular Function Terms From Human LAD and AA Proteins
Supplemental Figure 5	Enriched GO: Cellular Component Terms From Human LAD and AA Proteins
Supplemental Figure 6	Weighted Co-Expression Network Analysis of Human Abdominal Aortic (AA) Proteins
Supplemental Figure 7	Number of Identifiable Proteins from Human LAD and AA Arterial Samples
Supplemental Figure 8	Comparison of Extra Cellular Matrix Proteins in Normal LAD and AA Samples
Supplemental Figure 9	Elastic Net Modelling of Proteins Predicting Presence or Absence of Fibrous Plaque in LAD (N=99) Samples
Supplemental Figure 10	Convex Analysis of Mixtures (CAM) of AA Protein Data
Supplemental Figure 11	Convex Analysis of Mixtures (CAM) Identified Upregulated Fibrous Plaque Marker Proteins for LAD (n=99) and AA (n=99) Samples
Supplemental Figure 12	Comparison of Extracellular Matrix Proteins in FP vs NL Samples in LAD and AA Samples
Supplemental Figure 13	Design and Quality Control Analysis of Tissue-Derived Circulating Fibrous Plaque Marker Panel





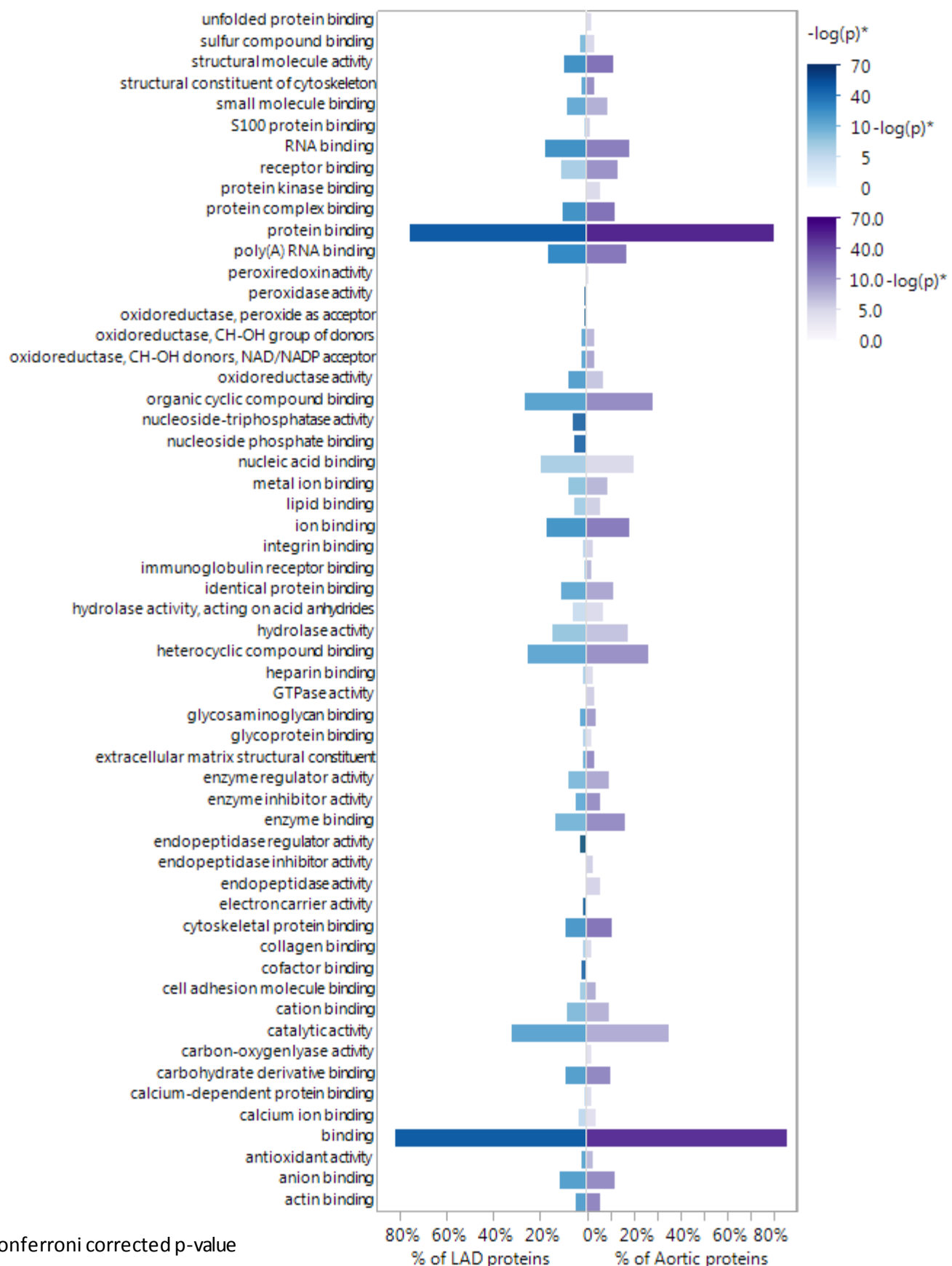
Supplemental Figure 2. Data Missingness, Imputation, Batch Effects and Anatomic Overlap. a.) Distribution of missingness for the LAD and AA data. The most common value for missingness was 0% in both the LAD and AA. However, there was a range of missingness including some unambiguously identified protein groups that were only present in a minority of samples. Missingness encoded models did not identify any proteins with >50% missingness that were significantly associated with disease status. b.) Using proteins with complete data (0% missingness) data sets simulating various rates (2.5%-50.0%), and types (random, inversely proportional with mean signal intensity) of missingness were used to test 11 different matrix completion methods. Based on the low normalized mean squared error, the NPIALS method was selected for imputation. c.) PCA analysis with color encoding for different protein extraction batches did not identify important batch effects or extreme outliers. d.) Proportional Venn diagrams indicating the overlap in identified and analyzed proteins in the LAD and AA territories.

Supplemental Figure 3. Enriched GO: Biological Process Terms from Human LAD and AA Proteins GO enrichment analysis was performed using 944 LAD proteins (left half of the plot – blue) and 725 AA proteins (right half of the plot – purple) that were included for subsequent analysis. GO terms with Bonferroni adjusted p-value <0.05 in either anatomic territory are presented.



Supplemental Figure 4. Enriched GO: Molecular Function Terms from Human LAD and AA Proteins

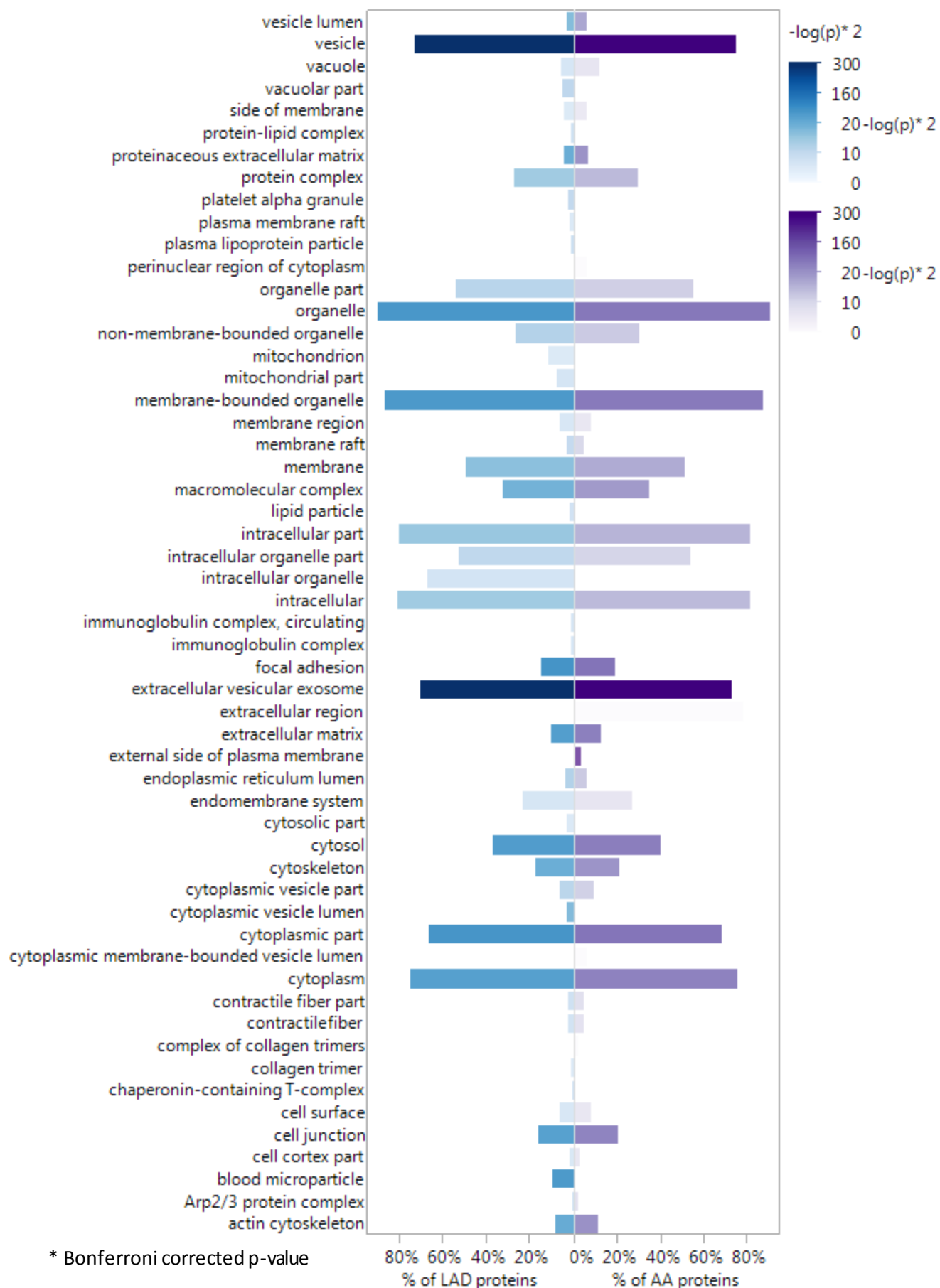
GO term enrichment analysis was performed using 944 LAD proteins (left half of the plot – blue) and 725 AA proteins (right half of the plot – purple) that were included for subsequent analysis. GO terms with Bonferroni adjusted p-value <0.05 in either anatomic territory are presented.



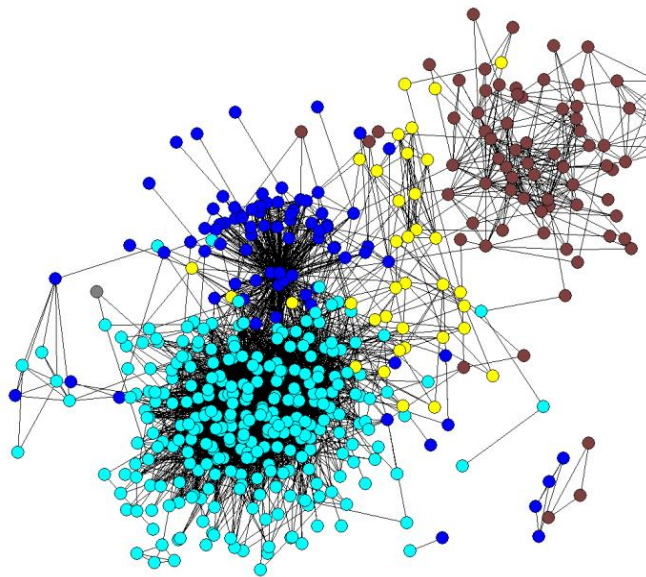
* Bonferroni corrected p-value

Supplemental Figure 5. Enriched GO: Cellular Component Terms from Human LAD and AA Proteins

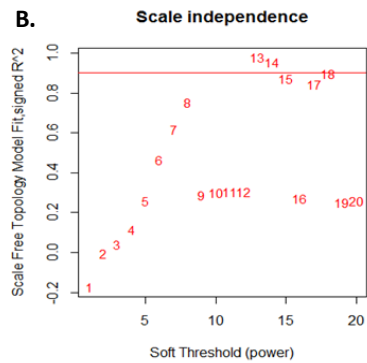
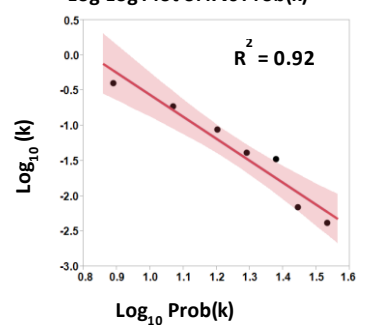
GO term enrichment analysis was performed using 944 LAD proteins (left half of the plot – blue) and 725 AA proteins (right half of the plot – purple) that were included for subsequent analysis. GO terms with Bonferroni adjusted p-value <0.05 in either anatomic territory are presented.



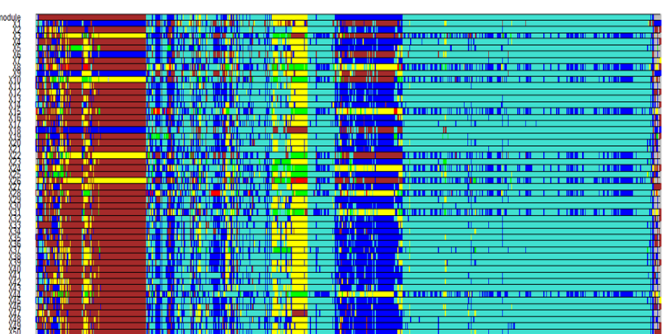
A.



B.

**Log-Log Plot of k vs Prob(k)**

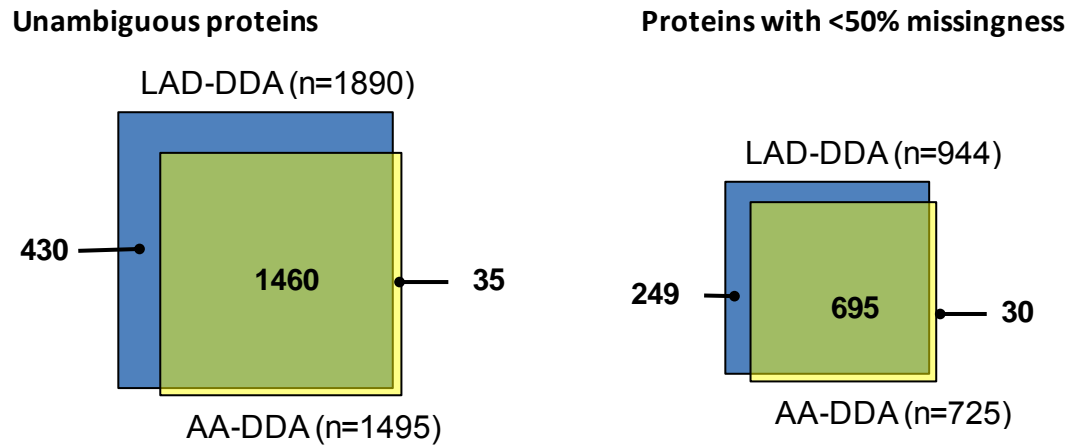
C.



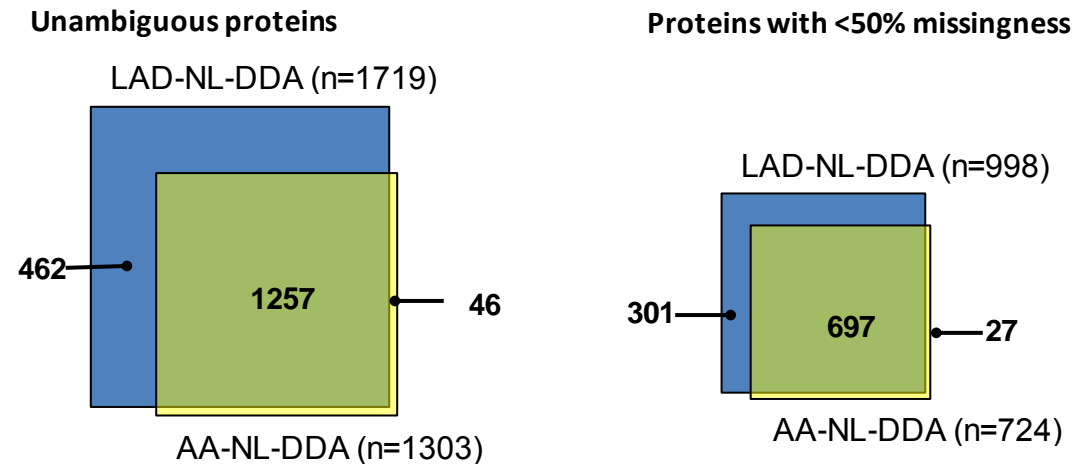
Supplemental Figure 6. Weighted Co-Expression Network Analysis of Human Abdominal Aortic (AA) Proteins
 A. Adjacency map of AA proteins color coded by module assignment based on hierarchical clustering of the topological overlap matrix (TOM)-based dissimilarity measure. For clarity of presentation only nodes (proteins) with at least one edge (adjacency measure (k)) > 98%tile are shown. B. Left panel shows that scale-free topology is well approximated when the adjacency power parameter $\beta= 8$. Right panel shows the log-log plot of adjacency (k) vs prob(k) with $\beta= 8$, supporting a power-law relationship in the connectivity of the expressed proteins. C. Module assignment for fifty 90% random samples of the data illustrating the overall stability of the modular structure of the protein expression patterns. Colors are assigned according cluster size which may vary with each random sample. As a result actual color assignment may vary from run to run, but module membership remains relatively stable.

Supplemental Figure 7. Number of Identifiable Proteins From Human LAD and AA Arterial Samples. a. All samples (n=99 samples from each territory). Left Venn diagram: proteins detected at least once in any sample according to anatomic territory; Right Venn diagram: proteins detected in >50% of the samples. GO term analysis of the LAD only proteins indicated significant enrichment of mitochondrial proteins (p-values: unambiguous proteins = 1.8e-28; proteins with <50% missingness = 1.7e-6) b. Normal samples only (n=30 from each territory). Left Venn diagram: proteins detected at least once in any sample according to anatomic territory; Right Venn diagram: proteins detected in >50% of the samples. GO term analysis of the LAD only proteins indicated significant enrichment of mitochondrial proteins (p-values: unambiguous proteins = 1.0e-13; proteins with <50% missingness p-value = 1.9e-12)

a. All Samples (LAD: n=99; AA: n=99)

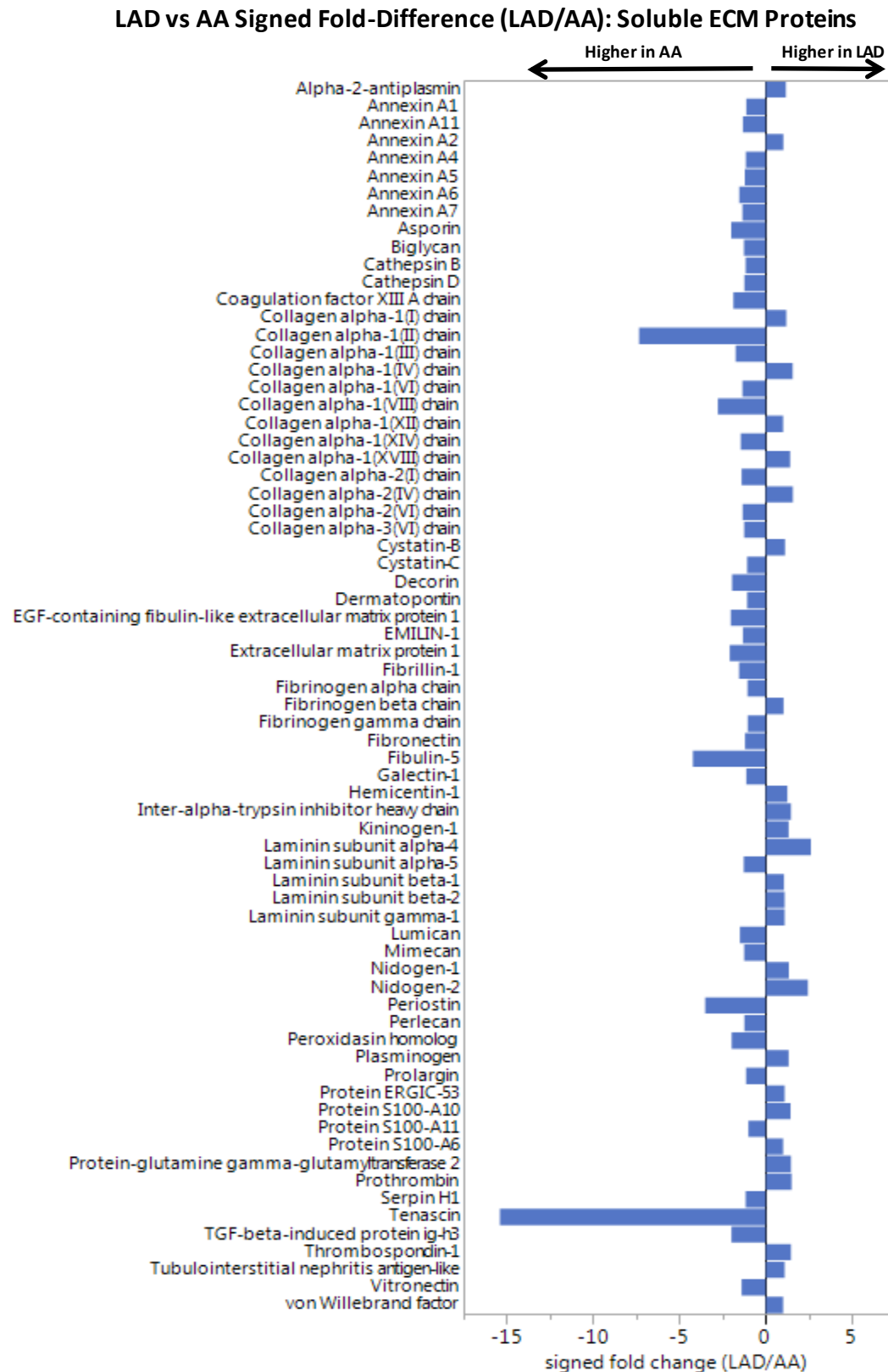


b. Normal Samples only (LAD: n=30; AA: n=30)



Supplemental Figure 8. Comparison of Extra Cellular Matrix Proteins in Normal LAD and AA

Samples. Data independent MS (SWATH) analysis of completely normal LAD and AA samples (n=15 from each anatomic location) with adjustment for age, sex, MYH11, RABA7A, TERA, G6PI. Mean fold-difference = 6% (AA>LAD), p= 0.01.

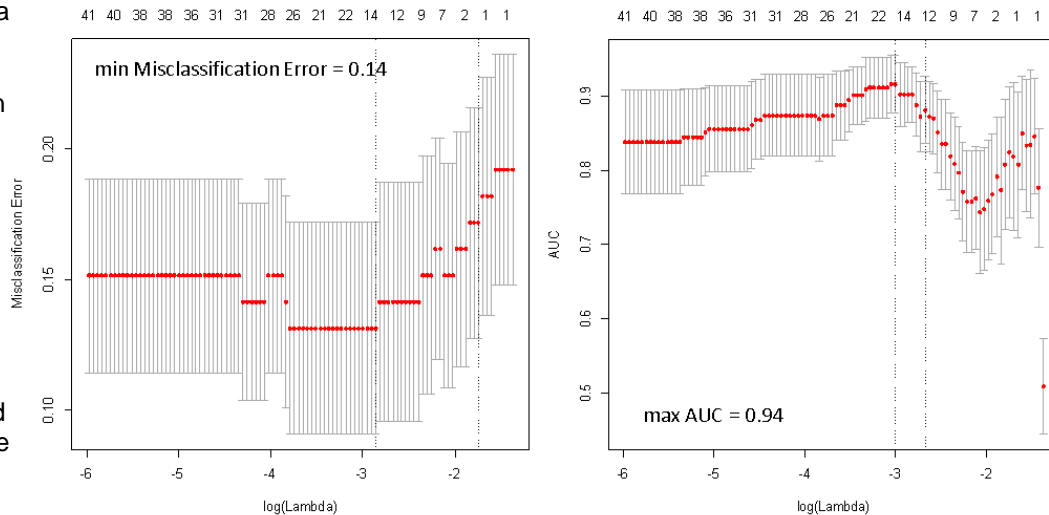


Supplemental Figure 9. Elastic Net Modelling of Proteins Predicting Presence or Absence of Fibrous Plaque in LAD (N=99) Samples. Graphs: Misclassification (left graph) and AUC (right graph) across a range of lambdas for two typical elastic net models predicting presence of fibrous plaque. Red points indicate the mean and bars indicate the SE for the estimate of misclassification or AUC across 10-folds in a cross-fold validation scheme. Numbers across the top indicate the number of variables (proteins) remaining in the model as the model progresses from the most inclusive (left) to the most parsimonious (right). **Table:** Models were developed using cross-fold validation to select the lambdas optimizing AUC or misclassification. To minimize the effect of chance in selecting folds for the cross-fold validation each model was run 100 times and the selected proteins and their respective beta coefficients were recorded. The table indicates the number of times each protein was selected in each of 100 models and the mean beta

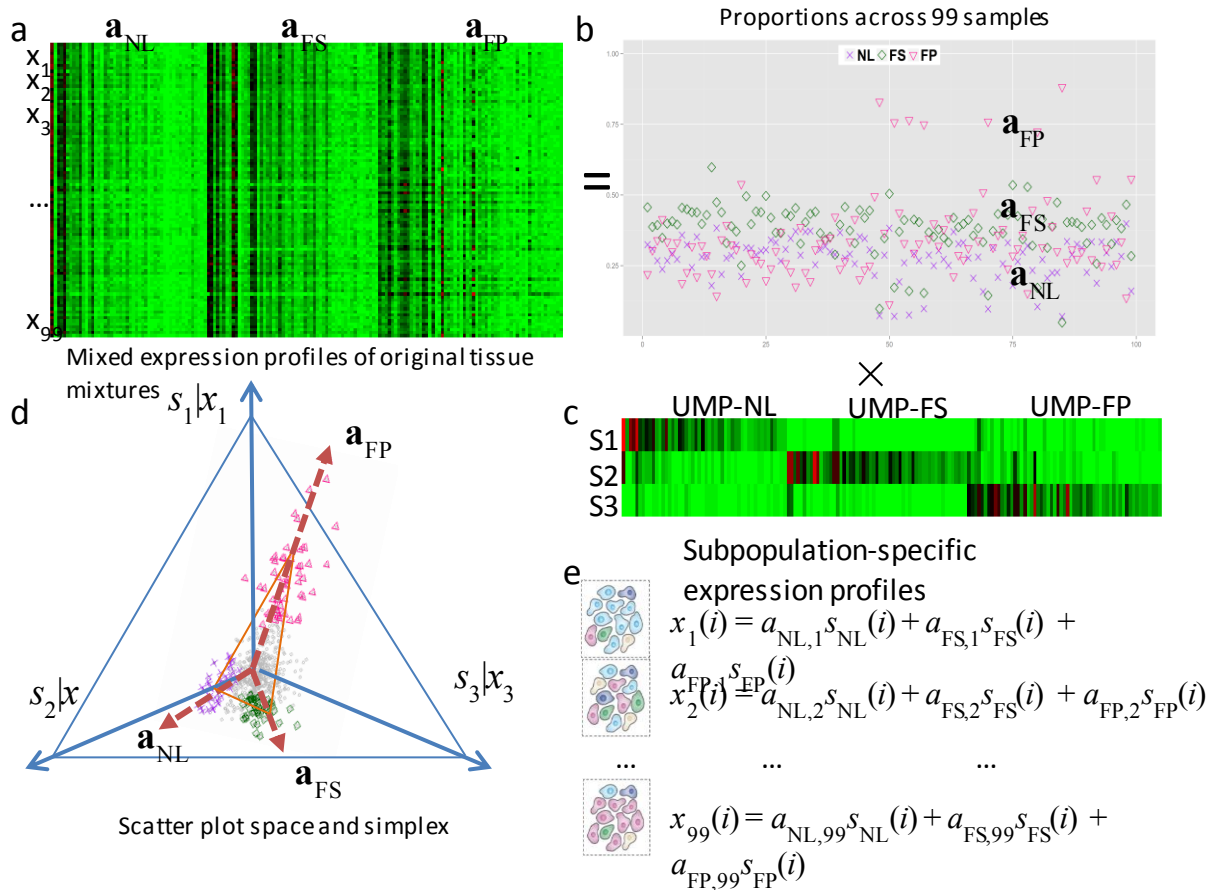
for the subset of models where the protein in question was included.

Proteins included in 10 or more models are indicated by bold in the # of models

columns. Several highly correlated proteins competed for entry into these models.



Uniprot ID	Protein	Gene	Maximizing AUC		Minimizing Misclassification	
			# of models	mean beta	# of models	mean beta
P24821	Tenascin	TNC	98	0.2186	99	0.4057
O43852	Calumenin	CALU	39	1.2896	76	0.3454
Q8NBX0	Saccharopine dehydrogenase-like oxidoreductase	SCCPDH	39	0.9419	46	0.5198
O43866	CD5 antigen-like	CD5L	39	0.8716	69	0.2865
O14773	Tripeptidyl-peptidase 1	TPP1	39	0.7078	76	0.1898
Q15063	Periostin	POSTN	39	0.5949	93	0.1174
P07602	Prosaposin	PSAP	39	0.4851	48	0.2585
HLA-H						
P13760	HLA class II histocompatibility antigen, DRB1-4 beta chain	DRB1	39	0.4804	99	0.1096
Q9UBR2	Cathepsin Z	CTSZ	39	0.2781	85	0.1031
Q6NZI2	Polymerase I and transcript release factor	PTRF	39	0.9566	46	0.5423
P07998	Ribonuclease pancreatic	RNASE1	38	0.0979	23	0.1233
P09543	2',3'-cyclic-nucleotide 3'-phosphodiesterase	CNP	38	0.2526	26	0.2877
Q03135	Caveolin-1	CAV1	38	0.2749	45	0.1503
P07858	Cathepsin B	CTSB	32	0.0764	95	0.0270
P04114	Apolipoprotein B-100	APOB	21	0.3371	11	0.5460
Q16853	Membrane primary amine oxidase	AOC3	19	0.0698	10	0.0813
P40261	Nicotinamide N-methyltransferase	NNMT	17	0.4705	8	0.9733
Q13200	26S proteasome non-ATPase regulatory subunit 2	PSMD2	15	0.6538	6	1.8703
P11586	C-1-tetrahydrofolate synthase, cytoplasmic	MTHFD1	13	0.1454	3	1.2007
P50395	Rab GDP dissociation inhibitor beta	GDI2	8	0.6810	3	2.5022
P63241	Eukaryotic translation initiation factor 5A-1	EIF5A	8	0.7468	3	3.2132
P08237	ATP-dependent 6-phosphofructokinase, muscle type	PFKM	7	0.5024	3	1.7951
Q06828	Fibromodulin	FMOD	7	2.3252	3	7.3673
P09960	Leukotriene A-4 hydrolase	LTA4H	6	0.9809	3	2.6087
Dolichyl-diphosphooligosaccharide--protein glycosyltransferase						
P04844	subunit 2	RPN2	2	3.3432	1	14.323
P34932	Heat shock 70 kDa protein 4	HSPA4	2	5.1045	1	20.526
P49908	Selenoprotein P	SEPP1	2	5.0315	1	17.382
P52209	6-phosphogluconate dehydrogenase, decarboxylating	PGD	2	3.5218	1	10.090
P84157	Matrix-remodeling-associated protein 7	MXRA7	2	4.9994	1	19.504
O95834	Echinoderm microtubule-associated protein-like 2	EML2	1	2.4512	1	3.3472
P14174	Macrophage migration inhibitory factor	MIF	1	2.0485	1	3.4632
P21926	CD9 antigen	CD9	1	0.8408	1	1.0123
P28482	Mitogen-activated protein kinase 1	MAPK1	1	3.6737	1	4.5044
P43652	Afamin	AFM	1	2.9634	1	3.4717

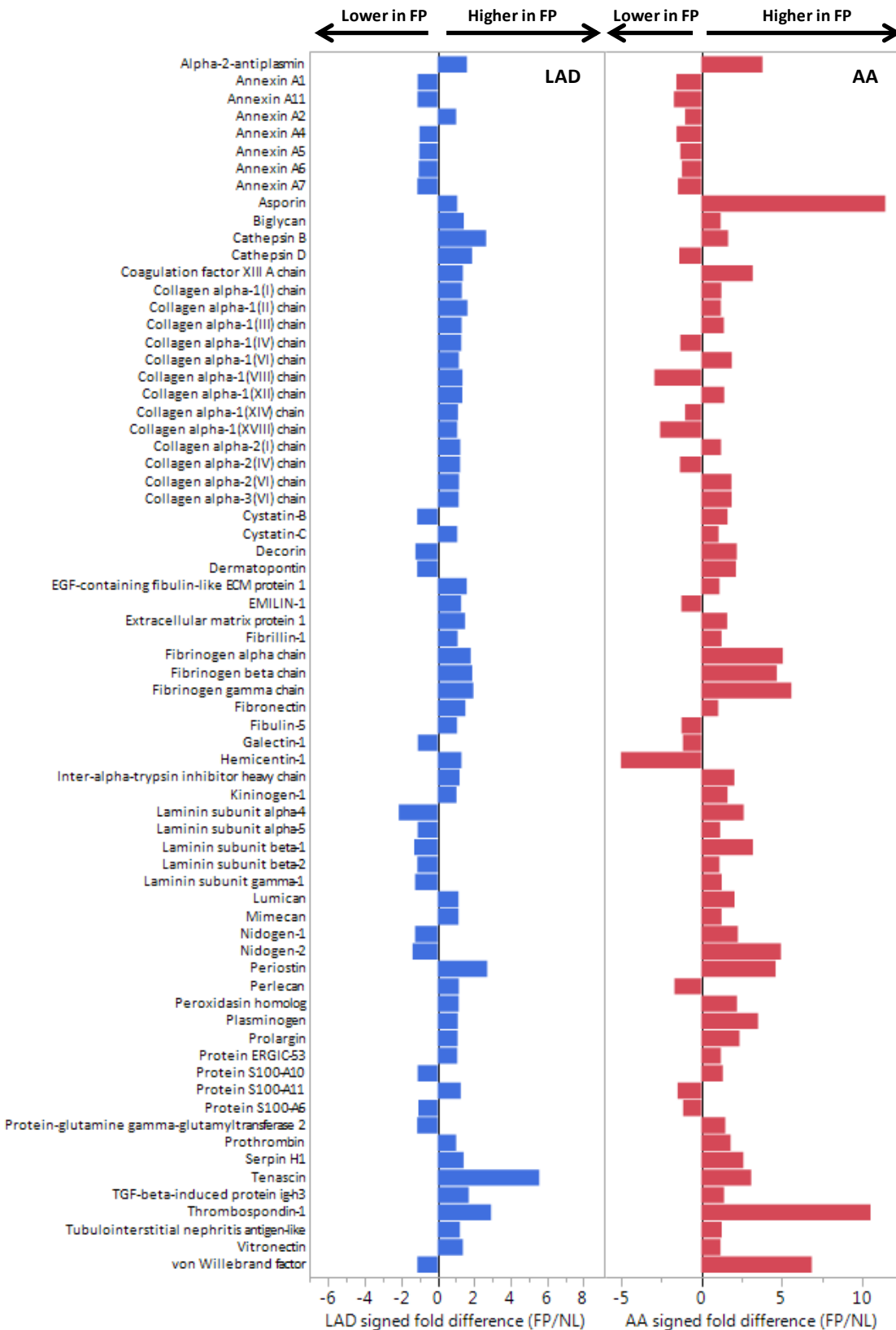


Supplemental Figure 10 Convex Analysis of Mixtures of AA Protein Data. a. Heatmap of mixed expressions of upregulated marker proteins (UMP) in 99 AA samples. b. Estimated proportions of NL, FS, and FP across 99 AA samples. Note: The AA data only supported identification of three vertices compared with four vertices in the LAD data. c. Heatmap of subpopulation-specific expressions of upregulated marker proteins. d. Geometry of the mixing operation in scatter space that produces a compressed and rotated scatter simplex whose vertices host subpopulation-specific upregulated marker proteins and correspond to mixing proportions. e. Mathematical description on the protein expression readout of multiple distinct subpopulations.

Supplemental Figure 11. Convex Analysis of Mixtures (CAM) Identified Upregulated Fibrous Plaque Marker Proteins for LAD (n=99) and AA (n=99) Samples.

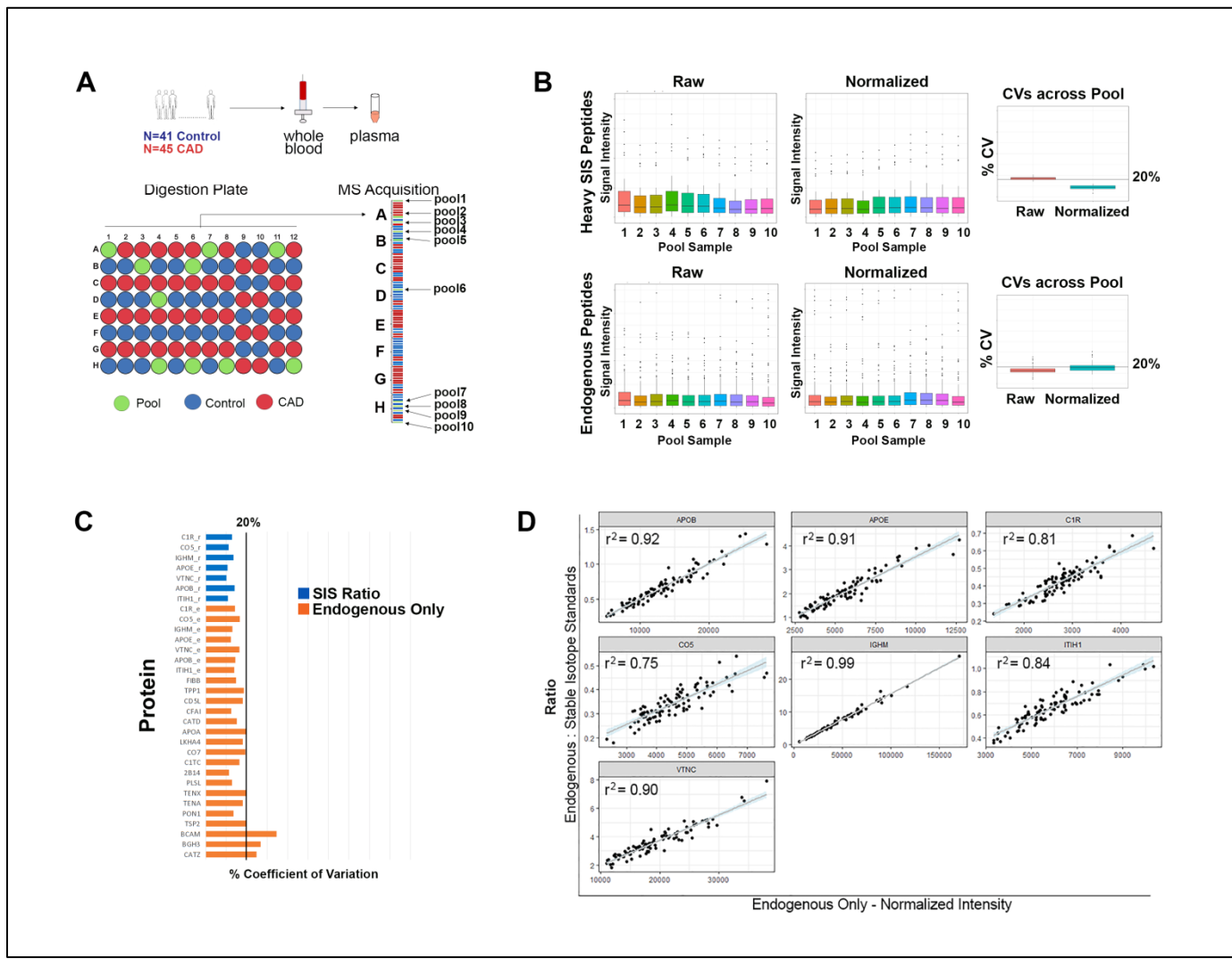
LAD CAM Fibrous Plaque Marker Proteins

19 (24%)		29 (37%)		30 (38%)				
AA CAM Fibrous Plaque Marker Proteins								
UniprotID	LAD Only Protein	Gene	UniprotID	LAD and AA Protein	Gene	UniprotID	AA Only Protein	Gene
Q8IUX7	Adipocyte enhancer-binding protein 1	AEBP1	P04114	Apolipoprotein B-100		APOB	P01023	Alpha-2-macroglobulin
P01024	Complement C3	C3	P02649	Apolipoprotein E		APOE	P02765	Alpha-2-HS-glycoprotein
P07358	Complement component C8 beta chain	C8B	Q14791	Apolipoprotein L1		APOL1	P05090	Apolipoprotein D
P07360	Complement component C8 gamma chain	C8G	P00736	Complement C1r subcomponent		C1R	P0COL5	Complement C4-B
Q99715	Collagen alpha-1(XII) chain COL12A1	P04003		C4b-binding protein alpha chain		C4BPA	P00751	Complement factor B
Q9UBR2	Cathepsin Z	CTSZ	P01031	Complement C5		C5	Q9BXR6	Complement factor H-related protein 5
P02751	Fibronectin	FN1	P10643	Complement component C7		C7	P00450	Ceruloplasmin
P13760	HLA class II HCAg, DRB1-4 beta chain	HLA-DRB1	P40121	Macrophage-capping protein		CAPG	P59665	Neutrophil defensin 1
Q92743	Serine protease HTRA1	HTRA1	Q43866	CD5 antigen-like		CD5L	P00488	Coagulation factor XIII A chain
P35858	IGF-binding protein complex acid labile subunit	IGFALS	P08603	Complement factor H		CFH	P00734	Prothrombin
P05783	Keratin, type I cytoskeletal 18	KRT18	P05156	Complement factor I		CR	P02671	Fibrinogen alpha chain
P08519	Apolipoprotein(a)	LPA	P31146	Coronin-1A		CORO1A	P02794	Ferritin heavy chain
P01620	Ig kappa chain V-III region SIE	none	P07858	Cathepsin B		CTS B	P02792	Ferritin light chain
Q15063	Periostin	POSTN	P07339	Cathepsin D		CTS D	P69905	Hemoglobin subunit alpha
P34096	Ribonuclease 4	RNASE4	P02675	Fibrinogen beta chain		FGB	P69891	Hemoglobin subunit gamma-1
P06702	Protein S100-A9	S100A9	P02679	Fibrinogen gamma chain		FGG	P01892	HLA class I HCAg, A-2 alpha chain
Q15582	TGFβ-induced protein ig-h3	TGFBI	P01871	Ig mu chain Cregion		IGHM	P00738	Haptoglobin
P07996	Thrombospondin-1	THBS1	P19827	Inter-alpha-trypsin inhibitor heavy chain H1		ITIH1	P00739	Haptoglobin-related protein
P04004	Vitronectin	VTN	P19823	Inter-alpha-trypsin inhibitor heavy chain H2		ITIH2	P04196	Histidine-rich glycoprotein
			P18428	Lipopolysaccharide-binding protein		LBP	P01877	Ig alpha-2 chain Cregion
			P13796	Plastin-2		LCP1	P06312	Ig kappa chain V-IV region (Fragment)
			P61626	Lysozyme C		LYZ	Q14624	Inter-alpha-trypsin inhibitor heavy chain H4
			P40261	Nicotinamide N-methyltransferase		NNMT	P01042	Kininogen-1
			Q96PD5	N-acetylmuramoyl-L-alanine amidase		PGLYRP2	P20700	Lamin-B1
			P27169	Serum paraoxonase/arylesterase 1		PON1	P01594	Ig kappa chain V-I region AU
			P05546	Heparin cofactor 2		SERPIN D1	P52209	6-phosphogluconate dehydrogenase, decarboxylating
			P02730	Band 3 anion transport protein		SLC4A1	P00747	Plasminogen
			P35442	Thrombospondin-2		THBS2	P20742	Pregnancy zone protein
			P24821	Tenascin		TNC	P05155	Plasmaprotease C1 inhibitor
							P04179	Superoxide dismutase [Mn], mitochondrial
								SOD2



Supplemental Figure 12. Comparison of Extracellular Matrix Proteins in FP vs NL Samples in LAD and AA Samples

Data independent acquisition (SWATH) analysis was used to compare a targeted set of mitochondrial proteins in LAD (FP n=15; NL n=30) and AA (FP n=9; NL n=18) samples after adjustment for age, sex, MYH11, RABA7A, TERA, G6PI. Histogram bars indicate relative difference between FP and NL samples in each anatomic location. LAD Mean FP/NL = 1.25, MANOVA p-value = 0.02; AA Mean FP/NL = 1.78, p-value = 0.017



Supplemental Figure 13. Design and Quality Control Analysis of Tissue-Derived Circulating Fibrous Plaque Marker Panel. (A) Plasma samples were processed from whole blood samples of female donors with established coronary artery disease (CAD, N=45) or apparently healthy controls (Control, N=41). An additional sample of normal control pooled plasma (Pool, N=10) was used in technical replicates to monitor workflow precision. Samples were randomized and acquired against an optimized multiplexed scheduled MRM assay to quantify the relative abundance of 33 candidate FP markers in human plasma. (B) Data quality monitoring of signal intensity for each fragment monitored across the 10 pool plasma technical replicates indicated a slight downward drift in signal intensity for both spiked stable isotope standard (SIS) peptides (upper left boxplot) and endogenous peptides (lower left boxplot) from the beginning to the end of acquisition, this drift was mitigated by normalizing all raw signals by the median intensity of all SIS peptides from a given injection (middle boxplots). This normalization maintained an appropriately low coefficient of variation (%CV) across pooled replicates (right most boxplots). (C) Final data processing strategy resulted in a final panel of 25 quantifiable plasma proteins as fibrous plaque biomarker candidates. As expected, proteins quantified by SIS ratios (dark blue bars) had slightly lower %CV than when the same proteins were quantified by the endogenous peptide workflow (orange bars), although nearly all proteins demonstrated excellent % CV in the pooled replicates. (D) As additional validation of the endogenous quantification workflow, overall correlations between SIS-quantified and endogenously-quantified proteins were very strong.

Proteomic Architecture of Human Coronary and Aortic Atherosclerosis

Online Supplemental Tables

Table of Contents

Supplemental Table 1	Human Arterial Proteins from Left Anterior Descending (LAD) Coronary Artery (N=99) and Distal Abdominal Aortic (AA) (N=99) Samples
Supplemental Table 2	Human LAD Protein GO Terms: Biologic Processes (top 100 GO Terms)
Supplemental Table 3	Human LAD Protein GO Terms: Molecular Functions (adj. p-value < 0.05*)
Supplemental Table 4	Human LAD Protein GO Terms: Cellular Component (adj. p-value < 0.05*)
Supplemental Table 5	Human Distal Aortic Protein GO Terms: Biologic Process (top 100 GO Terms)
Supplemental Table 6	Human Distal Aortic Protein GO Terms: Molecular Function (adj. p-value < 0.05*)
Supplemental Table 7	Human Distal Aortic Protein GO Terms: Cellular Component (adj. p-value < 0.05*)
Supplemental Table 8	Enriched Ingenuity Canonical Pathways among 944 Human LAD Proteins (FDR<0.001)
Supplemental Table 9	Enriched Ingenuity Canonical Pathways among 725 Human Distal Aortic Proteins (FDR<0.001)
Supplemental Table 10	Regression Models of Association between Individual Proteins and Extent of Surface Area Involved with Fibrous Plaque (FP) or Normal Intima (NML) in Human LAD Arterial Samples (top 100 proteins)
Supplemental Table 11	Regression Models of Association between Individual Proteins and Extent of Surface Area Involved with Fibrous Plaque (FP) or Normal (NML) in Human Abdominal Aorta Samples (top 100 proteins)
Supplemental Table 12	Up-Regulated Proteins in LAD Fibrous Plaque Samples (n=15) Compared with Normal LAD Samples (n=30)
Supplemental Table 13	Down-Regulated Proteins in LAD Fibrous Plaque Samples (n=15) Compared with Normal LAD Samples (n=30)

Supplemental Table 14	Predicted Upstream Master Regulators for Up- and Down-Regulated Fibrous Plaque Proteins
Supplemental Table 15	IPA Output for Analysis of Fibrous Plaque vs NL Marker Proteins with q-value ≤ 0.05 and fold change ≥ 1.7
Supplemental Table 16	Up-Regulated Proteins in Fibrous Plaque Enriched AA Samples (n=7) Compared with Normal AA Samples (n=15)
Supplemental Table 17	Down-Regulated Proteins in Fibrous Plaque Enriched AA Samples (n=7) Compared with Normal AA Samples (n=15)
Supplemental Table 17	Overlap of Patho-Proteomic Fibrous Plaque Proteins in Human LAD (n=99) and AA (n=99) Samples
Supplemental Table 19	IPA Output for Analysis of Fibrous Plaque vs NL Marker Proteins with q-value ≤ 0.01

Supplemental Table 1. Human Arterial Proteins from Left Anterior Descending (LAD) Coronary Artery (N=99) and Distal Abdominal Aortic (AA) (N=99) Samples

<see separate excel spreadsheet>

Supplemental Table 2 Human LAD Protein GO Terms: Biologic Processes (top 100 GO Terms)

GO Term ID	Description	# of proteins	log(p-value)*
GO:0044710	single-organism metabolic process	490	-69.46
GO:0044699	single-organism process	807	-62.11
GO:0044281	small molecule metabolic process	293	-53.18
GO:0044763	single-organism cellular process	737	-47.07
GO:0009987	cellular process	821	-41.91
GO:0071840	cellular component organization or biogenesis	445	-40.94
GO:0016192	vesicle-mediated transport	181	-40.34
GO:0030198	extracellular matrix organization	91	-40.29
GO:0043062	extracellular structure organization	91	-40.16
GO:0008152	metabolic process	661	-38.93
GO:0019752	carboxylic acid metabolic process	146	-36.47
GO:0006082	organic acid metabolic process	156	-35.83
GO:0006810	transport	341	-35.55
GO:0055114	oxidation-reduction process	110	-33.01
GO:0006950	response to stress	329	-32.61
GO:1901564	organonitrogen compound metabolic process	227	-32.56
GO:0006897	endocytosis	111	-32.55
GO:0071704	organic substance metabolic process	615	-32.36
GO:0051179	localization	390	-32.34
GO:0065008	regulation of biological quality	274	-31.59
GO:0009056	catabolic process	218	-31.57
GO:0009611	response to wounding	130	-30.88
GO:0044707	single-multicellular organism process	349	-27.85
GO:0006091	generation of precursor metabolites and energy	85	-27.46
GO:0050896	response to stimulus	513	-27.35
GO:0072376	protein activation cascade	61	-26.78
GO:0009605	response to external stimulus	201	-24.80
GO:0042060	wound healing	101	-24.20
GO:0050817	coagulation	92	-23.59
GO:0071822	protein complex subunit organization	167	-22.67
GO:0032501	multicellular organismal process	383	-22.47
GO:0022607	cellular component assembly	199	-21.77
GO:0002576	platelet degranulation	36	-21.35
GO:0002253	activation of immune response	99	-21.31
GO:0044238	primary metabolic process	565	-21.23
GO:0050878	regulation of body fluid levels	95	-21.10
GO:0042221	response to chemical	295	-20.70
GO:0006956	complement activation	51	-20.35
GO:0050778	positive regulation of immune response	104	-19.57
GO:0000904	cell morphogenesis involved in differentiation	111	-19.30
GO:0044237	cellular metabolic process	562	-19.28
GO:0044085	cellular component biogenesis	201	-19.08
GO:0030162	regulation of proteolysis	91	-19.07
GO:0051641	cellular localization	218	-18.51
GO:0006959	humoral immune response	61	-18.28
GO:0032502	developmental process	305	-17.68
GO:0006952	defense response	174	-17.37
GO:0006898	receptor-mediated endocytosis	65	-17.33
GO:0009141	nucleoside triphosphate metabolic process	49	-17.01
GO:0002376	immune system process	211	-16.81
GO:0072524	pyridine-containing compound metabolic process	35	-16.63
GO:0048584	positive regulation of response to stimulus	181	-16.60

GO:0046496	nicotinamide nucleotide metabolic process	34	-16.58
GO:0033036	macromolecule localization	185	-16.54
GO:0008104	protein localization	165	-16.03
GO:0048518	positive regulation of biological process	339	-15.70
GO:0061024	membrane organization	116	-15.42
GO:0019538	protein metabolic process	350	-15.32
GO:0046907	intracellular transport	160	-14.83
GO:0048583	regulation of response to stimulus	265	-14.71
GO:0040011	locomotion	145	-14.58
GO:0051128	regulation of cellular component organization	163	-14.39
GO:0006928	cellular component movement	157	-14.38
GO:0005975	carbohydrate metabolic process	101	-14.34
GO:0006508	proteolysis	128	-14.21
GO:0005996	monosaccharide metabolic process	48	-14.20
GO:0002252	immune effector process	93	-14.14
GO:0051186	cofactor metabolic process	54	-14.02
GO:0044711	single-organism biosynthetic process	148	-14.01
GO:0065007	biological regulation	582	-13.93
GO:0031589	cell-substrate adhesion	46	-13.71
GO:0002682	regulation of immune system process	149	-13.70
GO:0080134	regulation of response to stress	135	-13.56
GO:0044282	small molecule catabolic process	53	-13.12
GO:0070887	cellular response to chemical stimulus	207	-13.07
GO:0030029	actin filament-based process	72	-13.03
GO:0050789	regulation of biological process	553	-12.87
GO:0045087	innate immune response	128	-12.85
GO:0002673	regulation of acute inflammatory response	23	-12.80
GO:0032879	regulation of localization	166	-12.67
GO:0051130	positive regulation of cellular component organization	101	-12.60
GO:0006793	phosphorus metabolic process	212	-12.59
GO:0043086	negative regulation of catalytic activity	86	-12.58
GO:0006457	protein folding	40	-12.45
GO:0009636	response to toxic substance	32	-12.42
GO:1901135	carbohydrate derivative metabolic process	120	-12.26
GO:0061615	glycolytic process through fructose-6-phosphate	17	-12.10
GO:0051246	regulation of protein metabolic process	191	-12.05
GO:0019637	organophosphate metabolic process	99	-11.94
GO:0007010	cytoskeleton organization	96	-11.92
GO:0002526	acute inflammatory response	26	-11.89
GO:0034446	substrate adhesion-dependent cell spreading	24	-11.87
GO:0006935	chemotaxis	89	-11.84
GO:0048468	cell development	136	-11.83
GO:0022610	biological adhesion	109	-11.72
GO:0006955	immune response	155	-11.61
GO:0001775	cell activation	88	-11.51
GO:0072350	tricarboxylic acid metabolic process	18	-11.43
GO:1901657	glycosyl compound metabolic process	53	-11.26
GO:0052547	regulation of peptidase activity	52	-11.17

* Bonferroni corrected p-value

Supplemental Table 3. Human LAD Protein GO Terms: Molecular Functions (adj. p-value < 0.05*)

GO Term ID	Description	# of proteins	log(p-value)*
------------	-------------	---------------	---------------

GO:0005515	protein binding	719	-50.25
GO:0005488	binding	780	-49.47
GO:0044822	poly(A) RNA binding	160	-29.24
GO:0005198	structural molecule activity	94	-24.83
GO:0003723	RNA binding	169	-24.82
GO:0032403	protein complex binding	101	-24.66
GO:0043167	ion binding	165	-23.14
GO:0008092	cytoskeletal protein binding	86	-21.19
GO:0043168	anion binding	113	-17.67
GO:0097367	carbohydrate derivative binding	89	-17.58
GO:0003779	actin binding	46	-16.90
GO:0016491	oxidoreductase activity	79	-16.89
GO:0097159	organic cyclic compound binding	253	-15.65
GO:0003824	catalytic activity	310	-14.77
GO:0016209	antioxidant activity	23	-13.55
GO:1901363	heterocyclic compound binding	241	-13.24
GO:0005539	glycosaminoglycan binding	32	-12.80
GO:0005200	structural constituent of cytoskeleton	26	-12.64
	oxidoreductase activity, acting on the CH-OH group		
GO:0016616	group of donors, NAD or NADP as acceptor	26	-12.47
GO:0042802	identical protein binding	107	-11.64
GO:0036094	small molecule binding	81	-11.00
	oxidoreductase activity, acting on CH-OH group of donors	26	-10.98
GO:0004857	enzyme inhibitor activity	47	-10.48
GO:0005201	extracellular matrix structural constituent	20	-9.54
GO:0061135	endopeptidase regulator activity	28	-9.34
GO:0019899	enzyme binding	127	-9.25
GO:0030234	enzyme regulator activity	75	-8.88
GO:1901681	sulfur compound binding	29	-8.80
GO:0043169	cation binding	82	-8.74
GO:0046872	metal ion binding	75	-7.98
GO:0016787	hydrolase activity	141	-7.76
GO:0034987	immunoglobulin receptor binding	13	-7.27
GO:0050839	cell adhesion molecule binding	29	-7.08
	oxidoreductase activity, acting on peroxide as acceptor	14	-7.08
GO:0016684			
GO:0008289	lipid binding	53	-6.88
GO:0005102	receptor binding	104	-6.75
GO:0003676	nucleic acid binding	187	-6.62
GO:0008201	heparin binding	20	-6.30
GO:0044548	S100 protein binding	9	-6.24
GO:0005518	collagen binding	16	-6.24
GO:0004601	peroxidase activity	13	-6.13
GO:0001948	glycoprotein binding	18	-6.02
GO:0009055	electron carrier activity	20	-6.00
GO:0005178	integrin binding	19	-5.58
GO:0017111	nucleoside-triphosphatase activity	59	-5.27
GO:0005509	calcium ion binding	34	-5.26
GO:0048306	calcium-dependent protein binding	14	-5.15
GO:1901265	nucleoside phosphate binding	53	-4.84
GO:0048037	cofactor binding	23	-4.69
GO:0016817	hydrolase activity, acting on acid anhydrides	60	-4.59
GO:0000166	nucleotide binding	52	-4.46
GO:0070325	lipoprotein particle receptor binding	9	-4.00
GO:0051082	unfolded protein binding	15	-4.00
GO:0005496	steroid binding	15	-3.34
GO:0019900	kinase binding	46	-3.28
GO:0016853	isomerase activity	20	-3.20

GO:0046983	protein dimerization activity	64	-3.16
GO:0001848	complement binding	7	-2.98
GO:0008307	structural constituent of muscle	11	-2.98
GO:0017166	vinculin binding	6	-2.82
GO:0042803	protein homodimerization activity	53	-2.77
GO:0046914	transition metal ion binding	38	-2.75
GO:0003823	antigen binding	34	-2.74
GO:0043178	alcohol binding	14	-2.67
GO:0002020	protease binding	16	-2.53
GO:0016835	carbon-oxygen lyase activity	11	-2.52
GO:0051087	chaperone binding	13	-2.50
GO:0031625	ubiquitin protein ligase binding	29	-2.49
GO:0016860	intramolecular oxidoreductase activity	10	-2.43
GO:0044389	small conjugating protein ligase binding	29	-2.38
GO:0019003	GDP binding	11	-2.31
GO:0023026	MHC class II protein complex binding	7	-2.28
GO:0043394	proteoglycan binding	7	-2.28
GO:0055102	lipase inhibitor activity	6	-2.21
	oxidoreductase activity, acting on a sulfur group of donors	10	-2.09
GO:0016801	hydrolase activity, acting on ether bonds	5	-2.06
GO:0008233	peptidase activity	42	-1.99
GO:0004175	endopeptidase activity	30	-1.98
GO:0019001	guanyl nucleotide binding	18	-1.95
GO:0004064	arylesterase activity	4	-1.75
GO:0004301	epoxide hydrolase activity	4	-1.75
GO:0023023	MHC protein complex binding	7	-1.74
GO:0019865	immunoglobulin binding	5	-1.72
	oxidoreductase activity, acting on the aldehyde or oxo group of donors	10	-1.60
GO:0016903	cholesterol binding	9	-1.56
GO:0032561	guanyl ribonucleotide binding	17	-1.44
GO:0044325	ion channel binding	14	-1.38
GO:0060090	binding, bridging	19	-1.33

* Bonferroni corrected p-value

Supplemental Table 4. Human LAD Protein GO Terms: Cellular Component (adj. p-value < 0.05*)

<u>GO Term ID</u>	<u>Description</u>	<u># of proteins</u>	<u>log(p-value)*</u>
GO:0031982	vesicle	694	-300.00
GO:0070062	extracellular vesicular exosome	671	-300.00
GO:0005925	focal adhesion	142	-84.66
GO:0044444	cytoplasmic part	633	-81.64
GO:0043226	organelle	857	-77.12
GO:0043227	membrane-bounded organelle	825	-73.16
GO:0072562	blood microparticle	92	-71.56
GO:0005829	cytosol	352	-64.45
GO:0031012	extracellular matrix	98	-60.94
GO:0005737	cytoplasm	712	-55.97
GO:0030054	cell junction	154	-53.69
GO:0015629	actin cytoskeleton	83	-26.96
GO:0005578	proteinaceous extracellular matrix	45	-22.33
GO:0005856	cytoskeleton	165	-20.83
GO:0032991	macromolecular complex	309	-19.25
GO:0060205	cytoplasmic membrane-bounded vesicle lumen	31	-17.64
GO:0031983	vesicle lumen	31	-17.44
GO:0016020	membrane	473	-16.77
GO:0044424	intracellular part	763	-15.51
GO:0043234	protein complex	259	-14.65
GO:0005622	intracellular	768	-14.65
GO:0005788	endoplasmic reticulum lumen	38	-12.37
GO:0043228	non-membrane-bounded organelle	252	-12.26
GO:0044422	organelle part	511	-11.60
GO:0044433	cytoplasmic vesicle part	65	-11.38
GO:0044437	vacuolar part	52	-10.91
GO:0044446	intracellular organelle part	500	-10.79
GO:0031091	platelet alpha granule	22	-10.39
GO:0045121	membrane raft	34	-10.18
GO:0034358	plasma lipoprotein particle	13	-8.87
GO:0032994	protein-lipid complex	13	-8.21
GO:0044449	contractile fiber part	27	-8.16
GO:0005832	chaperonin-containing T-complex	8	-7.80
GO:0005885	Arp2/3 protein complex	8	-7.80
GO:0005811	lipid particle	17	-7.67
GO:0043292	contractile fiber	27	-7.38
GO:0043229	intracellular organelle	639	-7.26
GO:0042571	immunoglobulin complex, circulating	12	-6.87
GO:0044429	mitochondrial part	75	-6.87
GO:0012505	endomembrane system	225	-6.71
GO:0019814	immunoglobulin complex	12	-6.61
GO:0005773	vacuole	56	-6.55
GO:0009986	cell surface	63	-6.12
GO:0098589	membrane region	61	-6.12
GO:0044448	cell cortex part	19	-6.09
GO:0005581	collagen trimer	12	-5.69
GO:0044445	cytosolic part	32	-5.65
GO:0044853	plasma membrane raft	16	-5.53
GO:0005739	mitochondrion	114	-5.44
GO:0098552	side of membrane	46	-5.42
GO:0005759	mitochondrial matrix	43	-5.13
GO:0009897	external side of plasma membrane	24	-5.11
GO:0045259	proton-transporting ATP synthase complex	10	-5.10
GO:0048471	perinuclear region of cytoplasm	43	-5.06
GO:0005577	fibrinogen complex	7	-4.96

GO:0005783	endoplasmic reticulum	109	-4.68
GO:0005839	proteasome core complex	9	-4.60
GO:0001725	stress fiber	12	-4.60
GO:0032432	actin filament bundle	12	-4.44
GO:0098644	complex of collagen trimers	9	-4.10
GO:0005623	cell	818	-4.08
GO:0044464	cell part	817	-4.06
GO:0000502	proteasome complex	15	-3.90
GO:0042641	actomyosin	12	-3.74
GO:0005938	cell cortex	21	-3.74
GO:0044432	endoplasmic reticulum part	76	-3.63
GO:0042383	sarcolemma	12	-3.26
GO:0031090	organelle membrane	157	-3.11
GO:0005874	microtubule	25	-3.04
GO:0071944	cell periphery	273	-2.98
GO:0005884	actin filament	12	-2.63
GO:0036019	endolysosome	7	-2.59
GO:0030175	filopodium	12	-2.54
GO:0031252	cell leading edge	26	-2.49
GO:0030529	ribonucleoprotein complex	54	-2.42
GO:0016469	proton-transporting two-sector ATPase complex	10	-2.41
GO:0044455	mitochondrial membrane part	22	-2.27
GO:0005886	plasma membrane	265	-2.21
GO:0001527	microfibril	5	-2.15
GO:0042995	cell projection	71	-1.98
GO:0005768	endosome	55	-1.91
GO:0005796	Golgi lumen	15	-1.85
GO:0030496	midbody	16	-1.83
GO:0031975	envelope	67	-1.80
GO:0001726	ruffle	15	-1.62
GO:0005743	mitochondrial inner membrane	33	-1.40
GO:0001772	immunological synapse	7	-1.39

* Bonferroni corrected p-value

Supplemental Table 5. Human Distal Aortic Protein GO Terms: Biologic Process (top 100 GO Terms)

<u>GO Term ID</u>	<u>Description</u>	<u># of proteins</u>	<u>log(p-value)*</u>
GO:0044699	single-organism process	619	-48.11
GO:0044763	single-organism cellular process	563	-36.27
GO:0016192	vesicle-mediated transport	153	-35.49
GO:0071840	cellular component organization or biogenesis	341	-33.98
GO:0030198	extracellular matrix organization	65	-31.62
GO:0043062	extracellular structure organization	65	-31.50
GO:0009987	cellular process	627	-30.47
GO:0065008	regulation of biological quality	217	-29.55
GO:0006897	endocytosis	91	-28.49
GO:0009611	response to wounding	93	-27.77
GO:0051179	localization	312	-27.74
GO:0044710	single-organism metabolic process	305	-27.74
GO:0051234	establishment of localization	273	-27.69
GO:0044707	single-multicellular organism process	269	-25.07
GO:0072376	protein activation cascade	53	-24.66
GO:0050896	response to stimulus	394	-24.21
GO:0006950	response to stress	227	-23.16
GO:0009056	catabolic process	166	-22.89
GO:0022607	cellular component assembly	168	-22.02
GO:0032501	multicellular organismal process	299	-21.59
GO:0042060	wound healing	66	-20.86
GO:0002576	platelet degranulation	35	-20.30
GO:0051128	regulation of cellular component organization	154	-19.28
GO:0002253	activation of immune response	79	-18.96
GO:0050817	coagulation	55	-18.75
GO:0044085	cellular component biogenesis	172	-18.56
GO:0006956	complement activation	44	-18.46
GO:0071822	protein complex subunit organization	132	-18.41
GO:0030029	actin filament-based process	70	-18.28
GO:0050778	positive regulation of immune response	84	-17.99
GO:0048518	positive regulation of biological process	284	-17.96
GO:0044767	single-organism developmental process	237	-17.90
GO:0032502	developmental process	241	-17.11
GO:0002376	immune system process	164	-16.96
GO:0072524	pyridine-containing compound metabolic process	32	-16.94
GO:0048584	positive regulation of response to stimulus	146	-16.83
GO:0022610	biological adhesion	102	-16.71
GO:0006959	humoral immune response	52	-16.68
GO:0007155	cell adhesion	101	-16.42
GO:0065007	biological regulation	470	-16.36
GO:0050878	regulation of body fluid levels	58	-16.28
GO:0006457	protein folding	38	-15.70
GO:0050789	regulation of biological process	450	-15.68
GO:0046496	nicotinamide nucleotide metabolic process	29	-15.42
GO:0008152	metabolic process	464	-15.20
GO:0007010	cytoskeleton organization	87	-14.69
GO:0034446	substrate adhesion-dependent cell spreading	24	-14.53
GO:0061621	canonical glycolysis	17	-14.49
GO:0048583	regulation of response to stimulus	216	-14.37
GO:0006909	phagocytosis	49	-14.10
GO:0051130	positive regulation of cellular component organization	89	-13.45

GO:0002673	regulation of acute inflammatory response	22	-13.44
GO:0080134	regulation of response to stress	111	-13.32
GO:0030036	actin cytoskeleton organization	56	-13.31
GO:0002252	immune effector process	78	-13.28
GO:0002526	acute inflammatory response	25	-13.27
GO:0032879	regulation of localization	142	-13.25
GO:0002682	regulation of immune system process	114	-12.82
GO:0030162	regulation of proteolysis	68	-12.73
GO:0055114	oxidation-reduction process	58	-12.73
GO:0006928	cellular component movement	113	-12.60
GO:0051641	cellular localization	167	-12.51
GO:0009605	response to external stimulus	121	-12.35
GO:0048522	positive regulation of cellular process	233	-12.27
GO:0044281	small molecule metabolic process	132	-12.26
GO:0048519	negative regulation of biological process	225	-12.14
GO:1901564	organonitrogen compound metabolic process	146	-11.89
GO:0006955	immune response	116	-11.72
GO:0006508	proteolysis	110	-11.63
GO:0071704	organic substance metabolic process	428	-11.53
GO:0043086	negative regulation of catalytic activity	71	-11.48
GO:0006165	nucleoside diphosphate phosphorylation	21	-11.30
GO:0003012	muscle system process	44	-11.18
GO:0033036	macromolecule localization	141	-10.70
GO:0051246	regulation of protein metabolic process	149	-10.69
GO:0046939	nucleotide phosphorylation	21	-10.65
GO:0006952	defense response	105	-10.41
GO:0034329	cell junction assembly	31	-10.36
GO:0006796	phosphate-containing compound metabolic process	166	-10.31
GO:0006082	organic acid metabolic process	81	-10.23
GO:0008104	protein localization	125	-10.21
GO:0032101	regulation of response to external stimulus	74	-10.17
GO:0042221	response to chemical	192	-10.11
GO:0010941	regulation of cell death	92	-10.08
GO:0019752	carboxylic acid metabolic process	74	-9.90
GO:0009205	purine ribonucleoside triphosphate metabolic process	34	-9.73
GO:0044092	negative regulation of molecular function	80	-9.69
GO:0016052	carbohydrate catabolic process	26	-9.64
GO:0009888	tissue development	91	-9.63
GO:0050794	regulation of cellular process	408	-9.60
GO:0034330	cell junction organization	34	-9.47
GO:0006793	phosphorus metabolic process	166	-9.44
GO:0021762	substantia nigra development	17	-9.42
GO:0051716	cellular response to stimulus	308	-9.32
GO:0070887	cellular response to chemical stimulus	143	-9.31
GO:0046907	intracellular transport	123	-9.31
GO:0051604	protein maturation	40	-9.17
GO:0065009	regulation of molecular function	152	-9.02
GO:0009132	nucleoside diphosphate metabolic process	21	-8.86
GO:0061024	membrane organization	80	-8.81

* Bonferroni corrected p-value

Supplemental Table 6. Human Distal Aortic Protein GO Terms: Molecular Function (adj. p-value < 0.05*)

<u>GO Term ID</u>	<u>Description</u>	<u># of proteins</u>	<u>log(p-value)*</u>
GO:0005515	protein binding	583	-55.54
GO:0005488	binding	622	-50.52
GO:0032403	protein complex binding	88	-24.65
GO:0005198	structural molecule activity	82	-24.37
GO:0008092	cytoskeletal protein binding	78	-23.01
GO:0044822	poly(A) RNA binding	124	-22.28
GO:0043167	ion binding	133	-19.83
GO:0003723	RNA binding	132	-19.13
GO:0003779	actin binding	40	-15.67
GO:0097367	carbohydrate derivative binding	73	-15.32
GO:0043168	anion binding	88	-13.33
GO:0097159	organic cyclic compound binding	202	-13.19
GO:0005201	extracellular matrix structural constituent	22	-12.89
GO:0019899	enzyme binding	116	-12.87
GO:0005200	structural constituent of cytoskeleton	23	-12.12
GO:0004857	enzyme inhibitor activity	42	-11.07
GO:1901363	heterocyclic compound binding	191	-10.72
GO:0005102	receptor binding	95	-10.09
GO:0005539	glycosaminoglycan binding	25	-9.33
GO:0042802	identical protein binding	82	-8.64
GO:0016616	oxidoreductase activity, acting on the CH-OH group of donors, NAD or NADP as acceptor	22	-8.62
GO:0030234	enzyme regulator activity	67	-8.46
GO:0003824	catalytic activity	252	-8.28
GO:0050839	cell adhesion molecule binding	27	-8.14
GO:0036094	small molecule binding	63	-8.00
GO:0043169	cation binding	67	-7.86
GO:0046872	metal ion binding	62	-7.49
GO:0016614	oxidoreductase activity, acting on CH-OH group of donors	22	-7.44
GO:0016209	antioxidant activity	16	-7.42
GO:0034987	immunoglobulin receptor binding	12	-7.41
GO:0016787	hydrolase activity	125	-6.60
GO:0016491	oxidoreductase activity	52	-6.36
GO:0003924	GTPase activity	24	-5.80
GO:0004866	endopeptidase inhibitor activity	20	-5.73
GO:0008289	lipid binding	43	-5.68
GO:0044548	S100 protein binding	8	-5.64
GO:0005178	integrin binding	17	-5.56
GO:0004175	endopeptidase activity	43	-5.41
GO:1901681	sulfur compound binding	21	-5.15
GO:0003676	nucleic acid binding	147	-4.95
GO:0005518	collagen binding	13	-4.86
GO:0019901	protein kinase binding	39	-4.80
GO:0016817	hydrolase activity, acting on acid anhydrides	51	-4.75
GO:0008201	heparin binding	16	-4.71
GO:0051082	unfolded protein binding	14	-4.65
GO:0048306	calcium-dependent protein binding	12	-4.57
GO:0051920	peroxiredoxin activity	5	-4.38
GO:0001948	glycoprotein binding	14	-4.19
GO:0016835	carbon-oxygen lyase activity	13	-4.03
GO:0005509	calcium ion binding	27	-4.02
GO:0005496	steroid binding	14	-4.02
GO:0001848	complement binding	7	-3.81
GO:0016684	oxidoreductase activity, acting on peroxide as acceptor	10	-3.78
GO:1901265	nucleoside phosphate binding	42	-3.56

GO:0032561	guanyl ribonucleotide binding	18	-3.45
GO:0019001	guanyl nucleotide binding	18	-3.40
GO:0046914	transition metal ion binding	33	-3.25
GO:0008233	peptidase activity	47	-3.22
GO:0017171	serine hydrolase activity	31	-3.20
GO:0008307	structural constituent of muscle	10	-3.17
GO:0001882	nucleoside binding	33	-3.03
GO:0016829	lyase activity	18	-2.94
GO:0046983	protein dimerization activity	52	-2.88
GO:0070325	lipoprotein particle receptor binding	7	-2.71
GO:0016853	isomerase activity	17	-2.69
GO:0031625	ubiquitin protein ligase binding	25	-2.67
GO:0048037	cofactor binding	17	-2.64
GO:0044389	small conjugating protein ligase binding	25	-2.58
GO:0019003	GDP binding	10	-2.56
GO:0015485	cholesterol binding	9	-2.53
GO:0042803	protein homodimerization activity	43	-2.45
GO:0043178	alcohol binding	12	-2.32
GO:0044325	ion channel binding	13	-2.01
GO:0023026	MHC class II protein complex binding phosphatidylcholine-sterol O-acyltransferase	6	-1.87
GO:0060228	activator activity	4	-1.80
GO:0097493	structural molecule activity conferring elasticity	4	-1.80
GO:0001846	opsonin binding	5	-1.80
GO:0044183	protein binding involved in protein folding	5	-1.80
GO:0048407	platelet-derived growth factor binding	5	-1.80
GO:0005507	copper ion binding	8	-1.70
GO:0017127	cholesterol transporter activity	5	-1.58
GO:0003823	antigen binding	26	-1.58
GO:0008426	protein kinase C inhibitor activity	3	-1.52
GO:0070653	high-density lipoprotein particle receptor binding	3	-1.52
GO:0050998	nitric-oxide synthase binding	4	-1.44
GO:0023023	MHC protein complex binding	6	-1.42
GO:0016860	intramolecular oxidoreductase activity	8	-1.34
GO:0019843	rRNA binding	8	-1.34

* Bonferroni corrected p-value

Supplemental Table 7. Human Distal Aortic Protein GO Terms: Cellular Component (adj. p-value < 0.05*)

<u>GO Term ID</u>	<u>Description</u>	<u># of proteins</u>	<u>log(p-value)*</u>
GO:0070062	extracellular vesicular exosome	527	-290.88
GO:0031982	vesicle	542	-260.54
GO:0005576	extracellular region	566	-257.72
GO:0005925	focal adhesion	133	-90.24
GO:0072562	blood microparticle	85	-71.70
GO:0030054	cell junction	145	-61.99
GO:0044444	cytoplasmic part	491	-61.48
GO:0031012	extracellular matrix	87	-58.30
GO:0005829	cytosol	289	-54.61
GO:0043226	organelle	654	-52.71
GO:0043227	membrane-bounded organelle	631	-50.45
GO:0005737	cytoplasm	548	-40.32
GO:0015629	actin cytoskeleton	76	-29.42
GO:0005856	cytoskeleton	149	-26.01
	cytoplasmic membrane-bounded vesicle		
GO:0060205	lumen	37	-24.40
GO:0031983	vesicle lumen	37	-24.22
GO:0005578	proteinaceous extracellular matrix	41	-22.83
GO:0032991	macromolecular complex	250	-17.78
GO:0005788	endoplasmic reticulum lumen	37	-15.26
GO:0043228	non-membrane-bounded organelle	214	-15.03
GO:0044433	cytoplasmic vesicle part	62	-13.77
GO:0043234	protein complex	210	-13.72
GO:0016020	membrane	370	-13.17
GO:0031091	platelet alpha granule	23	-12.06
GO:0045121	membrane raft	31	-11.05
GO:0044449	contractile fiber part	27	-10.63
GO:0044424	intracellular part	587	-10.34
GO:0043292	contractile fiber	27	-9.83
GO:0005622	intracellular	591	-9.44
GO:0044437	vacuolar part	60	-8.97
GO:0005885	Arp2/3 protein complex	8	-8.76
GO:0005773	vacuole	81	-8.73
GO:0044422	organelle part	399	-8.62
GO:0005581	collagen trimer	13	-8.35
GO:0012505	endomembrane system	192	-8.34
GO:0034358	plasma lipoprotein particle	11	-7.38
GO:0044446	intracellular organelle part	387	-7.24
GO:0009986	cell surface	55	-7.05
GO:0032994	protein-lipid complex	11	-6.86
GO:0042571	immunoglobulin complex, circulating	11	-6.86
GO:0098589	membrane region	53	-6.82
GO:0048471	perinuclear region of cytoplasm	40	-6.76
GO:0098644	complex of collagen trimers	10	-6.51
GO:0005832	chaperonin-containing T-complex	7	-6.44
GO:0019814	immunoglobulin complex	11	-6.40
GO:0042383	sarcolemma	13	-5.30
GO:0044448	cell cortex part	16	-5.21
GO:0009897	external side of plasma membrane	21	-5.11
GO:0098552	side of membrane	38	-4.85
GO:0001725	stress fiber	11	-4.80
GO:0005884	actin filament	13	-4.72
GO:0032432	actin filament bundle	11	-4.66
GO:0071944	cell periphery	228	-4.54
GO:0043229	intracellular organelle	492	-4.40
GO:0042995	cell projection	66	-4.36
GO:0044853	plasma membrane raft	13	-4.31

GO:0005811	lipid particle	12	-4.09
GO:0005577	fibrinogen complex	6	-4.01
GO:0042641	actomyosin	11	-4.01
GO:0005874	microtubule	23	-3.96
GO:0044445	cytosolic part	25	-3.91
GO:0005886	plasma membrane	221	-3.64
GO:0031252	cell leading edge	24	-3.54
GO:0005938	cell cortex	18	-3.53
GO:0005768	endosome	49	-3.01
GO:0005783	endoplasmic reticulum	85	-2.95
GO:0001527	microfibril	5	-2.75
GO:0044464	cell part	635	-2.69
GO:0005623	cell	635	-2.58
GO:0005796	Golgi lumen	14	-2.50
GO:0045259	proton-transporting ATP synthase complex	7	-2.46
GO:0001726	ruffle	14	-2.33
GO:0005769	early endosome	25	-2.23
GO:0001772	immunological synapse	7	-2.16
GO:0044432	endoplasmic reticulum part	60	-2.10
GO:0098643	banded collagen fibril	5	-1.88
GO:0005882	intermediate filament	9	-1.69
GO:0031838	haptoglobin-hemoglobin complex	3	-1.60
GO:0030904	retromer complex	6	-1.37

* Bonferroni corrected p-value

Supplemental Table 8. Enriched Ingenuity Canonical Pathways Among 944 Human LAD Proteins (FDR<0.001)

	-log(B-H p-value)		-log(B-H p-value)
Acute Phase Response Signaling	23.60	α -Adrenergic Signaling	5.21
LXR/RXR Activation	22.00	ERK/MAPK Signaling	4.90
Complement System	19.00	Regulation of Cellular Mechanics by Calpain Protease	4.76
Clathrin-mediated Endocytosis Signaling	17.80	Protein Kinase A Signaling Noradrenaline and Adrenaline Degradation	4.71 4.64
FXR/RXR Activation	16.80	Phospholipase C Signaling	4.57
Integrin Signaling	16.40	HIPPO signaling	4.57
Mitochondrial Dysfunction	14.20	Dopamine Receptor Signaling	4.46
Glycolysis I	13.60	Paxillin Signaling	4.38
Actin Cytoskeleton Signaling	13.50	Extrinsic Prothrombin Activation Pathway IL-12 Signaling and Production in Macrophages	4.36 4.34
RhoGDI Signaling	13.00	Breast Cancer Regulation by Stathmin1	4.31
Signaling by Rho Family GTPases	11.90	PI3K/AKT Signaling	4.31
RhoA Signaling	11.60	Germ Cell-Sertoli Cell Junction Signaling	4.25
Regulation of Actin-based Motility by Rho	11.00	Glutaryl-CoA Degradation	4.12
Remodeling of Epithelial Adherens Junctions	10.10	EIF2 Signaling	4.08
Actin Nucleation by ARP-WASP Complex	9.65	Glutathione Redox Reactions I	4.00
NRF2-mediated Oxidative Stress Response	9.21	Superoxide Radicals Degradation	3.98
Coagulation System	9.21	IGF-1 Signaling	3.90
Gluconeogenesis I	9.21	Regulation of eIF4 and p70S6K Signaling	3.87
Atherosclerosis Signaling	8.53	Tryptophan Degradation III (Eukaryotic)	3.69
TCA Cycle II (Eukaryotic)	8.50	Isoleucine Degradation I	3.69
ILK Signaling	8.36	CCR3 Signaling in Eosinophils	3.64
Intrinsic Prothrombin Activation Pathway	7.29	Sertoli Cell-Sertoli Cell Junction Signaling	3.60
Cdc42 Signaling	7.28	Unfolded protein response	3.56
Production of Nitric Oxide and Reactive Oxygen Species in Macrophages	7.28	Thrombin Signaling	3.56
Ephrin Receptor Signaling	7.10	PPAR α /RXR α Activation	3.45
Virus Entry via Endocytic Pathways	6.88	Xenobiotic Metabolism Signaling	3.45
Protein Ubiquitination Pathway	6.87	Pentose Phosphate Pathway	3.44
Huntington's Disease Signaling	6.59	Role of Tissue Factor in Cancer	3.43
Oxidative Phosphorylation	6.43	Ethanol Degradation II	3.36
Epithelial Adherens Junction Signaling	6.43	mTOR Signaling	3.32
Caveolar-mediated Endocytosis Signaling	6.27	GDP-glucose Biosynthesis	3.32
phagosome maturation	6.14	Androgen Signaling	3.30
Glycogen Degradation II	6.02	Myc Mediated Apoptosis Signaling	3.24
Lipid Antigen Presentation by CD1	5.99	Methylglyoxal Degradation III	3.23
Agrin Interactions at Neuromuscular Junction	5.90	Neuroprotective Role of THOP1 in Alzheimer's Disease	3.22
Rac Signaling	5.89	Glutathione-mediated Detoxification	3.21
G Beta Gamma Signaling	5.63	Axonal Guidance Signaling	3.16
fMLP Signaling in Neutrophils	5.63	Synaptic Long Term Potentiation	3.06
CDK5 Signaling	5.59	14-3-3-mediated Signaling	3.06
p70S6K Signaling	5.58	Semaphorin Signaling in Neurons	3.02
Ephrin B Signaling	5.42	Glucose and Glucose-1-phosphate Degradation	3.02
Glycogen Degradation III	5.34	Aspartate Degradation II	3.02
Fcy Receptor-mediated Phagocytosis in Macrophages and Monocytes	5.31		

Supplemental Table 9. Enriched Ingenuity Canonical Pathways among 725 Human Distal Aortic Proteins (FDR<0.001)

	-log(B-H p-value)		-log(B-H p-value)
Acute Phase Response Signaling	22.80	IGF-1 Signaling	5.26
LXR/RXR Activation	20.90	Phospholipase C Signaling	5.26
Integrin Signaling	19.90	Axonal Guidance Signaling	5.16
Complement System	18.60	Extrinsic Prothrombin Activation Pathway	5.12
Clathrin-mediated Endocytosis Signaling	18.00	Huntington's Disease Signaling	4.93
FXR/RXR Activation	16.80	Germ Cell-Sertoli Cell Junction Signaling	4.87
Actin Cytoskeleton Signaling	16.80	Glutaryl-CoA Degradation	4.78
RhoGDI Signaling	15.80	Glycogen Degradation III	4.78
Glycolysis I	15.50	Thrombin Signaling	4.78
Signaling by Rho Family GTPases	14.40	Noradrenaline and Adrenaline Degradation	4.73
RhoA Signaling	13.70	Breast Cancer Regulation by Stathmin1	4.68
Regulation of Actin-based Motility by Rho	13.60	Ephrin B Signaling	4.68
Gluconeogenesis I	12.00	Protein Ubiquitination Pathway	4.57
Actin Nucleation by ARP-WASP Complex	11.70	Tryptophan Degradation III (Eukaryotic)	4.43
Remodeling of Epithelial Adherens Junctions	11.30	Agrin Interactions at Neuromuscular Junction	4.34
Intrinsic Prothrombin Activation Pathway	9.84	14-3-3-mediated Signaling	4.33
ILK Signaling	9.81	Sertoli Cell-Sertoli Cell Junction Signaling	4.26
Caveolar-mediated Endocytosis Signaling	9.71	IL-12 Signaling and Production in Macrophages	4.26
Coagulation System	8.42	Neuroprotective Role of THOP1 in Alzheimer's Disease	4.05
Epithelial Adherens Junction Signaling	7.88	Hepatic Fibrosis / Hepatic Stellate Cell Activation	3.99
Atherosclerosis Signaling	7.87	Pentose Phosphate Pathway	3.99
Ephrin Receptor Signaling	7.61	FAK Signaling	3.94
Cdc42 Signaling	7.36	Lipid Antigen Presentation by CD1	3.90
Production of Nitric Oxide and Reactive Oxygen Species in Macrophages	7.27	CCR3 Signaling in Eosinophils	3.89
Virus Entry via Endocytic Pathways	7.16	Unfolded protein response	3.85
phagosome maturation	6.64	Role of Tissue Factor in Cancer	3.56
G Beta Gamma Signaling	6.45	Myc Mediated Apoptosis Signaling	3.51
ERK/MAPK Signaling	6.34	Androgen Signaling	3.44
Rac Signaling	6.18	Cellular Effects of Sildenafil (Viagra)	3.44
p70S6K Signaling	5.97	Ethanol Degradation II	3.26
fMLP Signaling in Neutrophils	5.96	ERK5 Signaling	3.22
Regulation of Cellular Mechanics by Calpain Protease	5.96	Isoleucine Degradation I	3.22
PI3K/AKT Signaling	5.84	Synaptic Long Term Potentiation	3.22
CDK5 Signaling	5.84	Semaphorin Signaling in Neurons	3.19
Paxillin Signaling	5.84	Sucrose Degradation V (Mammalian)	3.19
Protein Kinase A Signaling	5.70	Superoxide Radicals Degradation	3.19
NRF2-mediated Oxidative Stress Response	5.64	Cardiac β -adrenergic Signaling	3.18
Mitochondrial Dysfunction	5.59	Dopamine Receptor Signaling	3.17
Fcy Receptor-mediated Phagocytosis in Macrophages and Monocytes	5.47	P2Y Purigenic Receptor Signaling Pathway	3.17
Glycogen Degradation II	5.29	Gαi Signaling	3.10
α -Adrenergic Signaling	5.28	eNOS Signaling	3.09
HIPPO signaling	5.28	Pentose Phosphate Pathway (Oxidative Branch)	3.00

Supplemental Table 10. Regression Models of Association Between Individual Proteins and Extent of Surface Area Involved with Fibrous Plaque (FP) or Normal Intima (NL) in Human LAD Arterial Samples (top 100 proteins). In models of %FP, the non-FP% fraction includes fatty streaks (FS) and NML intima. Likewise, in models of % NL, the non -NL fraction includes both FP and FS. Accordingly, we modeled both %FP and %NL separately. We also classified samples into three level ordinal categories of extent of FP and extent of NL and performed ordinal logistic regression (Ord LR). This approach is less statistically powerful, but makes fewer distributional assumptions about the measures of extent of disease. In addition, we used MANOVA to jointly model the distribution of %FP, %FS and %NL. P-values and q-values <0.05 are highlighted in green and pink respectively. **Proteins in bold (n=21) are also included in the top 100 AA proteins**

Uniprot ID	Protein	Gene	MANOVA (%FP,%FS)			GLM (%FP)			Ord LR (%FP)			GLM (% NML)			Ord LR (%NML)		
			p-value	q-value	beta	p-value	q-value	beta	p-value	q-value	beta	p-value	q-value	beta	p-value	q-value	
P07858	Cathepsin B	CTSB	9.3E-09	5.5E-06	16.5	2.4E-08	1.0E-05	-1.9	2.2E-05	1.5E-02	-20.1	1.0E-08	7.4E-06	2.3	9.8E-06	5.8E-03	
P24821	Tenascin	TNC	2.1E-08	6.3E-06	2.3	1.2E-08	1.0E-05	-0.3	7.1E-05	2.4E-02	-2.6	9.9E-08	3.6E-05	0.3	2.8E-04	4.2E-02	
Q15063	Periostin	POSTN	1.1E-06	2.1E-04	1.9	2.9E-06	7.5E-04	-0.2	3.8E-04	3.0E-02	-2.4	4.1E-07	9.9E-05	0.2	1.3E-04	2.5E-02	
P04114	Apolipoprotein B-100	APOB	3.5E-06	5.3E-04	0.6	3.1E-05	3.7E-03	-0.1	9.3E-04	4.5E-02	-0.9	6.6E-07	1.2E-04	0.1	8.0E-04	7.9E-02	
P07996	Thrombospondin-1	THBS1	6.3E-06	7.5E-04	2.7	3.3E-04	2.0E-02	-0.3	2.8E-03	8.6E-02	-4.3	9.2E-07	1.3E-04	0.4	1.3E-03	9.5E-02	
P13796	Plastin-2	LCP1	1.4E-05	1.2E-03	6.5	3.6E-06	7.5E-04	-0.7	2.0E-04	3.0E-02	-6.9	4.2E-05	3.7E-03	0.5	9.4E-04	7.9E-02	
P07339	Cathepsin D	CTSD	1.7E-05	1.3E-03	11.9	4.9E-06	8.3E-04	-1.4	2.6E-03	8.6E-02	-12.9	3.9E-05	3.7E-03	1.4	2.5E-03	1.1E-01	
Q9UBR2	Cathepsin Z	CTSZ	1.3E-05	1.2E-03	29.6	2.0E-05	2.7E-03	-3.9	2.2E-04	3.0E-02	-37.3	5.0E-06	6.0E-04	2.7	8.7E-04	7.9E-02	
P50895	Basal cell adhesion molecule	BCAM	4.4E-04	2.2E-02	-3.3	4.3E-02	4.0E-01	0.6	1.6E-02	2.3E-01	7.0	1.9E-04	1.4E-02	-1.0	4.1E-05	1.2E-02	
P40261	Nicotinamide N-methyltransferase	NNMT	3.1E-04	1.7E-02	27.3	6.3E-05	6.6E-03	-3.7	3.0E-04	3.0E-02	-22.6	6.5E-03	1.2E-01	2.2	5.8E-03	1.2E-01	
P13760	HLA class II HC Ag, DRB1-4 beta	HLA-DRB1	3.0E-04	1.7E-02	18.2	7.5E-05	7.0E-03	-1.9	8.4E-04	4.5E-02	-19.2	4.7E-04	2.6E-02	1.5	9.0E-03	1.5E-01	
P40121	Macrophage-capping protein	CAPG	5.1E-04	2.2E-02	13.4	1.0E-04	8.5E-03	-1.8	1.4E-04	3.0E-02	-13.1	1.6E-03	5.9E-02	1.3	1.6E-03	1.0E-01	
O43866	CD5 antigen-like	CD5L	5.0E-04	2.2E-02	11.7	1.3E-04	9.9E-03	-1.4	4.1E-04	3.0E-02	-12.4	6.7E-04	3.2E-02	0.9	6.2E-03	1.2E-01	
P35442	Thrombospondin-2	THBS2	8.4E-04	2.9E-02	2.3	3.4E-03	1.1E-01	-0.3	8.1E-03	1.7E-01	-3.5	1.6E-04	1.3E-02	0.2	1.0E-02	1.5E-01	
P07998	Ribonuclease pancreatic	RNASE1	2.8E-04	1.7E-02	73.8	1.7E-04	1.2E-02	-4.8	2.1E-02	2.4E-01	-45.5	5.7E-02	3.5E-01	2.8	1.4E-01	3.3E-01	
O14773	Tripeptidyl-peptidase 1	TPP1	7.7E-04	2.9E-02	20.8	1.8E-04	1.2E-02	-3.6	3.7E-04	3.0E-02	-16.3	1.6E-02	2.0E-01	1.6	1.1E-02	1.5E-01	
P01871	Ig mu chain C region	IGHM	8.3E-04	2.9E-02	2.2	4.6E-04	2.3E-02	-0.2	2.7E-03	8.6E-02	-2.7	3.7E-04	2.4E-02	0.2	2.8E-03	1.1E-01	
P22105	Tenascin-X	TNXB	9.1E-04	3.0E-02	2.4	4.6E-04	2.3E-02	-0.3	4.9E-04	3.0E-02	-2.9	4.3E-04	2.6E-02	0.2	3.4E-03	1.1E-01	
Q15582	TGFBI ig-h3	TGFBI	4.3E-03	9.5E-02	2.9	1.2E-03	5.6E-02	-0.4	4.4E-04	3.0E-02	-3.1	3.8E-03	8.9E-02	0.3	3.0E-03	1.1E-01	
P13667	Protein disulfide-isomerase A4	PDIA4	1.5E-03	4.1E-02	16.5	4.5E-04	2.3E-02	-1.7	3.5E-03	1.0E-01	-18.2	1.2E-03	5.1E-02	1.4	4.3E-03	1.1E-01	
P04004	Vitronectin	VTN	2.5E-03	6.2E-02	3.5	2.0E-02	3.2E-01	-0.4	3.1E-02	2.5E-01	-6.1	5.7E-04	3.0E-02	0.5	1.0E-02	1.5E-01	
P14618	Pyruvate kinase PKM	PKM	1.7E-02	1.9E-01	3.4	6.5E-03	1.8E-01	-0.6	9.2E-04	4.5E-02	-3.9	8.5E-03	1.5E-01	0.4	3.7E-03	1.1E-01	
P09960	Leukotriene A-4 hydrolase	LTA4H	9.6E-04	3.0E-02	6.0	5.4E-02	4.6E-01	-0.7	1.0E-01	3.7E-01	1.9	6.2E-01	6.6E-01	-0.3	3.5E-01	4.2E-01	
P00450	Ceruloplasmin	CP	1.1E-03	3.2E-02	2.6	7.9E-03	2.0E-01	-0.4	1.1E-02	1.9E-01	-0.5	6.7E-01	6.8E-01	0.0	8.2E-01	5.7E-01	
P04844	Ribophorin-2	RPN2	3.7E-03	8.4E-02	13.8	2.8E-03	1.0E-01	-1.7	5.2E-03	1.4E-01	-17.7	1.1E-03	5.1E-02	1.5	3.0E-03	1.1E-01	
Q08380	Galectin-3-binding protein	LGALS3B	5.7E-03	1.1E-01	6.4	8.8E-03	2.2E-01	-0.6	2.0E-02	2.4E-01	-9.2	1.3E-03	5.3E-02	0.7	1.3E-02	1.8E-01	
P08519	Apolipoprotein(a)	LPA	6.5E-03	1.2E-01	23.3	1.5E-02	2.7E-01	-3.0	7.8E-03	1.7E-01	-35.8	1.5E-03	5.6E-02	2.8	8.0E-03	1.4E-01	
Q03135	Caveolin-1	CAV1	4.6E-03	9.8E-02	-10.0	2.5E-03	9.4E-02	2.0	1.6E-03	6.9E-02	12.3	1.8E-03	6.1E-02	-1.1	3.8E-03	1.1E-01	
P07900	Heat shock protein HSP 90-alpha 1	HSP90AA1	1.6E-03	4.3E-02	1.6	1.2E-01	6.0E-01	0.0	8.1E-01	6.7E-01	1.0	4.1E-01	5.9E-01	-0.1	1.6E-01	3.5E-01	
P30153	PP2A subunit A isoform PR65-alpha	PPP2R1A	2.0E-03	5.1E-02	0.4	8.9E-01	8.8E-01	-0.1	8.9E-01	6.8E-01	7.8	3.4E-02	2.8E-01	-0.7	3.2E-02	2.2E-01	
P12955	Xaa-Pro dipeptidase	PEPD	6.8E-03	1.2E-01	32.3	2.1E-03	9.3E-02	-3.2	9.6E-03	1.8E-01	-35.3	4.8E-03	1.0E-01	2.6	1.6E-02	1.9E-01	
O15511	Actin-related protein 2/3 complex subunit 5	ARPC5	6.8E-03	1.2E-01	30.5	2.3E-03	9.4E-02	-3.9	2.1E-03	8.6E-02	-21.2	8.0E-02	4.0E-01	2.0	6.2E-02	2.8E-01	
P48163	NADP-dependent malic enzyme	ME1	9.4E-03	1.5E-01	-5.2	2.3E-02	3.3E-01	0.8	4.3E-02	2.9E-01	8.1	2.2E-03	7.2E-02	-1.0	3.8E-03	1.1E-01	
P01023	Alpha-2-macroglobulin	A2M	9.9E-03	1.5E-01	1.7	3.3E-03	1.1E-01	-0.3	2.2E-03	8.6E-02	-1.8	6.0E-03	1.2E-01	0.1	2.8E-02	2.1E-01	
Q8WX93	Palladin	PALLD	2.1E-02	2.2E-01	-2.6	9.8E-02	5.5E-01	0.6	1.2E-02	2.0E-01	4.9	6.6E-03	1.2E-01	-0.6	2.2E-03	1.1E-01	
Q6NZI2	Polymerase I and transcript release factor	PTRF	1.3E-02	1.7E-01	-5.9	1.9E-02	3.2E-01	1.6	2.5E-03	8.6E-02	8.7	3.2E-03	8.7E-02	-0.9	5.8E-03	1.2E-01	
O43396	Thioredoxin-like protein 1	TXNL1	8.0E-03	1.4E-01	45.9	2.5E-03	9.4E-02	-4.8	6.4E-03	1.5E-01	-33.4	6.7E-02	3.8E-01	2.5	9.2E-02	2.8E-01	
P27169	Serum paraoxonase/arylesterase 1	PON1	1.1E-02	1.5E-01	6.9	2.8E-02	3.4E-01	-0.6	8.2E-02	3.5E-01	-11.1	2.6E-03	7.8E-02	1.0	3.1E-02	2.2E-01	
Q9ZNZ4	EH domain-containing protein 2	EHD2	3.1E-03	7.4E-02	-1.2	2.0E-01	6.9E-01	0.2	4.7E-02	2.9E-01	3.3	2.6E-03	7.8E-02	-0.3	5.6E-03	1.2E-01	
P00352	Retinal dehydrogenase 1	ALDH1A1	1.4E-02	1.7E-01	-1.9	6.5E-03	1.8E-01	0.3	2.8E-03	8.6E-02	2.3	5.4E-03	1.1E-01	-0.2	8.1E-03	1.4E-01	
Q13885	Tubulin beta-2A chain	TUBB2A	8.5E-03	1.4E-01	-0.8	8.1E-02	5.3E-01	0.1	2.7E-02	2.5E-01	1.6	2.8E-03	8.1E-02	-0.1	1.1E-02	1.5E-01	
P09543	2',3'-cyclic-nucleotide 3'-phosphodiesterase	CNP	1.1E-02	1.5E-01	-8.7	7.5E-03	2.0E-01	2.3	8.9E-03	1.7E-01	11.4	3.2E-03	8.7E-02	-0.9	2.7E-02	2.1E-01	
P62158	Calmodulin	CALM1	3.6E-02	2.8E-01	-6.3	8.8E-02	5.4E-01	1.2	5.3E-02	3.0E-01	11.1	1.1E-02	1.7E-01	-1.5	3.4E-03	1.1E-01	
Q07065	Cytoskeleton-associated protein 4	CKAP4	2.6E-02	2.4E-01	14.6	1.0E-02	2.4E-01	-2.2	5.4E-03	1.4E-01	-16.9	1.2E-02	1.7E-01	1.8	3.5E-03	1.1E-01	
Q9BQE3	Tubulin alpha-1C chain	TUBA1C	8.7E-03	1.4E-01	-1.0	1.2E-01	6.0E-01	0.2	5.1E-02	2.9E-01	2.1	3.6E-03	8.9E-02	-0.2	2.6E-02	2.1E-01	

P02545	Adenyl cyclase-associated protein 1	CAP1	1.1E-02	1.5E-01	-1.6	8.9E-02	5.4E-01	0.3	4.6E-02	2.9E-01	3.2	3.6E-03	8.9E-02	-0.3	4.3E-03	1.1E-01
P61160	Actin-related protein 2	ACTR2	1.2E-02	1.6E-01	10.6	3.8E-03	1.2E-01	-1.1	2.0E-02	2.4E-01	-11.5	8.3E-03	1.5E-01	0.6	1.3E-01	3.2E-01
P10768	S-formylglutathione hydrolase	ESD	1.4E-02	1.7E-01	-5.7	5.1E-02	4.5E-01	0.8	4.7E-02	2.9E-01	10.0	3.8E-03	8.9E-02	-0.9	4.2E-03	1.1E-01
P55268	Cell division control protein 42 homolog	CDC42	4.1E-02	2.8E-01	-1.5	3.4E-02	3.6E-01	0.3	1.8E-02	2.4E-01	2.1	1.2E-02	1.7E-01	-0.3	3.9E-03	1.1E-01
P98095	Fibulin-2	FBLN2	1.6E-02	1.8E-01	3.3	2.6E-02	3.4E-01	-0.4	2.9E-02	2.5E-01	-5.0	4.1E-03	9.1E-02	0.3	3.5E-02	2.3E-01
P07602	Prosaposin	PSAP	1.5E-02	1.7E-01	23.5	4.2E-03	1.3E-01	-2.4	1.1E-02	1.9E-01	-24.7	1.2E-02	1.7E-01	1.9	2.0E-02	2.0E-01
P50395	Rab GDP dissociation inhibitor beta	GDI2	3.5E-02	2.7E-01	4.9	2.8E-02	3.4E-01	-0.9	4.3E-03	1.2E-01	-6.7	1.0E-02	1.7E-01	0.7	4.8E-03	1.1E-01
Q14108	Lysosome membrane protein 2	SCARB2	1.6E-02	1.8E-01	21.8	9.1E-02	5.4E-01	-2.7	4.5E-02	2.9E-01	-42.3	5.1E-03	1.1E-01	4.3	4.8E-03	1.1E-01
P13489	Ribonuclease inhibitor	RNH1	4.9E-03	1.0E-01	3.2	1.5E-01	6.1E-01	-0.4	2.6E-01	4.9E-01	1.9	4.8E-01	6.3E-01	-0.1	5.7E-01	5.0E-01
P06756	Integrin alpha-V	ITGAV	6.6E-03	1.2E-01	29.7	5.4E-03	1.6E-01	-2.5	3.7E-02	2.6E-01	-14.9	2.5E-01	5.1E-01	1.0	3.3E-01	4.2E-01
P52566	Rho GDP-dissociation inhibitor 2	ARHGDIB	2.7E-02	2.4E-01	11.3	1.1E-02	2.4E-01	-1.5	5.4E-03	1.4E-01	-7.3	1.8E-01	4.6E-01	0.5	2.1E-01	3.7E-01
P53396	ATP-citrate synthase	ACLY	2.4E-02	2.3E-01	-8.9	3.0E-02	3.5E-01	2.4	3.0E-02	2.5E-01	13.2	6.2E-03	1.2E-01	-2.0	8.4E-03	1.4E-01
Q15746	Myosin light chain kinase, smooth muscle	MYLK	3.2E-02	2.6E-01	-1.6	3.5E-01	7.4E-01	0.7	1.4E-02	2.1E-01	4.5	2.2E-02	2.3E-01	-0.5	6.9E-03	1.3E-01
P12111	Collagen alpha-3(VI) chain	COL6A3	6.8E-02	3.2E-01	0.6	2.0E-02	3.2E-01	-0.1	7.1E-03	1.6E-01	-0.6	5.8E-02	3.6E-01	0.0	7.4E-02	2.8E-01
P00488	Coagulation factor XIII A chain	F13A1	1.2E-01	3.8E-01	3.8	4.1E-02	4.0E-01	-0.6	7.6E-03	1.7E-01	-4.0	7.1E-02	3.9E-01	0.3	9.0E-02	2.8E-01
O43852	Calumenin	CALU	2.9E-02	2.6E-01	30.0	7.7E-03	2.0E-01	-3.0	2.3E-02	2.4E-01	-28.2	3.6E-02	2.9E-01	2.5	3.9E-02	2.4E-01
P49327	Protein Cuta	CUTA	4.6E-02	2.8E-01	-0.6	2.5E-02	3.4E-01	0.1	2.2E-02	2.4E-01	0.7	1.6E-02	2.0E-01	-0.1	8.3E-03	1.4E-01
P31146	Coronin-1A	CORO1A	4.7E-02	2.8E-01	7.8	1.4E-02	2.6E-01	-1.0	8.3E-03	1.7E-01	-6.6	7.9E-02	4.0E-01	0.6	5.4E-02	2.8E-01
Q9BXN1	Asporin	ASPN	3.1E-02	2.6E-01	11.4	1.1E-02	2.4E-01	-1.4	8.9E-03	1.7E-01	-12.9	1.6E-02	2.0E-01	0.9	4.3E-02	2.5E-01
Q15847	Adipogenesis regulatory factor	ADIRF	1.1E-01	3.8E-01	-12.9	4.8E-02	4.2E-01	1.8	8.3E-02	3.5E-01	15.1	5.1E-02	3.4E-01	-2.0	9.1E-03	1.5E-01
P02649	Apolipoprotein E	APOE	3.3E-02	2.7E-01	3.0	3.2E-02	3.5E-01	-0.3	7.8E-02	3.5E-01	-4.4	9.2E-03	1.6E-01	0.3	6.9E-02	2.8E-01
P31949	Protein S100-A11	S100A11	2.7E-02	2.4E-01	6.6	9.4E-03	2.3E-01	-0.5	1.0E-01	3.7E-01	-4.7	1.3E-01	4.3E-01	0.2	3.5E-01	4.2E-01
P08294	Extracellular superoxide dismutase [Cu-Zn]	SOD3	9.7E-03	1.5E-01	1.0	7.5E-01	8.6E-01	-0.1	8.6E-01	6.8E-01	6.2	9.5E-02	4.2E-01	-0.4	2.2E-01	3.7E-01
P43121	Cell surface glycoprotein MUC18	MCAM	5.2E-02	2.9E-01	-2.7	9.8E-02	5.5E-01	0.5	3.6E-02	2.6E-01	4.6	1.6E-02	2.0E-01	-0.5	9.9E-03	1.5E-01
P20231	Tryptase beta-2	TPSB2	3.2E-02	2.6E-01	6.4	2.1E-02	3.2E-01	-0.6	6.2E-02	3.2E-01	-8.4	1.0E-02	1.7E-01	0.5	5.6E-02	2.8E-01
P62258	14-3-3 protein epsilon	YWHAE	1.6E-02	1.8E-01	-1.2	6.6E-01	8.3E-01	0.2	5.4E-01	6.0E-01	7.1	3.2E-02	2.7E-01	-0.8	1.0E-02	1.5E-01
Q04828	Aldo-keto reductase family 1 member C1	AKR1C1	3.5E-02	2.7E-01	-4.4	1.0E-02	2.4E-01	0.7	1.9E-02	2.4E-01	4.6	2.7E-02	2.6E-01	-0.4	6.5E-02	2.8E-01
P02656	Apolipoprotein C-III	APOC3	3.7E-02	2.8E-01	-20.2	3.2E-02	3.5E-01	2.9	7.6E-02	3.5E-01	28.4	1.1E-02	1.7E-01	-1.7	1.2E-01	3.1E-01
P12277	Creatine kinase B-type	CKB	1.0E-01	3.6E-01	-3.2	9.0E-02	5.4E-01	0.6	2.8E-02	2.5E-01	4.8	3.2E-02	2.7E-01	-0.5	1.1E-02	1.5E-01
Q01518	Prelaminin-A/C	LMNA	1.1E-02	1.5E-01	2.7	1.1E-01	5.6E-01	-0.2	2.3E-01	4.9E-01	0.7	7.2E-01	6.9E-01	-0.2	2.1E-01	3.7E-01
Q969G5	Coronin-1B	CORO1B	2.1E-02	2.2E-01	-4.4	2.2E-01	7.1E-01	0.8	9.2E-02	3.5E-01	10.7	1.1E-02	1.7E-01	-0.9	1.7E-02	1.9E-01
P14625	Endoplasmic reticulum protein	HSP90B1	2.3E-02	2.3E-01	4.7	1.6E-02	2.8E-01	-0.7	1.1E-02	1.9E-01	-2.3	3.2E-01	5.4E-01	0.1	4.9E-01	4.8E-01
Q16527	Cysteine and glycine-rich protein 2	CSRP2	2.7E-02	2.4E-01	-6.7	1.2E-02	2.5E-01	0.8	2.3E-02	2.4E-01	8.0	1.1E-02	1.7E-01	-0.6	2.7E-02	2.1E-01
P12110	Collagen alpha-2(VI) chain	COL6A2	8.0E-02	3.3E-01	1.8	3.3E-02	3.5E-01	-0.3	1.2E-02	2.0E-01	-2.1	3.6E-02	2.9E-01	0.2	3.5E-02	2.3E-01
Q7Z7G0	Target of Nesh-SH3	ABI3BP	4.4E-02	2.8E-01	-3.9	5.9E-02	4.8E-01	0.6	3.1E-02	2.5E-01	6.1	1.2E-02	1.7E-01	-0.5	1.6E-02	1.9E-01
P10643	Complement component C7	CLIC6	4.5E-02	2.8E-01	5.7	1.3E-02	2.5E-01	-0.5	8.9E-02	3.5E-01	-5.1	5.8E-02	3.6E-01	0.2	3.3E-01	4.2E-01
Q96CX2	Chloride intracellular channel protein 6	COL12A1	4.2E-02	2.8E-01	11.1	1.3E-02	2.5E-01	-1.3	2.8E-02	2.5E-01	-8.7	1.0E-01	4.3E-01	0.7	1.2E-01	3.2E-01
Q99715	Collagen alpha-1(XII) chain	COL12A1	4.2E-02	2.8E-01	11.1	1.3E-02	2.5E-01	-1.3	2.8E-02	2.5E-01	-8.7	1.0E-01	4.3E-01	0.7	1.2E-01	3.2E-01
P62942	Peptidyl-prolyl cis-trans isomerase	FKBP1A	1.4E-02	1.7E-01	0.5	3.7E-01	7.5E-01	-0.1	3.6E-01	5.4E-01	-1.7	1.3E-02	1.8E-01	0.1	8.1E-02	2.8E-01
P19105	Myosin regulatory light chain 12A	MLYL12A	4.8E-02	2.8E-01	-10.8	7.4E-02	5.2E-01	1.1	2.0E-01	4.6E-01	17.6	1.4E-02	1.8E-01	-1.2	5.9E-02	2.8E-01
Q16853	Membrane primary amine oxidase	AOC3	2.2E-01	4.5E-01	-1.4	9.1E-02	5.4E-01	0.3	1.4E-02	2.1E-01	1.5	1.1E-01	4.3E-01	-0.1	1.2E-01	3.2E-01
P30040	Endoplasmic reticulum resident protein 29	ERP29	5.0E-02	2.9E-01	29.3	1.4E-02	2.7E-01	-2.7	7.2E-02	3.4E-01	-26.0	6.9E-02	3.8E-01	1.6	1.7E-01	3.5E-01
P09382	Galectin-1	LGALS1	5.7E-02	2.9E-01	-1.7	2.9E-01	7.2E-01	0.5	6.0E-02	3.2E-01	4.0	2.8E-02	2.7E-01	-0.5	1.4E-02	1.8E-01
Q16658	Fascin	FSCN1	4.3E-02	2.8E-01	18.0	1.4E-02	2.7E-01	-1.9	4.5E-02	2.9E-01	-19.7	2.5E-02	2.5E-01	1.3	8.8E-02	2.8E-01
P27824	Calnexin	CANX	3.2E-02	2.6E-01	6.6	1.5E-02	2.7E-01	-0.8	3.5E-02	2.6E-01	-4.0	2.3E-01	5.0E-01	0.1	7.0E-01	5.5E-01
P29401	Transketolase	TKT	8.7E-02	3.3E-01	-1.2	4.1E-01	7.6E-01	0.2	3.3E-01	5.4E-01	3.4	5.1E-02	3.4E-01	-0.5	1.5E-02	1.9E-01
P60981	Destrin	DSTN	6.8E-02	3.2E-01	-2.0	3.5E-01	7.4E-01	0.4	2.1E-01	4.7E-01	5.2	3.7E-02	2.9E-01	-0.6	1.6E-02	1.9E-01
P00736	Complement C1r subcomponent	C1R	2.2E-02	2.2E-01	4.7	2.1E-02	3.2E-01	-0.7	1.6E-02	2.3E-01	-2.0	4.2E-01	6.0E-01	0.1	7.2E-01	5.5E-01
Q12765	Utrophin	UTRN	1.7E-01	4.2E-01	-4.9	4.1E-01	7.6E-01	1.3	1.7E-01	4.4E-01	12.1	8.5E-02	4.1E-01	-1.8	1.6E-02	1.9E-01
P30048	Peroxiredoxin III	PRDX3	4.3E-02	2.8E-01	-13.6	2.2E-02	3.3E-01	1.0	2.1E-01	4.7E-01	16.9	1.6E-02	2.0E-01	-1.1	1.1E-01	3.0E-01
P15088	Mast cell carboxypeptidase A	CPA3	1.6E-01	4.2E-01	6.8	1.5E-01	6.3E-01	-1.2	4.5E-02	2.9E-01	-10.8	5.6E-02	3.5E-01	1.2	1.6E-02	1.9E-01
O60888	Fatty acid synthase	FASN	4.6E-02	2.8E-01	-7.3	1.7E-01	6.4E-01	1.0	1.9E-01	4.6E-01	14.7	1.7E-02	2.0E-01	-1.3	2.6E-02	2.1E-01
P35555	Fibrillin-1	FBN1	1.0E-01	3.7E-01	0.9	8.2E-02	5.3E-01	-0.2	1.7E-02	2.3E-01	-1.3	3.3E-02	2.8E-01	0.1	2.4E-02	2.1E-01
P17858	ATP-dependent 6-phosphofructokinase, liver type	PFKL	8.3E-02	3.3E-01	10.1	4.4E-02	4.0E-01	-1.6	1.7E-02	2.3E-01	-5.6	3.5E-01	5.6E-01	0.4	4.0E-01	4.5E-01
Q8NBX0	UV excision repair protein RAD23 homolog A	RAD23A	2.5E-01	4.5E-01	30.5	1.0E-01	5.5E-01	-5.0	1.7E-02	2.3E-01	-33.8	1.3E-01	4.3E-01	3.2	8.5E-02	2.8E-01

Supplemental Table 11. Regression Models of Association Between Individual Proteins and Extent of Surface Area Involved with Fibrous Plaque (FP) or Normal (NML) in Human Abdominal Aorta Samples (top 100 proteins). In models of %FP, the non-FP% fraction includes fatty streaks (FS) and NML intima. Likewise, in models of % NML, the non-NML fraction includes both FP and FS. Accordingly, we modeled both %FP and %NML separately. We also classified samples into three level ordinal categories of extent of FP and extent of NML and performed ordinal logistic regression (Ord LR). This approach is less statistically powerful, but makes fewer distributional assumptions about the measures of extent of disease. In addition, we used MANOVA to jointly model the distribution of %FP, %FS, and %NML. P-values and q-values ≤ 0.05 are highlighted in green and pink respectively. **Proteins in bold (n=21) are also included in the top 100 LAD proteins.**

Uniprot ID	Protein	Gene	MANOVA (%FP,%FS)		GLM (%FP)			Ord LR (%FP)			GLM (% NML)			Ord LR (%NML)		
			p-value	q-value	beta	p-value	q-value	beta	p-value	q-value	beta	p-value	q-value	beta	p-value	q-value
P04114	Apolipoprotein B-100	APOB	4.08E-15	1.64E-12	1.01	4.17E-16	1.42E-13	-0.11	6.33E-05	1.13E-02	-0.71	2.08E-04	2.82E-02	0.05	2.32E-02	4.19E-01
P02649	Apolipoprotein E	APOE	2.64E-14	5.31E-12	9.39	4.77E-15	8.12E-13	-0.72	3.96E-04	2.45E-02	-8.79	9.69E-07	4.72E-04	0.53	3.88E-03	4.19E-01
O43866	CD5 antigen-like	CD5L	2.28E-13	3.06E-11	23.47	2.16E-14	2.45E-12	-3.57	6.57E-06	2.35E-03	-17.32	2.20E-04	2.82E-02	0.97	2.49E-02	4.19E-01
P00747	Plasminogen	PLG	5.98E-12	6.01E-10	7.58	1.48E-12	1.26E-10	-0.56	1.42E-03	3.05E-02	-4.55	5.14E-03	1.43E-01	0.19	1.35E-01	5.04E-01
P19823	Inter-alpha-trypsin inhibitor	ITIH2	9.60E-11	7.72E-09	10.63	3.94E-11	2.68E-09	-0.92	8.50E-04	3.05E-02	-5.77	1.71E-02	2.61E-01	0.32	1.00E-01	4.76E-01
P07339	Cathepsin D	CTSD	2.08E-09	1.11E-07	21.06	2.59E-10	1.37E-08	-1.67	3.20E-03	4.29E-02	-18.24	1.72E-04	2.82E-02	1.07	1.86E-02	4.19E-01
P40121	Macrophage-capping protein	CAPG	4.22E-10	2.83E-08	23.61	2.82E-10	1.37E-08	-1.43	7.37E-03	6.43E-02	-25.64	1.48E-06	4.72E-04	2.57	1.96E-03	4.19E-01
P01892	HLA class I HC Ag, A-2 alpha	HLA-A	3.97E-09	1.77E-07	20.85	4.47E-10	1.90E-08	-1.76	4.80E-04	2.45E-02	-16.10	1.02E-03	5.59E-02	1.05	1.50E-02	4.19E-01
P27169	Serum paraoxonase 1	PON1	2.22E-09	1.11E-07	19.28	5.05E-10	1.91E-08	-1.62	9.99E-03	6.76E-02	-11.51	1.23E-02	2.18E-01	0.42	3.21E-01	6.30E-01
P00739	Haptoglobin-related protein	HPR	9.08E-09	3.04E-07	14.51	1.11E-09	3.79E-08	-1.30	3.52E-03	4.29E-02	-10.60	2.40E-03	7.80E-02	0.85	1.74E-02	4.19E-01
P24821	Tenascin	TNC	1.21E-08	3.46E-07	2.23	1.40E-09	4.34E-08	-0.11	1.90E-02	8.04E-02	-1.79	8.55E-04	5.59E-02	0.08	8.27E-02	4.70E-01
P07858	Cathepsin B	CTSB	1.07E-08	3.32E-07	17.11	1.80E-09	5.10E-08	-1.00	1.52E-02	7.52E-02	-11.05	8.26E-03	1.76E-01	0.59	1.45E-01	5.17E-01
P01871	Ig mu chain C region	IGHM	5.90E-09	2.37E-07	6.48	1.99E-09	5.21E-08	-0.77	1.10E-04	1.22E-02	-3.53	2.71E-02	3.02E-01	0.18	1.51E-01	5.17E-01
P13796	Plastin-2	LCP1	1.96E-08	5.25E-07	11.39	2.32E-09	5.64E-08	-0.60	1.15E-02	6.76E-02	-9.18	9.26E-04	5.59E-02	0.58	4.32E-02	4.59E-01
P05090	Apolipoprotein D	APOD	7.04E-09	2.57E-07	23.52	2.15E-08	4.29E-07	-1.90	9.70E-04	3.05E-02	-7.87	2.04E-01	5.95E-01	0.22	6.12E-01	7.29E-01
P04003	C4b-binding protein	C4BPA	6.70E-08	1.50E-06	6.27	8.23E-09	1.87E-07	-0.46	3.30E-03	4.29E-02	-4.96	1.64E-03	6.98E-02	0.36	1.08E-02	4.19E-01
P00734	Prothrombin	F2	5.62E-08	1.33E-06	10.31	1.82E-08	3.86E-07	-0.67	1.06E-02	6.76E-02	-5.57	3.80E-02	3.20E-01	0.41	8.28E-02	4.70E-01
P01023	Alpha-2-macroglobulin	A2M	2.34E-08	5.89E-07	2.87	2.26E-07	3.50E-06	-0.28	1.45E-03	3.05E-02	-0.62	4.42E-01	7.70E-01	0.00	9.33E-01	8.06E-01
P05546	Heparin cofactor 2	SERPIND	3.92E-07	7.16E-06	27.74	7.47E-08	1.41E-06	-1.90	6.08E-03	5.88E-02	-17.35	2.04E-02	2.90E-01	0.67	2.67E-01	6.04E-01
P20742	Pregnancy zone protein	PZP	1.38E-07	2.92E-06	26.87	1.63E-07	2.77E-06	-2.17	2.20E-02	8.33E-02	-10.27	1.70E-01	5.85E-01	0.10	8.52E-01	7.90E-01
P01031	Complement C5	C5	9.55E-07	1.60E-05	7.22	1.46E-07	2.61E-06	-0.65	3.59E-03	4.29E-02	-6.37	1.14E-03	5.59E-02	0.40	2.01E-02	4.19E-01
P02647	Apolipoprotein A-I	APOA1	2.07E-07	3.97E-06	7.40	1.86E-07	3.01E-06	-0.81	2.17E-03	3.64E-02	-3.01	1.45E-01	5.32E-01	-0.01	9.20E-01	8.06E-01
P04179	Superoxide dismutase	SOD2	1.90E-07	3.81E-06	55.81	2.58E-07	3.81E-06	-3.31	1.62E-02	7.64E-02	-20.26	1.99E-01	5.95E-01	0.17	8.79E-01	7.96E-01
P02671	Fibrinogen alpha chain	FGA	1.32E-06	2.12E-05	3.47	2.79E-07	3.95E-06	-0.23	1.09E-02	6.76E-02	-2.10	3.15E-02	3.10E-01	0.09	2.24E-01	5.97E-01
Q9UJ70	N-acetyl-D-glucosamine kinase	NAGK	3.50E-06	4.42E-05	70.08	5.24E-07	7.14E-06	-4.04	5.13E-02	1.22E-01	-59.67	2.68E-03	8.14E-02	2.25	2.05E-01	5.91E-01
O14791	Apolipoprotein L1	APOL1	2.61E-06	3.62E-05	33.46	5.64E-07	7.39E-06	-2.76	1.13E-02	6.76E-02	-20.07	3.72E-02	3.20E-01	0.87	3.16E-01	6.29E-01
P55268	Laminin subunit beta-2	LAMB2	5.70E-07	9.96E-06	-2.91	2.90E-06	2.74E-05	0.23	9.12E-03	6.76E-02	-0.59	5.08E-01	8.10E-01	-0.03	6.17E-01	7.29E-01
P02675	Fibrinogen beta chain	FGB	2.92E-06	3.91E-05	1.15	6.85E-07	8.40E-06	-0.06	2.28E-02	8.33E-02	-0.67	4.47E-02	3.43E-01	0.03	2.32E-01	5.99E-01
P35442	Thrombospondin-2	THBS2	4.77E-06	5.81E-05	5.24	6.91E-07	8.40E-06	-0.39	3.55E-03	4.29E-02	-4.11	6.38E-03	1.52E-01	0.25	3.54E-02	4.59E-01
P04080	Cystatin-B	CSTB	3.52E-06	4.42E-05	47.93	8.58E-07	1.01E-05	-4.84	1.72E-03	3.43E-02	-27.51	4.96E-02	3.51E-01	0.29	7.69E-01	7.66E-01
O14818	Proteasome subunit alpha-type-7	PSMA7	7.03E-06	7.85E-05	88.12	1.08E-06	1.23E-05	-5.38	2.07E-02	8.04E-02	-63.83	1.34E-02	2.29E-01	1.73	3.78E-01	6.54E-01
P02679	Fibrinogen gamma	FGG	5.91E-06	6.93E-05	2.44	1.21E-06	1.33E-05	-0.14	2.33E-02	8.33E-02	-1.50	3.78E-02	3.20E-01	0.07	2.14E-01	5.94E-01
P04004	Vitronectin	VTN	6.03E-06	6.93E-05	7.65	1.28E-06	1.37E-05	-0.62	7.66E-03	6.53E-02	-7.42	8.44E-04	5.59E-02	0.41	2.38E-02	4.19E-01
Q9NZU5	LIM and cysteine-rich domains protein 1	LMCD1	2.29E-06	3.41E-05	-7.02	1.57E-06	1.62E-05	0.82	4.61E-04	2.45E-02	2.88	1.72E-01	5.85E-01	-0.20	1.70E-01	5.37E-01
P11047	Laminin subunit gamma-1	LAMC1	2.28E-06	3.41E-05	-3.59	6.39E-05	4.63E-04	0.29	2.03E-02	8.04E-02	-0.14	9.13E-01	8.64E-01	0.00	9.74E-01	8.08E-01
P98160	Basement membrane-specific heparan sulfate	HSPG2	2.44E-06	3.50E-05	-1.03	2.30E-06	2.31E-05	0.14	8.44E-04	3.05E-02	0.38	2.28E-01	6.32E-01	-0.03	2.61E-01	6.04E-01
P0C0L5	Complement C4-B	C4B	1.77E-05	1.83E-04	3.14	2.83E-06	2.74E-05	-0.21	1.97E-02	8.04E-02	-2.29	1.66E-02	2.60E-01	0.14	6.14E-02	4.70E-01
P05155	Plasma protease C1 inhibitor	SERPING1	2.68E-05	2.69E-04	11.82	5.01E-06	4.56E-05	-0.94	1.56E-02	7.52E-02	-7.73	3.61E-02	3.20E-01	0.50	6.90E-02	4.70E-01
P11216	Glycogen phosphorylase, brain	PYGB	3.11E-05	3.02E-04	-8.84	5.09E-06	4.56E-05	1.29	1.36E-04	1.22E-02	7.49	6.19E-03	1.52E-01	-0.54	8.86E-03	4.19E-01
Q15124	Phosphoglucomutase-like protein 5	PGM5	3.16E-05	3.02E-04	-4.59	6.29E-06	5.48E-05	0.51	2.19E-03	3.64E-02	4.33	2.44E-03	7.80E-02	-0.26	2.00E-02	4.19E-01
O00159	Unconventional myosin-Ic	MYO1C	8.01E-06	8.70E-05	-5.81	4.43E-05	3.51E-04	0.60	4.68E-03	4.79E-02	0.67	7.42E-01	8.46E-01	-0.02	8.83E-01	7.96E-01
O15230	Laminin subunit alpha-5	LAMA5	8.97E-06	9.49E-05	-2.00	4.07E-05	3.30E-04	0.17	1.58E-02	7.52E-02	0.27	6.94E-01	8.46E-01	-0.01	8.63E-01	7.92E-01
P02792	Ferritin light chain	FTL	7.19E-05	6.42E-04	13.07	2.71E-05	2.31E-04	-0.60	1.33E-01	1.91E-01	-14.43	8.40E-04	5.59E-02	0.80	2.17E-02	4.19E-01
Q14315	Filamin-C	FLNC	1.98E-04	1.59E-03	-2.67	3.54E-05	2.94E-04	0.33	2.37E-03	3.68E-02	1.96	3.11E-02	3.10E-01	-0.11	9.75E-02	4.76E-01
P08133	Annexin A6	ANXA6	5.29E-05	4.95E-04	-4.62	5.31E-05	4.11E-04	0.52	1.08E-02	6.76E-02	1.39	3.91E-01	7.52E-01	-0.07	5.45E-01	7.03E-01
P01024	Complement C3	C3	2.13E-04	1.68E-03	1.78	5.90E-05	4.46E-04	-0.11	5.49E-02	1.26E-01	-0.96	1.24E-01	5.01E-01	0.05	2.86E-01	6.14E-01
P52209	6-phosphogluconate dehydrogenase	PGD	1.76E-04	1.47E-03	19.04	6.06E-05	4.48E-04	-0.77	1.96E-01	2.32E-01	-9.25	1.69E-01	5.85E-01	0.19	7.16E-01	7.49E-01
P02768	Serum albumin	ALB	7.09E-05	6.42E-04	0.24	6.86E-05	4.86E-04	-0.02	1.81E-02	8.03E-02	-0.07	3.99E-01	7.52E-01	0.00	4.40E-01	6.77E-01
Q9UBR2	Cathepsin Z	CTSZ	1.96E-04	1.59E-03	33.51	7.45E-05	5.12E-04	-2.14	3.35E-02	9.66E-02	-37.34	1.43E-03	6.52E-02	1.49	1.01E-01	4.76E-01
P21333	Filamin-A	FLNA	1.10E-04	9.59E-04	-0.50	7.52E-05	5.12E-04	0.05	9.91E-03	6.76E-02	0.18	3.26E-01	7.06E-01	-0.01	3.69E-01	6.54E-01
P08603	Complement factor H	CFH	4.27E-04	2.85E-03	2.85	8.70E-05	5.80E-04	-0.21	3.07E-02	9.31E-02	-2.60	1.04E-02	2.03E-01	0.13	8.81E-02	4.70E-01
Q15063	Periostin	POSTN	4.00E-04	2.82E-03	2.23	9.40E-05	6.05E-04	-0.19	1.07E-02	6.76E-02	-2.18	6.10E-03	1.52E-			

P04196	Histidine-rich glycoprotein	HRG	6.63E-04	4.23E-03	8.46	1.42E-04	8.81E-04	-0.85	8.89E-03	6.76E-02	-7.85	1.13E-02	2.07E-01	0.34	1.29E-01	5.04E-01
O76070	Gamma-synuclein	SNCG	7.68E-04	4.68E-03	15.28	1.47E-04	8.90E-04	-2.03	9.20E-04	3.05E-02	-11.71	3.77E-02	3.20E-01	0.70	9.01E-02	4.70E-01
P16112	Aggrecan core protein	ACAN	1.49E-04	1.28E-03	-2.93	2.28E-04	1.27E-03	0.52	1.35E-03	3.05E-02	0.59	5.97E-01	8.16E-01	-0.01	8.66E-01	7.92E-01
P00450	Ceruloplasmin	CP	3.74E-04	2.69E-03	4.15	1.68E-04	1.00E-03	-0.28	5.32E-02	1.25E-01	-1.73	2.66E-01	6.54E-01	0.07	5.15E-01	6.93E-01
Q9NR12	PDZ and LIM domain protein 7	PDLIM7	8.75E-04	5.05E-03	-7.92	1.77E-04	1.04E-03	1.01	1.99E-03	3.64E-02	5.53	6.18E-02	3.84E-01	-0.52	1.85E-02	4.19E-01
P19827	Inter-alpha-trypsin inhibitor heavy chain H1	ITIH1	1.09E-03	5.79E-03	6.68	2.16E-04	1.25E-03	-0.62	1.28E-02	7.15E-02	-5.58	2.70E-02	3.02E-01	0.32	8.01E-02	4.70E-01
P35749	Myosin-11	MYH11	6.78E-04	4.26E-03	-0.33	2.24E-04	1.27E-03	0.03	1.54E-02	7.52E-02	0.16	1.99E-01	5.95E-01	-0.01	1.11E-01	4.79E-01
P43121	Cell surface glycoprotein MUC18	MCAM	2.45E-04	1.86E-03	-3.74	4.66E-02	7.31E-02	0.36	1.80E-01	2.24E-01	-4.20	1.02E-01	4.54E-01	0.26	1.54E-01	5.17E-01
P00740	Coagulation factor IX	F9	4.14E-04	2.85E-03	11.84	2.56E-04	1.40E-03	-0.95	2.28E-02	8.33E-02	-14.56	1.06E-03	5.59E-02	0.72	3.45E-02	4.59E-01
P06312	Ig kappa chain V-IV region (Fragment)	IGKV4-1	2.61E-04	1.94E-03	19.67	7.48E-03	2.02E-02	-1.38	1.49E-01	2.05E-01	8.57	4.01E-01	7.52E-01	-0.74	3.02E-01	6.27E-01
O43707	Alpha-actinin-4	ACTN4	1.07E-03	5.75E-03	-1.23	2.70E-04	1.46E-03	0.13	1.13E-02	6.76E-02	0.72	1.31E-01	5.04E-01	-0.04	2.07E-01	5.91E-01
P12111	Collagen alpha-3(VI)	COL6A3	9.82E-04	5.56E-03	1.13	2.94E-04	1.56E-03	-0.06	1.40E-01	1.96E-01	-0.59	1.81E-01	5.91E-01	0.02	5.79E-01	7.20E-01
P18206	Vinculin	VCL	1.06E-03	5.75E-03	-2.28	3.29E-04	1.72E-03	0.26	7.85E-03	6.53E-02	1.16	1.93E-01	5.95E-01	-0.08	2.03E-01	5.91E-01
P30613	Pyruvate kinase PKLR	PKLR	1.28E-03	6.69E-03	65.77	6.80E-03	1.86E-02	-4.71	1.37E-01	1.95E-01	-	3.82E-04	4.07E-02	5.58	3.84E-02	4.59E-01
Q96HC4	PDZ and LIM domain protein 5	PDLIM5	4.20E-04	2.85E-03	-6.65	1.05E-02	2.58E-02	1.22	6.69E-03	6.19E-02	3.13	3.84E-01	7.52E-01	0.11	6.43E-01	7.34E-01
P37837	Transaldolase	TALDO1	8.79E-04	5.05E-03	43.34	4.24E-04	2.19E-03	-2.18	9.85E-02	1.66E-01	-51.49	2.34E-03	7.80E-02	0.58	6.33E-01	7.33E-01
P01834	Ig kappa chain C region	IGKC	4.33E-04	2.85E-03	3.37	4.14E-03	1.27E-02	-0.22	1.33E-01	1.91E-01	0.75	6.48E-01	8.31E-01	-0.12	3.17E-01	6.29E-01
Q06828	Fibromodulin	FMOD	5.13E-04	3.32E-03	-5.23	3.45E-02	5.84E-02	0.76	5.50E-02	1.26E-01	-4.56	1.80E-01	5.91E-01	0.20	4.03E-01	6.60E-01
P31146	Coronin-1A	CORO1A	2.53E-03	1.24E-02	15.69	5.55E-04	2.82E-03	-1.05	3.97E-02	1.07E-01	-13.97	2.70E-02	3.02E-01	0.49	2.78E-01	6.12E-01
O43294	Transforming growth factor beta-1-induced transcript 1 protein	TGFB1I1	2.70E-03	1.31E-02	-5.48	5.90E-04	2.95E-03	0.44	5.06E-02	1.21E-01	3.81	8.70E-02	4.31E-01	-0.24	1.31E-01	5.04E-01
P39060	Collagen alpha-1(XVIII) chain	COL18A1	2.07E-03	1.04E-02	-5.45	6.30E-04	3.11E-03	0.57	2.90E-02	9.09E-02	2.82	2.07E-01	5.96E-01	-0.04	8.12E-01	7.83E-01
P06727	Apolipoprotein A-IV	APOA4	3.01E-03	1.41E-02	7.40	6.61E-04	3.21E-03	-0.91	1.15E-02	6.76E-02	-5.19	8.72E-02	4.31E-01	0.16	4.52E-01	6.79E-01
P63244	Guanine nucleotide-binding protein G(B1L)	GNB2L1	2.88E-03	1.36E-02	28.04	6.73E-04	3.22E-03	-2.07	6.95E-02	1.39E-01	-26.09	2.26E-02	3.02E-01	0.73	3.67E-01	6.54E-01
Q9Y490	Talin-1	TLN1	1.88E-03	9.58E-03	-1.45	7.12E-04	3.36E-03	0.21	3.45E-03	4.29E-02	0.65	2.82E-01	6.69E-01	-0.08	5.45E-02	4.70E-01
P05156	Complement factor I	CFI	7.24E-04	4.48E-03	17.78	1.42E-03	5.95E-03	-0.77	2.59E-01	2.63E-01	-1.56	8.41E-01	8.58E-01	-0.30	5.86E-01	7.20E-01
P00488	Coagulation factor XIII A chain	F13A1	3.57E-03	1.63E-02	9.72	7.67E-04	3.58E-03	-0.72	2.81E-02	8.97E-02	-8.01	4.64E-02	3.47E-01	0.54	8.38E-02	4.70E-01
P01620	Ig kappa chain V-III region SIE	IGKV3-20	8.15E-04	4.89E-03	12.69	4.33E-03	1.31E-02	-0.53	3.02E-01	2.86E-01	1.84	7.67E-01	8.46E-01	-0.18	6.69E-01	7.44E-01
P00736	Complement C1r subcomponent	C1R	3.35E-03	1.55E-02	11.46	8.30E-04	3.82E-03	-0.78	8.33E-02	1.57E-01	-7.05	1.41E-01	5.28E-01	0.03	9.23E-01	8.06E-01
Q08431	Lactadherin	MFGE8	8.32E-04	4.92E-03	-3.70	3.63E-03	1.20E-02	0.43	2.02E-02	8.04E-02	-0.37	8.36E-01	8.58E-01	-0.01	9.32E-01	8.06E-01
P59665	Neutrophil defensin 1	DEF A1	1.00E-03	5.60E-03	28.10	9.28E-04	4.21E-03	-3.00	1.24E-02	7.05E-02	-6.59	5.80E-01	8.16E-01	-0.02	9.83E-01	8.08E-01
Q14112	Nidogen-2	NID2	4.44E-03	1.94E-02	28.59	1.04E-03	4.66E-03	-3.01	5.49E-03	5.45E-02	-26.02	3.14E-02	3.10E-01	1.73	5.85E-02	4.70E-01
P50895	Basal cell adhesion molecule	BCAM	1.05E-03	5.75E-03	-5.67	1.99E-03	7.62E-03	0.51	4.69E-02	1.19E-01	0.41	8.72E-01	8.64E-01	-0.01	9.38E-01	8.06E-01
Q96PD5	N-acetylmuramoyl-L-alanine amidase	PGLYRP2	2.77E-03	1.33E-02	13.60	1.09E-03	4.83E-03	-1.19	2.75E-02	8.97E-02	-5.84	3.16E-01	7.06E-01	0.12	7.72E-01	7.67E-01
P12109	Collagen alpha-1(VI) chain	COL6A1	4.92E-03	2.13E-02	2.64	1.14E-03	4.96E-03	-0.21	7.63E-02	1.48E-01	-1.81	1.10E-01	4.70E-01	0.09	2.66E-01	6.04E-01
Q99497	Protein deglycase DJ-1	PARK7	2.55E-02	6.17E-02	-9.80	6.84E-03	1.86E-02	2.08	1.29E-03	3.05E-02	8.74	8.05E-02	4.21E-01	-0.70	5.58E-02	4.70E-01
P05062	Fructose-biphosphate aldolase B	ALDOB	2.26E-02	5.85E-02	-7.17	8.01E-03	2.12E-02	1.50	1.30E-03	3.05E-02	7.92	3.29E-02	3.10E-01	-0.49	7.12E-02	4.70E-01
Q9BXR6	Complement factor H-related protein 5	CFHR5	5.32E-03	2.23E-02	28.81	1.31E-03	5.66E-03	-1.34	2.10E-01	2.38E-01	-18.32	1.43E-01	5.30E-01	0.06	9.48E-01	8.08E-01
Q13361	Microfibrillar-associated protein 5	MFAP5	6.17E-03	2.45E-02	33.64	1.41E-03	5.95E-03	-2.13	1.08E-01	1.72E-01	-28.59	5.05E-02	3.51E-01	-0.71	4.89E-01	6.91E-01
P46952	3-hydroxyanthranilate 3,4-dioxygenase	HAAO	3.23E-02	7.13E-02	-14.05	8.90E-03	2.23E-02	5.09	1.42E-03	3.05E-02	12.53	9.08E-02	4.31E-01	-0.84	1.12E-01	4.80E-01
P08758	Annexin A5	ANXA5	5.21E-03	2.20E-02	-6.24	1.46E-03	6.07E-03	0.94	6.86E-03	6.19E-02	3.50	2.01E-01	5.95E-01	-0.33	9.23E-02	4.70E-01
Q13418	Integrin-linked protein kinase	ILK	1.68E-03	8.65E-03	-7.10	1.48E-03	6.07E-03	0.87	8.57E-03	6.76E-02	1.61	6.06E-01	8.16E-01	-0.01	9.75E-01	8.08E-01
P21291	Cysteine and glycine-rich protein 1	CSRP1	6.65E-03	2.57E-02	-6.17	1.55E-03	6.27E-03	0.83	1.20E-02	6.92E-02	4.34	1.10E-01	4.70E-01	-0.29	1.33E-01	5.04E-01
P10909	Clusterin	CLU	6.62E-03	2.57E-02	6.63	1.70E-03	6.81E-03	-0.35	1.94E-01	2.32E-01	-6.35	2.97E-02	3.10E-01	0.32	1.37E-01	5.04E-01
P00738	Haptoglobin	HP	4.41E-03	1.94E-02	1.15	1.82E-03	7.20E-03	-0.07	8.10E-02	1.54E-01	-0.47	3.59E-01	7.32E-01	0.05	2.05E-01	5.91E-01
Q92747	Actin-related protein 2/3 complex subunit 1A	ARPC1A	8.33E-03	2.93E-02	-85.33	1.92E-03	7.50E-03	13.45	4.31E-03	4.57E-02	66.51	8.16E-02	4.21E-01	-1.70	5.24E-01	6.95E-01
P51884	Lumican	LUM	8.38E-03	2.93E-02	6.76	1.98E-03	7.62E-03	-0.71	1.78E-02	8.03E-02	-4.82	1.13E-01	4.73E-01	0.15	4.72E-01	6.89E-01

Supplemental Table 12. Up-Regulated Proteins in LAD Fibrous Plaque Samples (n=15) Compared with Normal LAD Samples (n=30). Samples were selected using patho-proteomic phenotyping designed to integrate pathologist assessment of extent of disease and CAM deconvolution of global protein profiles (fold-change = mean FP / mean NL).

Uniprot ID		Protein	Gene	Fold change	q-value
P24821	Tenascin		TNC	13.04	1.08E-03
P07996	Thrombospondin-1		THBS1	10.05	2.06E-03
P13796	Plastin-2		LCP1	3.87	9.80E-04
P04114	Apolipoprotein B-100		APOB	3.65	6.26E-04
P07858	Cathepsin B		CTSB	3.63	3.13E-04
P40121	Macrophage-capping protein		CAPG	2.72	6.89E-03
P35442	Thrombospondin-2		THBS2	2.69	4.40E-04
P13760	HLA class II histocompatibility antigen, DRB1-4 beta chain		HLA-DRB1	2.57	1.02E-02
P05783	Keratin, type I cytoskeletal 18		KRT18	2.55	4.20E-02
P27169	Serum paraoxonase/arylesterase 1		PON1	2.21	3.75E-02
Q9UBR2	Cathepsin Z		CTSZ	2.20	9.53E-04
P01871	Ig mu chain C region		IGHM	2.15	8.14E-03
P31146	Coronin-1A		CORO1A	2.13	1.22E-02
O43866	CD5 antigen-like		CD5L	2.10	1.22E-02
P08519	Apolipoprotein(a)		LPA	1.97	1.08E-02
Q15063	Periostin		POSTN	1.94	5.47E-04
P01031	Complement C5		C5	1.89	1.58E-02
Q15582	Transforming growth factor-beta-induced protein ig-h3		TGFBI	1.86	2.41E-03
P02649	Apolipoprotein E		APOE	1.79	1.28E-02
P40261	Nicotinamide N-methyltransferase		NNMT	1.74	1.08E-02
Q8IUX7	Adipocyte enhancer-binding protein 1		AEBP1	1.71	4.77E-03

Supplemental Table 13. Down-Regulated Proteins in LAD Fibrous Plaque Samples (n=15) Compared with Normal LAD Samples (n=30). Samples were selected using patho-proteomic phenotyping designed to integrate pathologist assessment of extent of disease and CAM deconvolution of global protein profiles. (For down regulated proteins Fold-change = -1* mean NL/mean FP.)

Uniprot ID	Protein	Gene	Fold-change	q-value
P07197	Neurofilament medium polypeptide	NEFM	-5.70	3.42E-02
P49327	Fatty acid synthase	FASN	-5.40	1.55E-05
P15090	Fatty acid-binding protein, adipocyte	FABP4	-3.58	6.87E-03
P07196	Neurofilament light polypeptide	NEFL	-3.27	2.45E-02
Q96Q06	Perilipin-4	PLIN4	-2.53	2.90E-04
P09543	2',3'-cyclic-nucleotide 3'-phosphodiesterase	CNP	-2.50	2.77E-04
P33121	Long-chain-fatty-acid-CoA ligase 1	ACSL1	-2.41	4.90E-04
P11586	C-1-tetrahydrofolate synthase, cytoplasmic	MTHFD1	-2.28	1.55E-05
O60240	Perilipin-1	PLIN1	-2.24	3.13E-04
P22695	Cytochrome b-c1 complex subunit 2, mitochondrial	UQCRC2	-2.19	3.13E-04
P23634	Plasma membrane calcium-transporting ATPase 4	ATP2B4	-2.18	2.77E-04
Q68CZ2	Tensin-3	TNS3	-2.17	2.22E-03
Q05469	Hormone-sensitive lipase	LIPE	-2.16	1.36E-03
O43301	Heat shock 70 kDa protein 12A	HSPA12A	-2.13	4.90E-04
Q86TX2	Acyl-coenzyme A thioesterase 1	ACOT1	-2.11	9.01E-04
Q16363	Laminin subunit alpha-4	LAMA4	-2.10	4.90E-04
O43175	D-3-phosphoglycerate dehydrogenase	PHGDH	-2.09	2.77E-04
Q16698	2,4-dienoyl-CoA reductase, mitochondrial	DECR1	-2.08	5.47E-04
P11532	Dystrophin	DMD	-2.07	5.47E-04
P16930	Fumarylacetoacetate	FAH	-2.05	9.53E-04
Q02952	A-kinase anchor protein 12	AKAP12	-2.03	3.13E-04
Q9UN36	Protein NDRG2	NDRG2	-2.02	2.06E-03
Q9HBL0	Tensin-1	TNS1	-2.01	5.58E-04
P21695	Glycerol-3-phosphate dehydrogenase [NAD(+)], cytoplasmic	GPD1	-1.99	1.96E-04
Q9BSJ8	Extended synaptotagmin-1	ESYT1	-1.98	1.07E-03
O75112	LIM domain-binding protein 3	LDB3	-1.98	1.70E-02
P49748	Very long-chain specific acyl-CoA dehydrogenase, mitochondrial	ACADVL	-1.96	4.41E-04
P53396	ATP-citrate synthase	ACLY	-1.95	2.06E-03
O95810	Serum deprivation-response protein	SDPR	-1.95	5.67E-04
P48163	NADP-dependent malic enzyme	ME1	-1.95	3.46E-03
P31323	cAMP-dependent protein kinase type II-beta regulatory subunit	PRKAR2B	-1.94	2.05E-02
Q99685	Monoglyceride lipase	MGLL	-1.94	1.55E-03
Q13683	Integrin alpha-7	ITGA7	-1.90	3.46E-03
Q2UY09	Collagen alpha-1(XXVIII) chain	COL28A1	-1.90	1.92E-03
P46821	Microtubule-associated protein 1B	MAP1B	-1.90	4.59E-03
Q96JY6	PDZ and LIM domain protein 2	PDLIM2	-1.89	3.61E-03
O75390	Citrate synthase, mitochondrial	CS	-1.88	1.88E-03
P13804	Electron transfer flavoprotein subunit alpha, mitochondrial	ETFA	-1.87	2.77E-04
P21397	Amine oxidase [flavin-containing] A	MAOA	-1.87	5.24E-04
Q6YN16	Hydroxysteroid dehydrogenase-like protein 2	HSDL2	-1.86	5.47E-04

P31930	Cytochrome b-c1 complex subunit 1, mitochondrial	UQCRC1	-1.86	1.10E-03
P23141	Liver carboxylesterase 1	CES1	-1.86	9.39E-03
Q9BT4	Transmembrane protein 43	TMEM43	-1.84	1.08E-03
Q15836	Vesicle-associated membrane protein 3	VAMP3	-1.82	1.86E-03
Q14112	Nidogen-2	NID2	-1.81	5.47E-04
Q13011	Delta(3,5)-Delta(2,4)-dienoyl-CoA isomerase, mitochondrial	ECH1	-1.81	4.59E-03
Q99798	Aconitate hydratase, mitochondrial	ACO2	-1.80	1.96E-04
P09622	Dihydrolipoyl dehydrogenase, mitochondrial	DLD	-1.80	3.88E-04
P11177	Pyruvate dehydrogenase E1 component subunit beta, mitochondrial	PDHB	-1.80	1.08E-03
P14854	Cytochrome c oxidase subunit 6B1	COX6B1	-1.79	6.94E-04
Q96AM1	Mas-related G-protein coupled receptor member F	MRGPRF	-1.79	7.86E-03
P17540	Creatine kinase S-type, mitochondrial	CKMT2	-1.79	4.43E-02
P35611	Alpha-adducin	ADD1	-1.78	2.15E-03
P07451	Carbonic anhydrase 3	CA3	-1.78	1.08E-02
P27816	Microtubule-associated protein 4	MAP4	-1.78	1.28E-02
P06737	Glycogen phosphorylase, liver form	PYGL	-1.78	2.34E-02
Q02218	2-oxoglutarate dehydrogenase, mitochondrial	OGDH	-1.77	1.24E-02
P07099	Epoxide hydrolase 1	EPHX1	-1.77	4.10E-02
Q9UHD8	Septin-9	SEP9	-1.76	1.68E-03
P50213	Isocitrate dehydrogenase [NAD] subunit alpha, mitochondrial	IDH3A	-1.74	5.06E-03
P10620	Microsomal glutathione S-transferase 1	MGST1	-1.73	2.06E-03
Q16891	MICOS complex subunit MIC60	IMMT	-1.72	2.88E-03
P51911	Calponin-1	CNN1	-1.71	1.88E-03
Q6PCB0	von Willebrand factor A domain-containing protein 1	VWA1	-1.71	1.70E-02
P21399	Cytoplasmic aconitate hydratase	ACO1	-1.71	7.94E-03
P30084	Enoyl-CoA hydratase, mitochondrial	ECHS1	-1.71	1.36E-03
Q01082	Spectrin beta chain, non-erythrocytic 1	SPTBN1	-1.71	5.24E-04
O43491	Band 4.1-like protein 2	EPB41L2	-1.71	7.31E-03

Supplemental Table 14. Predicted Upstream Master Regulators for Up- and Down-Regulated Fibrous Plaque Proteins

A. LAD Samples

Overrepresented Pathways with Consistent Evidence of Activation or Inhibition

Upstream Regulator	Molecule Type	p-value of overlap	Predicted Activation	Activation z-score
INSR	kinase	8.56E-16	Inhibited	-2.493
PPARG	ligand-dependent nuclear receptor	2.42E-13	Inhibited	-2.805
PPARA	ligand-dependent nuclear receptor	4.22E-10	Inhibited	-3.060
TNF	cytokine	2.64E-07	Activated	3.043

Overrepresented Pathways without Consistent Evidence of Activation or Inhibition

Upstream Regulator	Molecule Type	p-value of overlap	Predicted Activation	Activation z-score
TP53	transcription regulator	5.60E-08	n/a	-0.723
MGEA5	enzyme	2.40E-06	n/a	0.302
PTEN	phosphatase	2.48E-06	n/a	-0.950
ESR2	ligand-dependent nuclear receptor	1.61E-05	n/a	-0.239
MYC	transcription regulator	2.34E-04	n/a	0.000
ERBB2	kinase	4.20E-04	n/a	n/a*
TGFB1	growth factor	1.79E-03	n/a	0.720

* not enough information in the Ingenuity database to estimate

B. AA Samples

Overrepresented Pathways with Consistent Evidence of Activation or Inhibition

Upstream Regulator	Molecule Type	p-value of overlap	Predicted Activation	Activation z-score
TGFB1	growth factor	8.53E-11	Inhibited	-3.147
APOE	transporter	4.53E-09	Inhibited	-2.611
APP	other	2.76E-06	Activated	2.148
TNF	cytokine	1.92E-05	Activated	2.192
IL1B	cytokine	2.31E-05	Activated	2.676
MGEA5	enzyme	9.02E-04	Activated	2.714
IL6	cytokine	1.05E-03	Activated	2.195

Overrepresented Pathways without Consistent Evidence of Activation or Inhibition

Upstream Regulator	Molecule Type	p-value of overlap	Predicted Activation	Activation z-score
TP53	transcription regulator	5.16E-11	n/a	-1.918
HRAS	enzyme	7.29E-11	n/a	0.617
MYC	transcription regulator	8.34E-08	n/a	-0.650
MYCN	transcription regulator	3.17E-07	n/a	1.612

PRL	cytokine	1.02E-05	n/a	0.818
JUN	transcription regulator	2.60E-05	n/a	0.859
	ligand-dependent nuclear			
AR	receptor	5.86E-05	n/a	-0.816
MAPK1	kinase	7.29E-05	n/a	0.000
KRAS	enzyme	7.39E-05	n/a	-0.043
NFKBIA	transcription regulator	2.55E-04	n/a	1.310
HTT	transcription regulator	4.65E-04	n/a	0.447
	ligand-dependent nuclear			
ESR1	receptor	1.03E-03	n/a	0.905
SP1	transcription regulator	1.84E-03	n/a	0.342
ERBB2	kinase	3.98E-03	n/a	-1.154
SMARCA4	transcription regulator	4.67E-03	n/a	-1.949
STAT3	transcription regulator	6.15E-03	n/a	1.680
FOS	transcription regulator	1.22E-02	n/a	-1.069
CTNNB1	transcription regulator	1.32E-02	n/a	0.000

Up-stream regulators common to both territories are indicated in **bold**

Supplemental Table 15. IPA Output for Analysis of Fibrous Plaque vs NL Marker Proteins with q-value ≤ 0.05 and $|fold\ change| \geq 1.7$

<see Excel file: Supplemental Table 15.xlsx>

Supplemental Table 16. Up-Regulated Proteins in Fibrous Plaque Enriched AA Samples (n=7) Compared with Normal AA Samples (n=15). Samples were selected using patho-proteomic phenotyping designed to integrate pathologist assessment of extent of disease and CAM deconvolution of global protein profiles (fold-change = mean FP/ mean NL).

<u>Uniprot</u>	<u>ID</u>	<u>Protein</u>	<u>Gene</u>	<u>Fold-change</u>	<u>q-value</u>
P04114		Apolipoprotein B-100	APOB	11.68	4.87E-03
P13796		Plastin-2	LCP1	9.22	4.50E-04
P02675		Fibrinogen beta chain	FGB	6.03	1.73E-03
P07858		Cathepsin B	CTSB	5.99	4.84E-03
P00734		Prothrombin	F2	5.30	5.92E-04
P00738		Haptoglobin	HP	4.26	1.36E-03
P01892		HLA class I histocompatibility antigen, A-2 alpha chain	HLA-A	4.16	4.73E-03
P20742		Pregnancy zone protein	PZP	4.04	3.90E-02
P27169		Serum paraoxonase/arylesterase 1	PON1	4.04	3.42E-02
P19823		Inter-alpha-trypsin inhibitor heavy chain H2	ITIH2	4.00	7.61E-04
P40121		Macrophage-capping protein	CAPG	3.88	1.09E-02
P35442		Thrombospondin-2	THBS2	3.82	1.36E-03
P00488		Coagulation factor XIII A chain	F13A1	3.77	5.86E-03
P01031		Complement C5	C5	3.64	5.07E-03
P02679		Fibrinogen gamma chain	FGG	3.53	3.90E-03
P04003		C4b-binding protein alpha chain	C4BPA	3.45	1.24E-03
P00739		Haptoglobin-related protein	HPR	3.41	5.26E-03
P31146		Coronin-1A	CORO1A	3.30	3.13E-05
P05090		Apolipoprotein D	APOD	3.29	2.90E-04
P24821		Tenascin	TNC	3.17	2.70E-03
P05546		Heparin cofactor 2	SERPIND1	3.12	1.03E-02
P02649		Apolipoprotein E	APOE	3.06	2.06E-04
Q14624		Inter-alpha-trypsin inhibitor heavy chain H4	ITIH4	3.04	3.70E-04
P02671		Fibrinogen alpha chain	FGA	3.03	1.26E-03
P52209		6-phosphogluconate dehydrogenase, decarboxylating	PGD	2.99	4.57E-02
P05155		Plasma protease C1 inhibitor	SERPING1	2.85	1.08E-04
P00747		Plasminogen	PLG	2.73	4.08E-04
POCOL5		Complement C4-B	C4B	2.72	3.13E-05
Q9BXR6		Complement factor H-related protein 5	CFHR5	2.64	2.00E-02
O43866		CD5 antigen-like	CD5L	2.63	1.62E-02
O14791		Apolipoprotein L1	APOL1	2.58	3.29E-02
P00736		Complement C1r subcomponent	C1R	2.56	3.13E-02
P02792		Ferritin light chain	FTL	2.54	4.01E-04
Q9UBR2		Cathepsin Z	CTS2	2.51	1.40E-02
P19827		Inter-alpha-trypsin inhibitor heavy chain H1	ITIH1	2.50	1.95E-05
P18428		Lipopolysaccharide-binding protein	LBP	2.48	1.02E-04
P01871		Ig mu chain C region	IGHM	2.43	2.07E-02
P04196		Histidine-rich glycoprotein	HRG	2.41	1.52E-06
P20700		Lamin-B1	LMNB1	2.40	1.62E-02
P04179		Superoxide dismutase [Mn], mitochondrial	SOD2	2.36	1.04E-03
P61626		Lysozyme C	LYZ	2.31	1.72E-02
P02794		Ferritin heavy chain	FTH1	2.21	5.16E-04
Q96PD5		N-acetylmuramoyl-L-alanine amidase	PGLYRP2	2.16	1.40E-02

P07358	Complement component C8 beta chain	C8B	2.15	3.93E-02
P01023	Alpha-2-macroglobulin	A2M	2.11	8.38E-04
P07339	Cathepsin D	CTSD	2.05	4.12E-03
P59665	Neutrophil defensin 1	DEFA1	2.04	1.75E-02
P01877	Ig alpha-2 chain C region	IGHA2	2.02	2.90E-03
P05156	Complement factor I	CFI	1.98	8.48E-03
P08603	Complement factor H	CFH	1.98	6.41E-06
Q14764	Major vault protein	MVP	1.97	2.54E-02
P00740	Coagulation factor IX	F9	1.88	1.16E-02
P00751	Complement factor B	CFB	1.85	1.94E-02
P13671	Complement component C6	C6	1.85	7.56E-03
P01594	Ig kappa chain V-I region AU		1.84	4.49E-02
P00450	Ceruloplasmin	CP	1.83	7.34E-05
P10643	Complement component C7	C7	1.82	1.97E-03
P04004	Vitronectin	VTN	1.81	9.08E-04
Q9UJ70	N-acetyl-D-glucosamine kinase	NAGK	1.80	3.61E-02
O14818	Proteasome subunit alpha type-7	PSMA7	1.79	1.75E-02
P01042	Kininogen-1	KNG1	1.79	1.84E-03

Supplemental Table 17. Down-Regulated Proteins in Fibrous Plaque Enriched AA Samples (n=7) Compared with Normal AA Samples (n=15). Samples were selected using patho-proteomic phenotyping designed to integrate pathologist assessment of extent of disease and CAM deconvolution of global protein profiles. (For down regulated proteins Fold-change=-1* mean NL/mean FP)

<u>Uniprot ID</u>	<u>Protein</u>	<u>Gene</u>	<u>Fold-change</u>	<u>q-value</u>
Q8N2S1	Latent-transforming growth factor beta-binding protein 4	LTBP4	-6.38	4.00E-07
P55083	Microfibril-associated glycoprotein 4	MFAP4	-4.92	6.64E-05
Q7Z4I7	LIM and senescent cell antigen-like-containing domain protein 2	LIMS2	-4.47	5.95E-05
P17661	Desmin	DES	-4.36	1.95E-05
P46821	Microtubule-associated protein 1B	MAP1B	-4.11	4.00E-07
P11216	Glycogen phosphorylase, brain form	PYGB	-3.74	7.51E-07
Q9HBL0	Tensin-1	TNS1	-3.72	1.73E-05
Q9H223	EH domain-containing protein 4	EHD4	-3.69	1.52E-06
Q0ZGT2	Nexilin	NEXN	-3.62	5.65E-05
P16112	Aggrecan core protein	ACAN	-3.55	6.64E-05
Q14315	Filamin-C	FLNC	-3.54	7.34E-05
Q53GG5	PDZ and LIM domain protein 3	PDLIM3	-3.48	1.22E-05
P50895	Basal cell adhesion molecule	BCAM	-3.46	1.77E-06
O00151	PDZ and LIM domain protein 1	PDLIM1	-3.37	4.28E-05
O43175	D-3-phosphoglycerate dehydrogenase	PHGDH	-3.31	4.90E-06
O00159	Unconventional myosin-Ic	MYO1C	-3.19	3.56E-06
P53814	Smoothelin	SMTN	-3.14	7.75E-07
P29536	Leiomodin-1	LMOD1	-3.12	5.80E-07
Q7Z7G0	Target of Nesh-SH3	ABI3BP	-3.05	1.55E-04
Q8WX93	Palladin	PALLD	-3.05	3.56E-06
P60660	Myosin light polypeptide 6	MYL6	-3.03	2.64E-04
Q9NR12	PDZ and LIM domain protein 7	PDLIM7	-2.98	4.12E-05
Q01082	Spectrin beta chain, non-erythrocytic 1	SPTBN1	-2.86	2.07E-04
Q9Y4G6	Talin-2	TLN2	-2.84	3.06E-05
Q96A00	Protein phosphatase 1 regulatory subunit 14A	PPP1R14A	-2.82	3.88E-05
Q8IVN8	Somatomedin-B and thrombospondin type-1 domain-containing protein	SBSPON	-2.79	1.87E-05
Q15746	Myosin light chain kinase, smooth muscle	MYLK	-2.77	5.54E-06
Q9NVD7	Alpha-parvin	PARVA	-2.69	5.54E-06
Q9NZU5	LIM and cysteine-rich domains protein 1	LMCD1	-2.68	1.08E-05
Q9UMS6	Synaptopodin-2	SYNPO2	-2.68	1.53E-04
P19105	Myosin regulatory light chain 12A	MYL12A	-2.57	1.95E-05
P17655	Calpain-2 catalytic subunit	CAPN2	-2.50	1.26E-04
Q96HC4	PDZ and LIM domain protein 5	PDLIM5	-2.48	5.89E-05
O75112	LIM domain-binding protein 3	LDB3	-2.48	3.29E-04
Q07954	Prolow-density lipoprotein receptor-related protein 1	LRP1	-2.47	9.83E-05
Q9BX66	Sorbin and SH3 domain-containing protein 1	SORBS1	-2.45	4.10E-04
Q9BZQ8	Protein Niban	FAM129A	-2.45	3.34E-04
Q15942	Zyxin	ZYX	-2.40	8.03E-06
Q9UGI8	Testin	TES	-2.39	3.47E-05
O94875	Sorbin and SH3 domain-containing protein 2	SORBS2	-2.38	1.85E-04
O14974	Protein phosphatase 1 regulatory subunit 12A	PPP1R12A	-2.38	2.97E-05

Q15365	Poly(rC)-binding protein 1	PCBP1	-2.37	2.20E-04
P09651	Heterogeneous nuclear ribonucleoprotein A1	HNRNPA1	-2.37	6.11E-03
P16615	Sarcoplasmic/endoplasmic reticulum calcium ATPase 2	ATP2A2	-2.36	4.13E-04
P48059	LIM and senescent cell antigen-like-containing domain protein 1	LIMS1	-2.33	8.29E-04
Q14BN4	Sarcolemmal membrane-associated protein	SLMAP	-2.30	5.89E-05
Q8WUP2	Filamin-binding LIM protein 1	FBLIM1	-2.27	1.33E-04
P51911	Calponin-1	CNN1	-2.26	6.30E-04
Q93052	Lipoma-preferred partner	LPP	-2.26	9.77E-05
O43294	Transforming growth factor beta-1-induced transcript 1 protein	TGFBI1	-2.25	6.93E-04
Q14204	Cytoplasmic dynein 1 heavy chain 1	DYNC1H1	-2.24	1.66E-03
Q05682	Caldesmon	CALD1	-2.24	2.94E-04
Q16836	Hydroxyacyl-coenzyme A dehydrogenase, mitochondrial	HADH	-2.22	6.78E-04
O15061	Synemin	SYNM	-2.21	1.72E-02
Q9BTV4	Transmembrane protein 43	TMEM43	-2.21	1.16E-03
Q9Y696	Chloride intracellular channel protein 4	CLIC4	-2.21	5.54E-06
P43121	Cell surface glycoprotein MUC18	MCAM	-2.18	1.28E-05
P09104	Gamma-enolase	ENO2	-2.17	3.96E-04
Q13976	cGMP-dependent protein kinase 1	PRKG1	-2.16	3.88E-04
Q03252	Lamin-B2	LMNB2	-2.15	1.03E-02
Q13813	Spectrin alpha chain, non-erythrocytic 1	SPTAN1	-2.14	5.45E-04
Q15019	Septin-2	2-Sep	-2.11	1.58E-03
Q15124	Phosphoglucomutase-like protein 5	PGM5	-2.08	1.36E-03
Q9UBX5	Fibulin-5	FBLN5	-2.08	9.44E-04
P02511	Alpha-crystallin B chain	CRYAB	-2.06	7.93E-03
O14558	Heat shock protein beta-6	HSPB6	-2.05	9.05E-05
P13861	cAMP-dependent protein kinase type II-alpha regulatory subunit	PRKAR2A	-2.05	2.43E-04
P53708	Integrin alpha-8	ITGA8	-2.02	1.15E-03
P27816	Microtubule-associated protein 4	MAP4	-2.01	3.71E-04
O15230	Laminin subunit alpha-5	LAMA5	-2.01	7.86E-04
P20073	Annexin A7	ANXA7	-2.01	4.50E-03
P55268	Laminin subunit beta-2	LAMB2	-2.01	9.55E-04
Q03135	Caveolin-1	CAV1	-1.98	2.33E-03
Q96AC1	Fermitin family homolog 2	FERMT2	-1.95	6.78E-04
Q01995	Transgelin	TAGLN	-1.95	7.34E-05
Q14240	Eukaryotic initiation factor 4A-II	EIF4A2	-1.93	4.44E-03
P08670	Vimentin	VIM	-1.92	3.35E-04
Q92599	Septin-8	8-Sep	-1.92	1.68E-02
Q9NZN4	EH domain-containing protein 2	EHD2	-1.92	1.66E-03
Q04917	14-3-3 protein eta	YWHAH	-1.89	1.16E-03
Q00577	Transcriptional activator protein Pur-alpha	PURA	-1.89	1.73E-04
Q9UBI6	Guanine nucleotide-binding protein G(I)/G(S)/G(O) subunit gamma-12	GNG12	-1.88	2.96E-03
Q13555	Calcium/calmodulin-dependent protein kinase type II subunit gamma	CAMK2G	-1.88	5.82E-03
P30084	Enoyl-CoA hydratase, mitochondrial	ECHS1	-1.87	2.10E-02
Q08257	Quinone oxidoreductase	CRYZ	-1.87	7.25E-04
Q16555	Dihydropyrimidinase-related protein 2	DPYSL2	-1.86	7.75E-07
Q96S97	Myeloid-associated differentiation marker	MYADM	-1.85	1.68E-04
Q16181	Septin-7	7-Sep	-1.85	5.25E-03
Q9H4M9	EH domain-containing protein 1	EHD1	-1.84	1.71E-03
Q8WUM4	Programmed cell death 6-interacting	PDCD6IP	-1.84	9.46E-03

	protein			
Q15847	Adipogenesis regulatory factor	ADIRF	-1.84	8.01E-03
P11047	Laminin subunit gamma-1	LAMC1	-1.84	5.83E-04
Q9NZN3	EH domain-containing protein 3	EHD3	-1.83	3.53E-03
P36871	Phosphoglucomutase-1	PGM1	-1.81	2.31E-03
P05388	60S acidic ribosomal protein P0	RPLPO	-1.79	2.10E-03
Q6NZI2	Polymerase I and transcript release factor	PTRF	-1.78	2.41E-03
P12277	Creatine kinase B-type	CKB	-1.77	1.09E-02
P31150	Rab GDP dissociation inhibitor alpha	GDI1	-1.76	7.96E-03
P62140	Serine/threonine-protein phosphatase PP1-beta catalytic subunit	PPP1CB	-1.76	6.41E-03
P35749	Myosin-11	MYH11	-1.75	3.46E-04
Q9UL25	Ras-related protein Rab-21	RAB21	-1.73	4.72E-03
P21333	Filamin-A	FLNA	-1.73	3.57E-04
Q969G5	Protein kinase C delta-binding protein	PRKCDBP	-1.73	1.18E-02
P39060	Collagen alpha-1(XVIII) chain	COL18A1	-1.72	3.46E-04
P63167	Dynein light chain 1, cytoplasmic	DYNLL1	-1.70	3.39E-04
Q63ZY3	KN motif and ankyrin repeat domain-containing protein 2	KANK2	-1.70	1.38E-02

Supplemental Table 18. Overlap of Patho-Proteomic Fibrous Plaque Proteins in Human LAD

(n=99) and AA (n=99) Samples Twelve proteins were significantly ($q \leq 0.05$) up-regulated in fibrous plaque enriched samples compared to normal samples in both the LAD and AA. With the exception of cathepsin Z, all of the up-regulated proteins were also identified as fibrous plaque proteins in both LAD and AA using CAM. Similarly, seven proteins were significantly down-regulated in fibrous plaque samples compared to normal.

Uniprot ID	Protein	Gene	Fold-change	q-value	Fold-change	q-value
P24821	Tenascin	TNC	13.04	1.08E-03	3.17	2.70E-03
P04114	Apolipoprotein B-100	APOB	3.65	6.26E-04	11.68	4.87E-03
P13796	Plastin-2	LCP1	3.87	9.80E-04	9.22	4.50E-04
P07858	Cathepsin B	CTSB	3.63	3.13E-04	5.99	4.84E-03
P40121	Macrophage-capping protein	CAPG	2.72	6.89E-03	3.88	1.09E-02
P35442	Thrombospondin-2	THBS2	2.69	4.40E-04	3.82	1.36E-03
P01031	Complement C5	C5	1.89	1.58E-02	3.64	5.07E-03
P31146	Coronin-1A	CORO1A	2.13	1.22E-02	3.30	3.13E-05
P02649	Apolipoprotein E	APOE	1.79	1.28E-02	3.06	2.06E-04
O43866	CD5 antigen-like	CD5L	2.10	1.22E-02	2.63	1.62E-02
Q9UBR2	Cathepsin Z	CTSZ	2.20	9.53E-04	2.51	1.40E-02
P01871	Ig mu chain C region	IGHM	2.15	8.14E-03	2.43	2.07E-02
P46821	Microtubule-associated protein 1B	MAP1B	-1.90	4.59E-03	-4.11	4.00E-07
Q9HBL0	Tensin-1	TNS1	-2.01	5.58E-04	-3.72	1.73E-05
O43175	D-3-phosphoglycerate dehydrogenase	PHGDH	-2.09	2.77E-04	-3.31	4.90E-06
O75112	LIM domain-binding protein 3	LDB3	-1.98	1.70E-02	-2.48	3.29E-04
P51911	Calponin-1	CNN1	-1.71	1.88E-03	-2.26	6.30E-04
P27816	Microtubule-associated protein 4	MAP4	-1.78	1.28E-02	-2.01	3.71E-04
P30084	Enoyl-CoA hydratase, mitochondrial	ECHS1	-1.71	1.36E-03	-1.87	2.10E-02

Supplemental Table 19. IPA Output for Analysis of Fibrous Plaque vs NL Marker Proteins with q-value ≤ 0.01

<see Excel file: Supplemental Table 19.xlsx>

SUPPLEMENTAL REFERENCES

1. Strong JP, Malcom GT, McMahan CA, Tracy RE, Newman WP, 3rd, Herderick EE and Cornhill JF. Prevalence and extent of atherosclerosis in adolescents and young adults: implications for prevention from the Pathobiological Determinants of Atherosclerosis in Youth Study. *JAMA*. 1999;281:727-735.
2. Suna G, Wojakowski W, Lynch M, Barallobre-Barreiro J, Yin X, Mayr U, Baig F, Lu R, Fava M, Hayward R, Molenaar C, White SJ, Roleder T, Milewski KP, Gasior P, Buszman PP, Buszman P, Jahangiri M, Shanahan CM, Hill J and Mayr M. Extracellular Matrix Proteomics Reveals Interplay of Aggrecan and Aggrecanases in Vascular Remodeling of Stented Coronary Arteries. *Circulation*. 2018;137:166-183.
3. de Castro Bras LE, Ramirez TA, DeLeon-Pennell KY, Chiao YA, Ma Y, Dai Q, Halade GV, Hakala K, Weintraub ST and Lindsey ML. Texas 3-step decellularization protocol: looking at the cardiac extracellular matrix. *J Proteomics*. 2013;86:43-52.
4. Chambers MC, Maclean B, Burke R, Amodei D, Ruderman DL, Neumann S, Gatto L, Fischer B, Pratt B, Egertson J, Hoff K, Kessner D, Tasman N, Shulman N, Frewen B, Baker TA, Brusniak MY, Paulse C, Creasy D, Flashner L, Kani K, Moulding C, Seymour SL, Nuwaysir LM, Lefebvre B, Kuhlmann F, Roark J, Rainer P, Detlev S, Hemenway T, Huhmer A, Langridge J, Connolly B, Chadick T, Holly K, Eckels J, Deutsch EW, Moritz RL, Katz JE, Agus DB, MacCoss M, Tabb DL and Mallick P. A cross-platform toolkit for mass spectrometry and proteomics. *Nat Biotechnol*. 2012;30:918-920.
5. Craig R and Beavis RC. TANDEM: matching proteins with tandem mass spectra. *Bioinformatics*. 2004;20:1466-1467.
6. Geer LY, Markey SP, Kowalak JA, Wagner L, Xu M, Maynard DM, Yang X, Shi W and Bryant SH. Open mass spectrometry search algorithm. *J Proteome Res*. 2004;3:958-964.
7. Elias JE and Gygi SP. Target-decoy search strategy for increased confidence in large-scale protein identifications by mass spectrometry. *Nat Methods*. 2007;4:207-214.
8. Apweiler R, Bairoch A, Wu CH, Barker WC, Boeckmann B, Ferro S, Gasteiger E, Huang H, Lopez R, Magrane M, Martin MJ, Natale DA, O'Donovan C, Redaschi N and Yeh LS. UniProt: the Universal Protein knowledgebase. *Nucleic Acids Res*. 2004;32:D115-119.
9. Keller A, Eng J, Zhang N, Li XJ and Aebersold R. A uniform proteomics MS/MS analysis platform utilizing open XMLfile formats. *Mol Syst Biol*. 2005;1:2005.0017.
10. Keller A, Nesvizhskii AI, Kolker E and Aebersold R. Empirical statistical model to estimate the accuracy of peptide identifications made by MS/MS and database search. *Anal Chem*. 2002;74:5383-5392.
11. Shteynberg D, Deutsch EW, Lam H, Eng JK, Sun Z, Tasman N, Mendoza L, Moritz RL, Aebersold R and Nesvizhskii AI. iProphet: multi-level integrative analysis of shotgun proteomic data improves peptide and protein identification rates and error estimates. *Mol Cell Proteomics*. 2011;10:M111.007690.
12. Nesvizhskii AI, Keller A, Kolker E and Aebersold R. A statistical model for identifying proteins by tandem mass spectrometry. *Anal Chem*. 2003;75:4646-4658.
13. Vogel C and Marcotte EM. Label-free protein quantitation using weighted spectral counting. *Methods Mol Biol*. 2012;893:321-341.
14. Candès E and Recht B. Exact Matrix Completion via Convex Optimization. *Foundations of Computational mathematics* 2009;9.6:717-772.
15. Zhang B and Horvath S. A general framework for weighted gene co-expression network analysis. *Stat Appl Genet Mol Biol*. 2005;4:Article17.
16. Buettner F, Natarajan KN, Casale FP, Proserpio V, Scialdone A, Theis FJ, Teichmann SA, Marioni JC and Stegle O. Computational analysis of cell-to-cell heterogeneity in single-cell RNA-sequencing data reveals hidden subpopulations of cells. *Nat Biotechnol*. 2015;33:155-160.
17. Lake BB, Ai R, Kaeser GE, Salathia NS, Yung YC, Liu R, Wildberg A, Gao D, Fung HL, Chen S, Vijayaraghavan R, Wong J, Chen A, Sheng X, Kaper F, Shen R, Ronaghi M, Fan JB, Wang W, Chun J and Zhang K. Neuronal subtypes and diversity revealed by single-nucleus RNA sequencing of the human brain. *Science*. 2016;352:1586-1590.

18. Quintivano J, Aryee MJ and Kaminsky ZA. A cell epigenotype specific model for the correction of brain cellular heterogeneity bias and its application to age, brain region and major depression. *Epigenetics*. 2013;8:290-302.
19. Kuhn A, Thu D, Waldvogel HJ, Faull RL and Luthi-Carter R. Population-specific expression analysis (PSEA) reveals molecular changes in diseased brain. *Nat Methods*. 2011;8:945-947.
20. Rahmani E, Zaitlen N, Baran Y, Eng C, Hu D, Galanter J, Oh S, Burchard EG, Eskin E, Zou J and Halperin E. Sparse PCA corrects for cell type heterogeneity in epigenome-wide association studies. *Nat Methods*. 2016;13:443-445.
21. Chan T, Ma W, Chi C and Wang Y. A convex analysis framework for blind separation of non-negative sources. *IEEE Trans Signal Processing*. 2008;56:5120-5134.
22. Wang N, Hoffman EP, Chen L, Chen L, Zhang Z, Liu C, Yu G, Herrington DM, Clarke R and Wang Y. Mathematical modelling of transcriptional heterogeneity identifies novel markers and subpopulations in complex tissues. *Sci Rep*. 2016;6:18909.
23. Chen L, Chan TH, Choyke PL, Hillman EM, Chi CY, Bhujwalla ZM, Wang G, Wang SS, Szabo Z and Wang Y. CAM-CM: a signal deconvolution tool for in vivo dynamic contrast-enhanced imaging of complex tissues. *Bioinformatics*. 2011;27:2607-2609.
24. Chen L, Choyke PL, Chan TH, Chi CY, Wang G and Wang Y. Tissue-specific compartmental analysis for dynamic contrast-enhanced MR imaging of complex tumors. *IEEE Trans Med Imaging*. 2011;30:2044-2058.
25. Frey BJ and Dueck D. Clustering by passing messages between data points. *Science*. 2007;315:972-976.
26. Boyle EI, Weng S, Gollub J, Jin H, Botstein D, Cherry JM and Sherlock G. GO::TermFinder--open source software for accessing Gene Ontology information and finding significantly enriched Gene Ontology terms associated with a list of genes. *Bioinformatics*. 2004;20:3710-3715.
27. Supek F, Bosnjak M, Skunca N and Smuc T. REVIGO summarizes and visualizes long lists of gene ontology terms. *PLoS One*. 2011;6:e21800.
28. Mitra K, Carvunis AR, Ramesh SK and Ideker T. Integrative approaches for finding modular structure in biological networks. *Nat Rev Genet*. 2013;14:719-732.
29. Hu JX, Thomas CE and Brunak S. Network biology concepts in complex disease comorbidities. *Nat Rev Genet*. 2016;17:615-629.
30. Hudson NJ, Dalrymple BP and Reverter A. Beyond differential expression: the quest for causal mutations and effector molecules. *BMC Genomics*. 2012;13:356.
31. Zhang B, Tian Y, Jin L, Li H, Shih Ie M, Madhavan S, Clarke R, Hoffman EP, Xuan J, Hilakivi-Clarke L and Wang Y. DDN: a caBIG(R) analytical tool for differential network analysis. *Bioinformatics*. 2011;27:1036-1038.
32. Tian Y, Zhang B, Hoffman EP, Clarke R, Zhang Z, Shih Ie M, Xuan J, Herrington DM and Wang Y. Knowledge-fused differential dependency network models for detecting significant rewiring in biological networks. *BMC Syst Biol*. 2014;8:87.
33. Tian Y, Zhang B, Hoffman EP, Clarke R, Zhang Z, Shih Ie M, Xuan J, Herrington DM and Wang Y. KDDN: an open-source Cytoscape app for constructing differential dependency networks with significant rewiring. *Bioinformatics*. 2015;31:287-289.
34. MacLean B, Tomazela DM, Shulman N, Chambers M, Finney GL, Frewen B, Kern R, Tabb DL, Liebler DC and MacCoss MJ. Skyline: an open source document editor for creating and analyzing targeted proteomics experiments. *Bioinformatics*. 2010;26:966-968.
35. Tibshirani R. Regression Shrinkage and Selection via the Lasso. *Journal of the Royal Statistical Society*. 1996;Series B, 58:267-288.
36. Zou H and Hastie T. Regularization and Variable Selection via the Elastic Net. *Journal of the Royal Statistical Society*. 2005;Series B, 67:301-320.
37. Zou H and Zhang H. On the Adaptive Elastic-Net with A Diverging Number of Parameters. *Annals of Statistics*. 2009;37:1733-1751.
38. Efron B. Nonparametric Standard Errors and Confidence Intervals. *The Canadian Journal of Statistics* 1981;9:139-158.

